MAGIC III: AN AUTOMATED GENERAL PURPOSE SYSTEM FOR STRUCTURAL ANALYSIS

VOLUME I: ENGINEER'S MANUAL

JAMES R. BATT
STEPHEN JORDAN

FOREWORD

This report was prepared by Textron's Bell Aerospace Company (BAC), Buffalo, New York under USAF Contract No. F 33615-71-C-1390. This contract is an extension of previous work initiated under Project No. 1467, "Structural Analysis Methods", Task No. 146702, "Thermal Elastic Analysis Methods." The program was administered by the Air Force Flight Dynamics Laboratory (AFFDL), under the cognizance of Mr. G. E. Maddux, AFFDL Program Manager. The program was carried out by the Structural Systems Department, Bell Aerospace Company, during the period 15 March 1971 to 15 March 1972, under the direction of Mr. Stephen Jordan, BAC Program Manager.
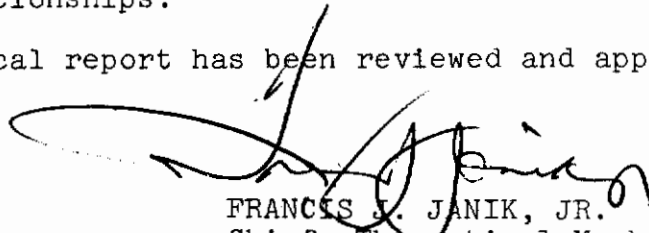
This report, "MAGIC III: An Automated General Purpose System for Structural Analysis," is published in three volumes, "Volume I: Engineer's Manual," "Volume II; User's Manual," and Volume III: Programmer's Manual." The manuscript for Volume I was released by the authors in July, 1972 as an AFFDL Technical Report.

The authors wish to express appreciation to colleagues in the Advanced Structural Design Technology Section of the Structural Design Technology Section of the Structural Systems Department and Research Department for their individually significant, and collectively indispensable contributions to this effort.

Special appreciation is given to Dr. Robert H. Mallett for the evaluation of the quadrilateral thin shell element in Section II-H of this report. Appreciation is also given to Mr. Michael Apostal for his contributions with regard to the derivation and evaluation of the triangular ring element with asymmetric load which is described in Section II-G of this report.

The authors wish to express appreciation also to Miss Beverly J. Dale and her staff for the expert computer programming that transformed the analytical development into a practical working tool. Particular gratitude is given to Mr. Walter Luberacki for his efforts in coding and checkoutof the lengthy solid element relationships.

This technical report has been reviewed and approved.

FRANCIS J. JANIK, JR.
Chief, Theoretical Mechanics Branch
Structures Division

ABSTRACT

An automated general purpose system for analysis is presented. This system, identified by the acronym, "MAGIC III" for Matrix Analysis via Generative and Interpretive Computations, is an extension of the structural analysis capability available in the initial MAGIC System. MAGIC III provides a powerful framework for implementation of the finite element analysis technology and provides diversified capability for displacement, stress, vibration and stability analyses.

Additional elements have been added to the MAGIC element library in this phase of MAGIC development. These are the solid elements; rectangular prism, tetrahedron, triangular prism, symmetric triangular prism, and triangular ring (asymmetrical loading). Also included are the symmetric shear web element and a revised quadrilateral thin shell element. The finite elements listed include matrices for stiffness, mass, prestrain load, thermal load, distributed mechanical load, pressure and stress.

The MAGIC III System for structural analysis is presented as an integral part of the overall design cycle. Considerations in this regard include, among other things, preprinted input data forms, automated data generation, data confirmation features, restart options, automated output data reduction and readable output displays.

Documentation of the MAGIC III System is presented in three parts; namely, Volume I: Engineer's Manual, Volume II: User's Manual and Volume III: Programmer's Manual. The subject document, Volume I (Engineer's Manual) is an extension of the primary Technical documents. Included are the theoretical developments for the additional finite elements included in the MAGIC III System as well as a discussion of newly added computational procedures.

TABLE OF CONTENTS

v

TABLE OF CONTENTS (CONCLUDED)

TABLE OF CONTENTS (CONCLUDED)

LIST OF FIGURES

LIST OF FIGURES (Concluded)

LIST OF TABLES

x

SECTION I

INTRODUCTION

The MAGIC III System for structural analysis is an extension
of the MAGIC I and MAGIC II Systems reported in References 1 to 6.
All capabilities available in the original systems have been
retained and improved upon. Extension of the MAGIC System has
been in the following areas:

(a) Incorporation of four (4) solid elements
   (1) Rectangular Prism
   (2) Tetrahedron
   (3) Triangular Prism
   (4) Symmetric Triangular Prism

(b) Incorporation of a Triangular Cross-Section Ring which
     accommodates asymmetric mechanical and thermal loading.

(c) Incorporation of the Symmetric Shear Web element.

(d) Incorporation of a revised Quadrilateral Thin Shell
     element which reflects high aspect ratio usage.

(e) Incorporation of new equation solvers into the
     MAGIC III System.

(f) Inclusion of additional computational procedures to
     support the analysis process.

The work reported herein is a discussion of the extensions
listed above. The discussion encompasses three volumes of which
this is the first. This Volume, Engineer's Manual, (Volume I) is
an addendum to the technical reports given in References 1 and 4
and as such should be used in conjunction with these references to
effectively utilize the MAGIC III System. The second Volume, User's
Manual, Reference 7, includes detailed specifications for the
preparation of input data for the additional elements included in
this third version of MAGIC. The last volume, Volume III,

Programmer's Manual, Reference 8, presents information on the organization of the MAGIC III System as well as its operational characteristics.

Section II of this report presents the theoretical basis of the additional finite elements and gives explicit expressions for their characteristic matrices. These elements are:

(a) Rectangular Prism

(b) Tetrahedron

(c) Triangular Prism

(d) Symmetric Triangular Prism

(e) Triangular Cross-Section Ring (Asymmetric Loading)

(f) Symmetric Shear Web

(g) Revised Quadrilateral Thin Shell

Figures I-1 to I-3 depict these newly added elements as well as previously existing elements of the MAGIC System.

A discussion of new computational features incorporated into the MAGIC III System is given in Section III. Included are a discussion of the ANALIC (Analysis In Core) Module and the out-of-core variable bandwidth equation solver based on Cholesky triangularization.

The body of the technical report is concluded with a general retrospective discussion in Section IV. An overview of the MAGIC III System is presented.

2

c. Triangular Prism

b. Tetrahedron

a. Rectangular Prism

f. Triangular Cross-Section Ring
(Asymmetric Loads)

Plane of Symmetry

c. Symmetrical Shear Web

Plane of Symmetry

d. Symmetrical Triangular Prism
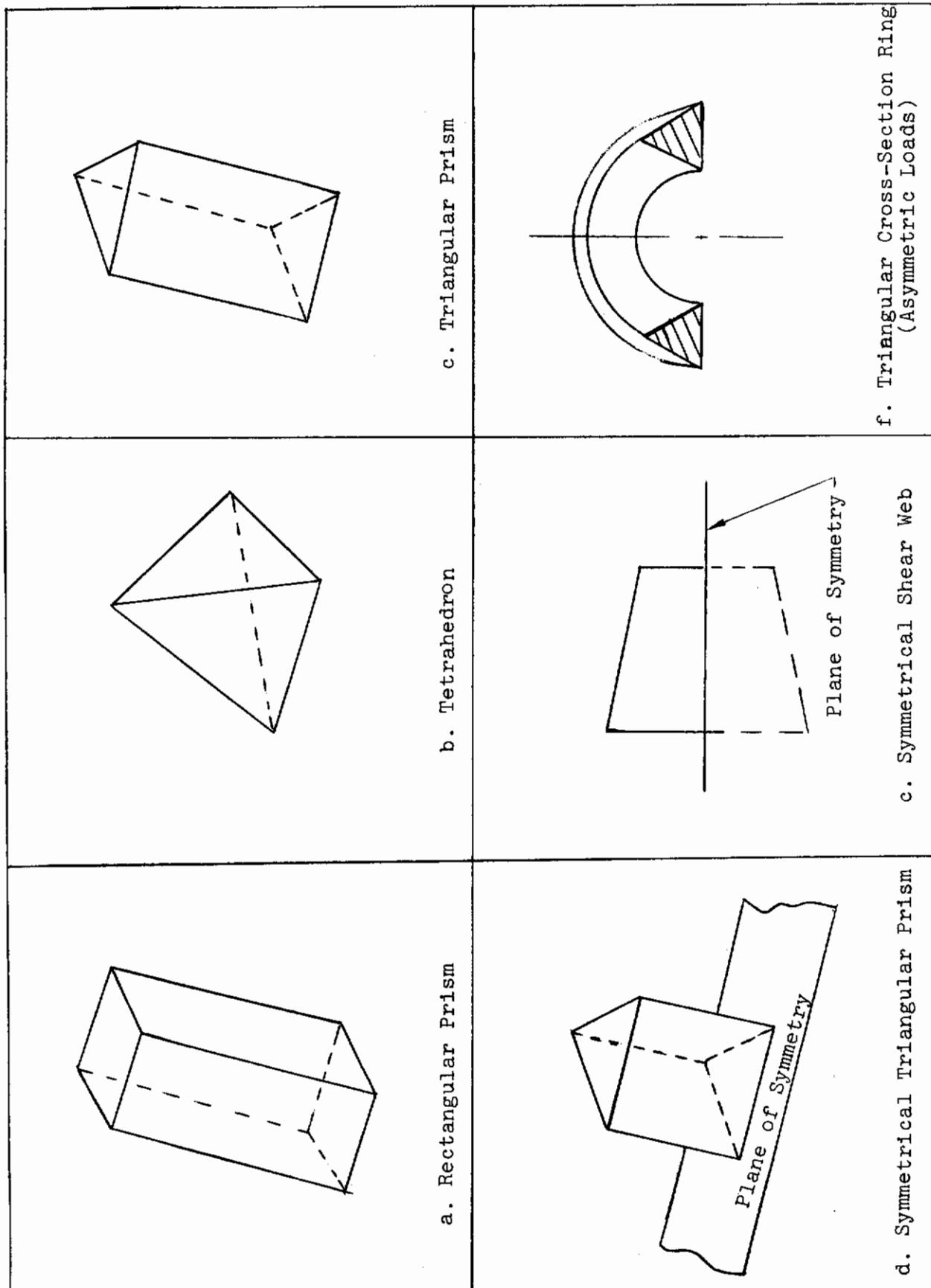
FIGURE I-1   MAGIC III ADDITIONAL FINITE ELEMENTS

3

g. Trapezoidal Cross-Section Ring (Core) Element

h. Quadrilateral Plate Element

i. Triangular Plate Element

j. Incremental Frame Element
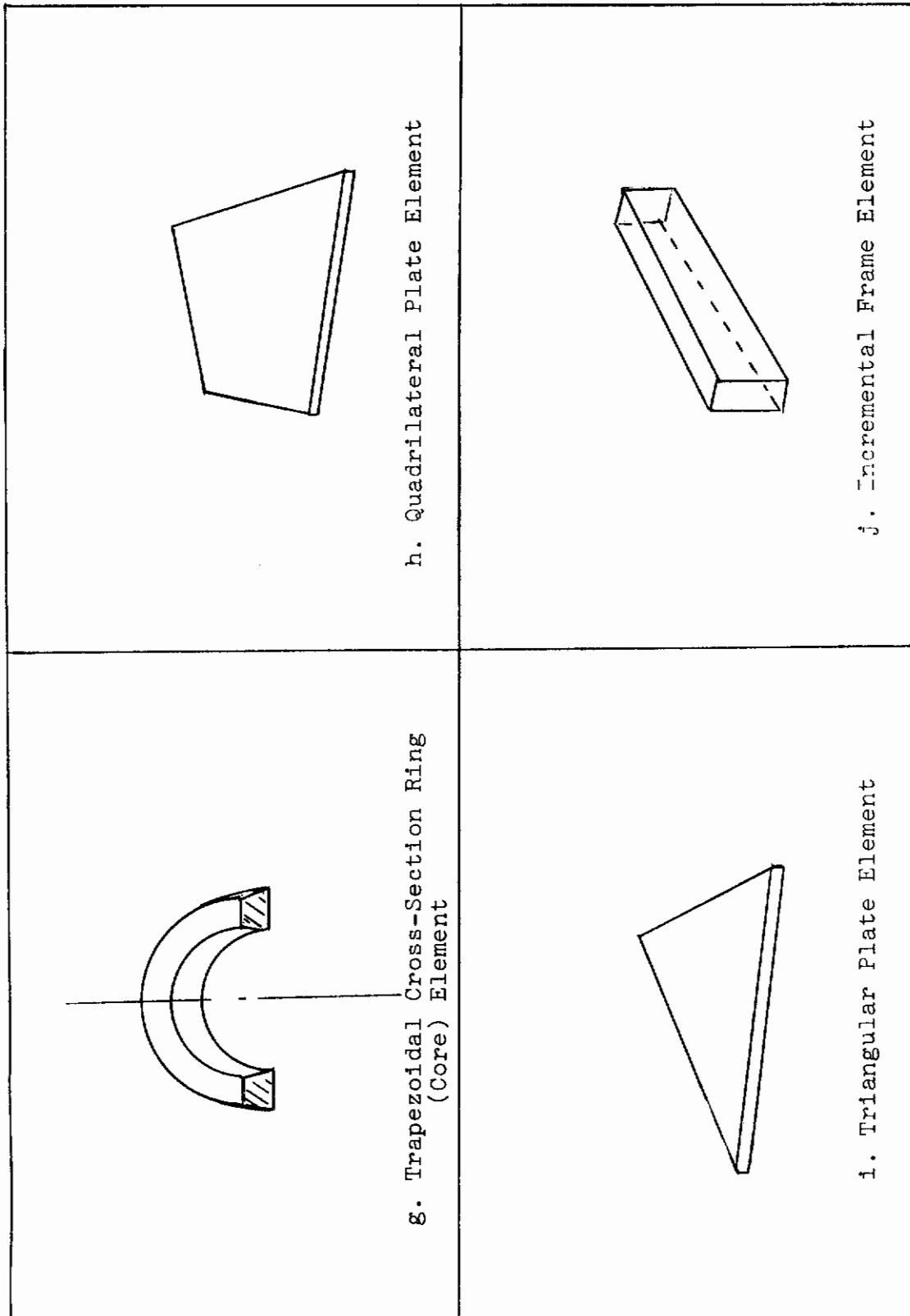
FIGURE I-2   MAGIC II ADDITIONAL FINITE ELEMENTS

4
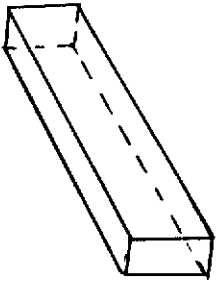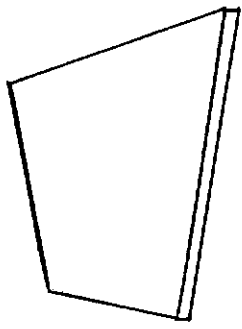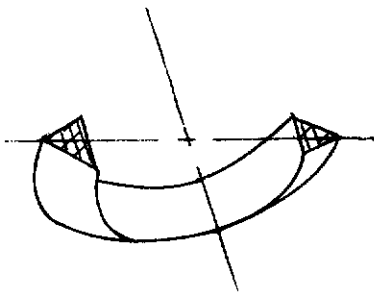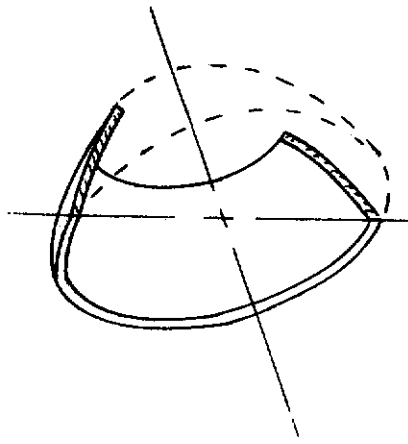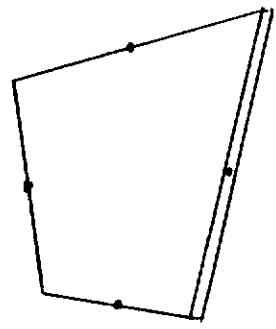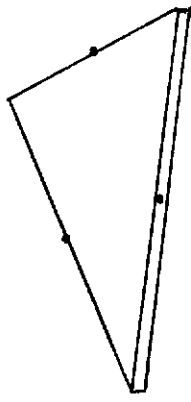
k. Frame and Axial Force Element

l. Quadrilateral Shear Panel Element

m. Triangular Cross-Section Ring Element

n. Toroidal Thin Shell Ring Element

o. Mallett Quadrilateral Thin Shell Element (Mid-Side Nodes)

p. Helle Triangular Thin Shell Element (Mid-Side Nodes)

FIGURE I-3   MAGIC FINITE ELEMENTS

5

SECTION II

ADDITIONAL FINITE ELEMENTS

A.   INTRODUCTION

The MAGIC III System incorporates seventeen finite elements. Ten of these elements; namely frame, shear panel, triangular cross-section ring, toroidal thin shell ring, quadrilateral thin shell, triangular thin shell, trapezoidal cross-section ring, quadrilateral plate, triangular plate and incremental frame were available in the initial MAGIC and MAGIC II Systems and are described in detail in References 1 and 4.

Seven additional elements; namely rectangular prism, tetrahedron, triangular prism, symmetric triangular prism, symmetric shear web, triangular cross-section ring and a revised quadrilateral thin shell element have been incorporated into the MAGIC III System. Characteristic matrices have been derived for these elements and include stiffness, stress, prestrain load, pressure load, thermal load, and consistent mass matrices. The derivation of these matrices for each finite element is presented in the following sections.

B.   RECTANGULAR PRISM ELEMENT

I.   Introduction

The formulation of an element stiffness matrix for the rectangular prism discrete element was first documented in Reference 9, and the approach used here is one of three suggested therein.

The rectangular prism element is a powerful tool for the analysis of solid structures, thick plates, and beams. It can be used in conjunction with the triangular prism and tetrahedral discrete elements for the analysis of arbitrary solid geometries, or with plate elements for the analysis of built-up regions.

An appropriate mathematical model for the rectangular prism discrete element is formulated on the basis of the variational principles of continuum mechanics. From an admissible assumed displacement function only, algebraic expressions for various element matrices which describe the mathematical behavior of the element are derived by use of the Lagrange variational equation.

Consistent with the state of the art, the discrete element representation for the subject element is taken to consist of algebraic expressions for the following matrices:

a. Stiffness $[K]$

b. Stress $[S]$

c. Prestrain Load $\{F_\epsilon\}$

d. Thermal Load $\{F_T\}$

e. Consistent Mass $[M]$

f. Pressure Load $\{F_p\}$

These matrices arise as coefficient matrices in the generalized form of the Lagrange equations. The form of these equations, necessary for the complete element representation listed above, are:

$$\frac{\partial \Phi_p}{\partial q_r} + \frac{d}{dt}\left(\frac{\partial \Phi_\kappa}{\partial \dot{q}_r}\right) = 0 \qquad (1)$$

where:

$q_r \sim r^{th}$ generalized displacement

$\dot{q}_r \sim r^{th}$ generalized velocity

$\Phi_p \sim$ total potential energy

$\Phi_k \sim$ total kinetic energy

II.   Geometry

Figure II-1 depicts the geometry of the rectangular prism element. Also shown are the local and global axes systems; namely, local x, y, z and global X, Y, Z. The local axes are fixed at the centroid of the element. Use of vector analysis permits definition of the dimensions of the prism to be:

$$a = 1/2 \ |\bar{r}_x| \tag{2}$$

$$b = 1/2 \ |\bar{r}_y| \tag{3}$$

$$c = 1/2 \ |\bar{r}_z| \tag{4}$$

Where:

$$|\bar{r}_x| = |\bar{r}_4 - \bar{r}_8| = \left[(X_4 - X_8)^2 + (Y_4 - Y_8)^2 + (Z_4 - Z_8)^2 \right]^{1/2} \tag{5}$$

$$|\bar{r}_y| = |\bar{r}_7 - \bar{r}_8| = \left[(X_7 - X_8)^2 + (Y_7 - Y_8)^2 + (Z_7 - Z_8)^2 \right]^{1/2} \tag{6}$$

$$|\bar{r}_z| = |\bar{r}_5 - \bar{r}_8| = \left[(X_5 - X_8)^2 + (Y_5 - Y_8)^2 + (Z_5 - Z_8)^2 \right]^{1/2} \tag{7}$$

The quantities $\bar{r}_4$, $\bar{r}_5$, $\bar{r}_7$, and $\bar{r}_8$ are vectors emanating from the origin of the global axes to prism grid points 4, 5, 7 and 8. The vectors $\bar{r}_x$, $\bar{r}_y$, $\bar{r}_z$ form a mutually orthogonal set (see Figure II-1).

A rotational and translational transformation matrix from local to global coordinates is formed using these vectors. This transformation is given below.

8
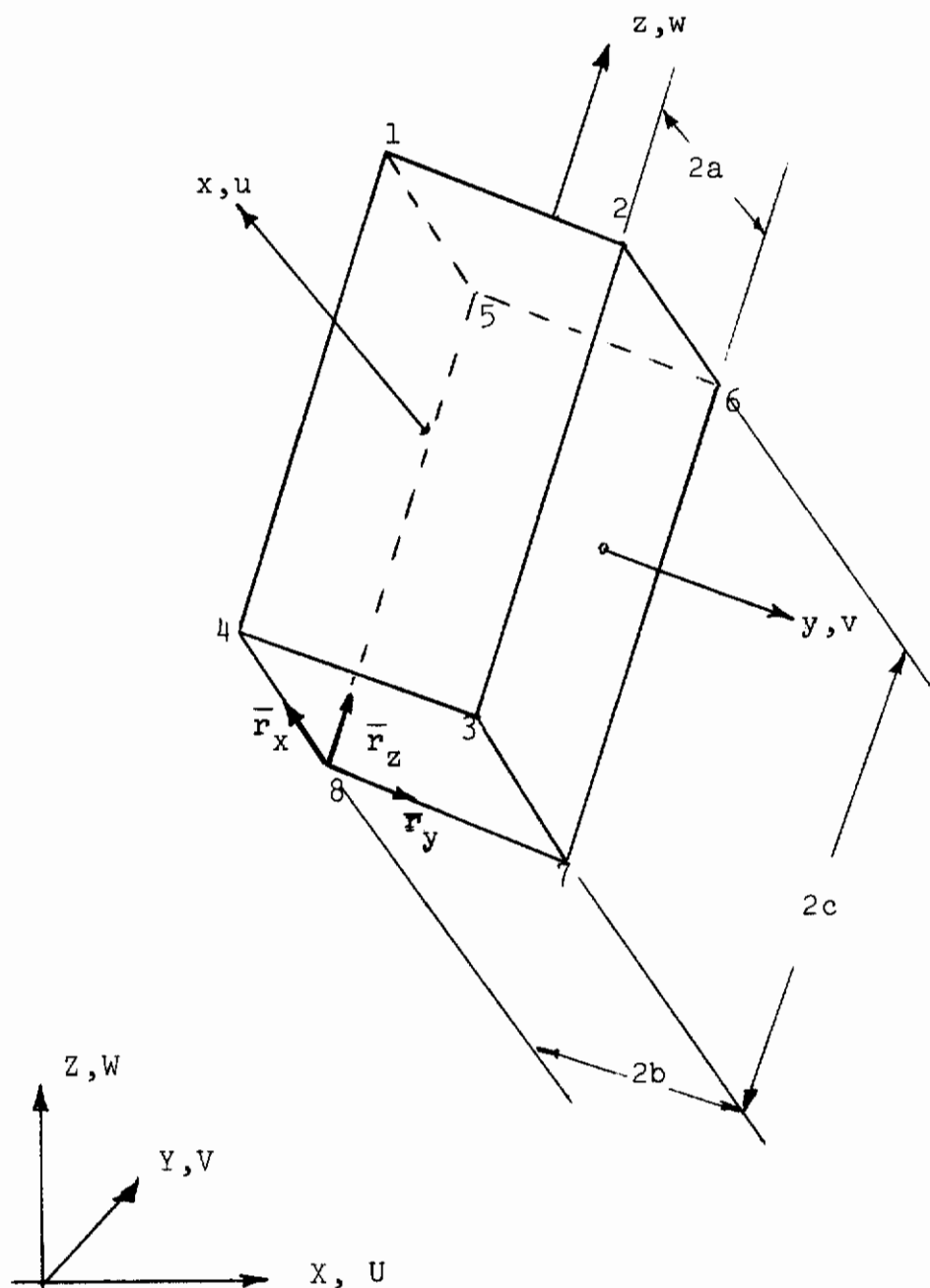
FIGURE II-1   RECTANGULAR PRISM GEOMETRY

9

$$\{x^{(\ell)}\} = [\tilde{T}_{g\ell}]\{\{X^{(g)}\} - \{X_c\}^{(g)}\}\} \tag{8}$$

where:

$$\{x^{(\ell)}\}^T = \lfloor x^{(\ell)}, \ y^{(\ell)}, \ z^{(\ell)} \rfloor \text{ are the local coordinates}$$

$$\{X^{(g)}\}^T = \lfloor X^{(g)}, \ Y^{(g)}, \ Z^{(g)} \rfloor \text{ are the global coordinates}$$

$$\{X_c^{(g)}\}^T = \lfloor X_c^{(g)}, \ Y_c^{(g)}, \ Z_c^{(g)} \rfloor \text{ are the centroidal global coordinates}$$

$$[\tilde{T}_{g\ell}] = \begin{bmatrix} e_{x_1}, & e_{x_2}, & e_{x_3} \\ & & \\ e_{y_1}, & e_{y_2}, & e_{y_3} \\ & & \\ e_{z_1}, & e_{z_2}, & e_{z_3} \end{bmatrix} \quad \begin{array}{l} \text{is the matrix of} \\ \text{direction cosines} \end{array}$$

$$e_{x_1} = \frac{1}{2a}(X_4 - X_8), \ e_{x_2} = \frac{1}{2a}(Y_4 - Y_8), \ e_{x_3} = \frac{1}{2a}(Z_4 - Z_8)$$

$$e_{y_1} = \frac{1}{2b}(X_7 - X_8), \ e_{y_2} = \frac{1}{2b}(Y_7 - Y_8), \ e_{y_3} = \frac{1}{2b}(Z_7 - Z_8)$$

$$e_{z_1} = \frac{1}{2c}(X_5 - X_8), \ e_{z_2} = \frac{1}{2c}(Y_5 - Y_8), \ e_{z_3} = \frac{1}{2c}(Z_5 - Z_8)$$

The transformation matrix $[\tilde{T}_{g\ell}]$ is used not only for coordinate transformations but deformation transformations also.

III. Assumed Displacement Functions

A structural element is mathematically discretized into a finite number of displacement degrees of freedom by the assumption of displacement mode shapes. For the simple geometry of the rectangular prism element, trilinear Lagrangian interpolation formulas are constructed. The displacement is given by

$$\delta^{(j)}(x,y,z) = 1/8abc \; [-f_1\bar{f}_2 f_3 \delta_1^{(j)} + f_1 f_2 f_3 \delta_2^{(j)} - f_1 f_2 \bar{f}_3 \delta_3^{(j)}$$

$$+ f_1 \bar{f}_2 \bar{f}_3 \; \delta_4^{(j)} + \bar{f}_1 \bar{f}_2 f_3 \delta_5^{(j)}$$

$$-\bar{f}_1 f_2 f_3 \delta_6^{(j)} + \bar{f}_1 f_2 \bar{f}_3 \delta_7^{(j)} - \bar{f}_1 \bar{f}_2 \bar{f}_3 \delta_8^{(j)}] \qquad (9)$$

where

$$f_1 = (x+a) \qquad f_2 = (y+b) \qquad f_3 = (z+c)$$

$$\bar{f}_1 = (x-a) \qquad \bar{f}_2 = (y-b) \qquad \bar{f}_3 = (z-c) \qquad (10)$$

and a, b, and c are the half-dimensions of the prism as shown in Figure II-1.

Note that $\delta_k^{(j)}$, k = 1, 2, ... 8 are the grid point displacements where j = 1, 2, 3 corresponds to the u, v, and w displacements.

Equation (9) can be written in matrix form as

$$\delta^{(j)} = \lfloor \tilde{B} \rfloor \; \{\delta_k^{(j)}\} \div 8 \; abc \qquad (11)$$

where

$$\{\tilde{B}\}^T = \lfloor -f_1\bar{f}_2 f_3, \; f_1 f_2 f_3, \; -f_1 f_2 \bar{f}_3, \; f_1 \bar{f}_2 \bar{f}_3, \bar{f}_1 \bar{f}_2 f_3, \; -\bar{f}_1 f_2 f_3,$$

$$\bar{f}_1 f_2 \bar{f}_3, \; -\bar{f}_1 \bar{f}_2 \bar{f}_3 \rfloor \qquad (12)$$

and

$$\{\delta_k^{(j)}\}^T = \lfloor \delta_1^{(j)}, \; \delta_2^{(j)}, \delta_3^{(j)}, \delta_4^{(j)}, \delta_5^{(j)}, \delta_6^{(j)}, \delta_7^{(j)}, \delta_8^{(j)} \rfloor$$

$$(13)$$

11

It is instructive to examine the nature of these assumed displacement functions by considering the allowable deformation of each face of the prism. For example, the displacement of the planes $x = a$, $y = b$, and $z = c$ can be written for $x = a$

$$\delta^{(j)}(a,y,z) = (k_1 yz + k_2' y + k_3 z + k_4'')(-\delta_1^{(j)} + \delta_2^{(j)} - \delta_3^{(j)} + \delta_4^{(j)}) \tag{14}$$

for $y = b$

$$\delta^{(j)}(x,b,z) = (k_1 xz + k_2 x + k_3 z + k_4)(\delta_2^{(j)} - \delta_3^{(j)} - \delta_6^{(j)} + \delta_7^{(j)}) \tag{15}$$

for $z = c$

$$\delta^{(j)}(x,y,c) = (k_1 xy + k_2 x + k_3 y + k_4)(-\delta_1^{(j)} + \delta_2^{(j)} + \delta_5^{(j)} - \delta_6^{(j)}) \tag{16}$$

and similarly for $x = -a$, $y = -b$, $z = -c$. It is noted that the k_1 are arbitrary constants. Referring to Figure II-1, it is seen that the displacements on these planes are functions only of the displacements of the gridpoints defining the planes. Hence, the assumed functions are admissible in that they satisfy the requirements of displacement continuity along interelement boundaries. Due to the assumption of linear interpolation formulas, the edges of the prism remain linear in deformation. A direct consequence of the above observations is that although a single element maywarp under a force-couple, it may not bend under any conditions.

The foregoing assumed displacement functions lead to three translational displacement degrees of freedom at each of the eight corner gridpoints; thus the complete element deformation is described by twenty-four displacement degrees of freedom.

The definition of assumed displacement functions permits the derivation of the strain-displacement relationships. The element strain components are expressed as functions of the assumed displacement modes by

$$\varepsilon_x = \delta^{(1)}_{,x} = \frac{\partial \delta^{(1)}}{\partial x} \tag{17}$$

$$\varepsilon_y = \delta^{(2)}_{,y} = \frac{\partial \delta^{(2)}}{\partial y} \tag{18}$$

$$\varepsilon_z = \delta^{(3)}_{,z} = \frac{\partial \delta^{(3)}}{\partial z} \tag{19}$$

$$\varepsilon_{xy} = \delta^{(1)}_{,y} + \delta^{(2)}_{,x} = \frac{\partial \delta^{(1)}}{\partial y} + \frac{\partial \delta^{(2)}}{\partial x} \tag{20}$$

$$\varepsilon_{yz} = \delta^{(2)}_{,z} + \delta^{(3)}_{,y} = \frac{\partial \delta^{(2)}}{\partial z} + \frac{\partial \delta^{(3)}}{\partial y} \tag{21}$$

$$\varepsilon_{zx} = \delta^{(1)}_{,z} + \delta^{(3)}_{,x} = \frac{\partial \delta^{(1)}}{\partial z} + \frac{\partial \delta^{(3)}}{\partial x} \tag{22}$$

Performing the necessary differentiations on the displacement functions yields:

$$\delta^{(j)}_{,x} = \frac{1}{8\,abc} \lfloor D_x \rfloor \{\delta^{(j)}_k\} \tag{23}$$

$$\delta^{(j)}_{,y} = \frac{1}{8\,abc} \lfloor D_y \rfloor \{\delta^{(j)}_k\} \tag{24}$$

$$\delta^{(j)}_{,z} = \frac{1}{8\,abc} \lfloor D_z \rfloor \{\delta^{(j)}_k\} \tag{25}$$

13

where

$$\{D_x\}^T = \lfloor -\bar{f}_2 f_3, \ f_2 f_3, \ -f_2 \bar{f}_3, \ \bar{f}_2 \bar{f}_3, \ \bar{f}_2 f_3, \ -f_2 f_3 \qquad (26)$$

$$f_2 \bar{f}_3, \ -\bar{f}_2 \bar{f}_3 \rfloor$$

$$\{D_y\}^T = \lfloor -f_1 f_3, \ f_1 f_3, \ -f_1 \bar{f}_3, \ f_1 \bar{f}_3, \ \bar{f}_1 \bar{f}_3, \ -\bar{f}_1 f_3,$$

$$\bar{f}_1 \bar{f}_3, \ -\bar{f}_1 \bar{f}_3 \rfloor \qquad (27)$$

$$\{D_z\}^T = \lfloor -f_1 \bar{f}_2, \ f_1 f_2, \ -f_1 f_2, \ f_1 \bar{f}_2, \ \ \bar{f}_1 \bar{f}_2, - \ \bar{f}_1 f_2$$

$$\bar{f}_1 f_2, \ -\bar{f}_1 \bar{f}_2 \rfloor \qquad (28)$$

and

$$\{\delta_k^{(j)}\}^T = \lfloor \delta_1^{(j)}, \ \delta_2^{(j)}, \ \delta_3^{(j)}, \ \delta_4^{(j)}, \ \delta_5^{(j)},$$

$$\delta_6^{(j)}, \ \delta_7^{(j)}, \ \delta_8^{(j)} \rfloor \ . \qquad (29)$$

These equations are assembled into a single matrix expression relating the strain components to the displacement degrees of freedom,

$$\{\epsilon\} = \frac{1}{8 \ abc} \ [D] \ \{\delta^{(j)}\} \qquad (30)$$

where

$$\{\epsilon\}^T = \lfloor \epsilon_x, \ \epsilon_y, \ \epsilon_z, \ \epsilon_{xy}, \ \epsilon_{yz}, \ \epsilon_{zx} \rfloor \qquad (31)$$

$$\{\delta^{(j)}\}^T = \lfloor \delta_k^{(1)}, \ \delta_k^{(2)}, \ \delta_k^{(3)} \rfloor \qquad (32)$$

14

and

$$[D] = \begin{bmatrix} \lfloor D_x \rfloor & 0 & 0 \\ 0 & \lfloor D_y \rfloor & 0 \\ 0 & 0 & \lfloor D_z \rfloor \\ \lfloor D_y \rfloor & \lfloor D_x \rfloor & 0 \\ 0 & \lfloor D_z \rfloor & \lfloor D_y \rfloor \\ \lfloor D_z \rfloor & 0 & \lfloor D_x \rfloor \end{bmatrix}$$

(33)

15

IV.   <u>Potential Energy</u>

The potential energy of the element is

$$\Phi_p = U - W \tag{34}$$

where

$$U = \int_V \int_{\{0\}}^{\{\varepsilon\}} \lfloor d\varepsilon \rfloor \{\sigma\} \, dV \tag{35}$$

$$W \text{ are external work contributions} \tag{36}$$

$$\{\varepsilon\}^T = \lfloor \varepsilon_x, \; \varepsilon_y, \; \varepsilon_z, \; \varepsilon_{xy}, \; \varepsilon_{yz}, \; \varepsilon_{zx} \rfloor \tag{37}$$

$$\{\sigma\}^T = \lfloor \sigma_x, \; \sigma_y, \; \sigma_z, \; \sigma_{xy}, \; \sigma_{yz}, \; \sigma_{zx} \rfloor . \tag{38}$$

Linear elastic materials behaviour is assumed from an initial state of strain $\{\bar{\varepsilon}\}$ to a final state of stress $\{\sigma\}$ and strain $\{\varepsilon\}$. From the generalized Hooke's Law,

$$\{\sigma\} = [E]\Big\{\{\varepsilon\} - \{\bar{\varepsilon}\}\Big\} \tag{39}$$

where [E] is the symmetric matrix of elastic constants which, for three-dimensional orthotropic material, can be written

$$[E] = 1/\Delta \begin{bmatrix} E_x(1-\nu_{yz}\nu_{zy}), & E_x(\nu_{yx} + \nu_{zx}\nu_{yz}), & E_x(\nu_{zx}+\nu_{yx}\nu_{zy}) \\ & E_y(1-\nu_{zx}\nu_{xz}), & E_y(\nu_{zy} + \nu_{xy}\nu_{zx}) \; 0, \; 0, \; 0 \\ & & E_z(1-\nu_{xy}\nu_{yx}) \quad\quad 0, \; 0, \; 0 \\ & & \quad\quad\quad\quad , \Delta G_{xy}, \; 0, \; 0 \\ \text{-Symmetric-} & & \quad\quad\quad\quad\quad , \Delta G_{yz}, \; 0 \\ & & \quad\quad\quad\quad\quad\quad , \Delta G_{zx} \end{bmatrix} \tag{40}$$

16

where

$$\Delta = 1 - \nu_{xy}\nu_{yx} - \nu_{yz}\nu_{zy} - \nu_{zx}\nu_{xz} - \nu_{xy}\nu_{yz}\nu_{zx} - \nu_{xz}\nu_{yx}\nu_{zy} \qquad (41)$$

and ν_{ij} is defined as the resulting strain in the jth direction due to a stress in the ith direction. [E] can be expressed in more concise form as

$$[E] = \begin{bmatrix} E_{11} & E_{12} & E_{13} & 0 & 0 & 0 \\ & E_{22} & E_{23} & 0 & 0 & 0 \\ & & E_{33} & 0 & 0 & 0 \\ & & & E_{44} & 0 & 0 \\ & & & & E_{55} & 0 \\ \text{Symmetric} & & & & & E_{66} \end{bmatrix} \qquad (42)$$

Substitution of Equation (39) into the strain energy function and integrating yields

$$U = \int_V (1/2 \lfloor \epsilon \rfloor [E] \{\epsilon\} - \lfloor \epsilon \rfloor [E] \{\bar{\epsilon}\}) dV . \qquad (43)$$

This is the desired form of potential energy Φ_p.

17

V. Element Static Matrices

5.1 Introduction

To effect the discretization of the element the assumed displacement functions are introduced into the potential energy function which in turn is substituted into the Lagrange equations to yield element matrices with respect to grid point displacement degrees of freedom. An exception is the element stress matrix which is derived from strain-displacement and stress-strain relationships.

5.2 Stiffness Matrix

The energy contribution to the linear elastic stiffness is given by

$$\Phi_p = 1/2 \int_V \lfloor \varepsilon \rfloor [E] \{\varepsilon\} \, dV . \tag{44}$$

Recalling the strain-displacement relations

$$\{\varepsilon\} = \frac{1}{8\,abc} [D] \{\delta^{(J)}\} \tag{30}$$

and substituting these into Equation (44) yields

$$\Phi_p = \frac{1}{2} \left(\frac{1}{8abc}\right)^2 \int_V \lfloor \delta^{(J)} \rfloor [D]^T [E] [D] \{\delta^{(J)}\} \, dV . \tag{45}$$

Performing the matrix multiplication, and noting that the grid point displacement degrees of freedom are not functions of the local coordinate system, the potential energy function may be expressed as shown by Equation 46. Taking the first

18

$$\Phi_P = \frac{1}{2}\left(\frac{1}{8\ abc}\right)^2 \int_V \left\lfloor \dot{\delta}^{(J)}\right\rfloor^2
\begin{bmatrix}
E_{11}\{D_x\}\lfloor D_x\rfloor + E_{44}\{D_y\}\lfloor D_y\rfloor + E_{66}\{D_z\}\lfloor D_z\rfloor, \\[4pt]
E_{12}\{D_y\}\lfloor D_x\rfloor + E_{44}\{D_x\}\lfloor D_y\rfloor,\quad E_{22}\{D_y\}\lfloor D_y\rfloor + E_{44}\{D_x\}\lfloor D_x\rfloor + E_{55}\{D_z\}\lfloor D_z\rfloor, \\[4pt]
E_{13}\{D_z\}\lfloor D_x\rfloor + E_{66}\{D_x\}\lfloor D_z\rfloor,\quad E_{23}\{D_z\}\lfloor D_y\rfloor + E_{55}\{D_y\}\lfloor D_z\rfloor,\quad E_{33}\{D_z\}\lfloor D_z\rfloor + E_{55}\{D_y\}\lfloor D_y\rfloor + E_{66}\{D_x\}\lfloor D_x\rfloor
\end{bmatrix}
dV\{\delta^{(J)}\}$$

$$\tag{46}$$

or

$$\Phi_P = \frac{1}{2}\left(\frac{1}{8\ abc}\right)^2 \lfloor \delta^{(J)}\rfloor\ \tilde{[K]}\ \{\delta^{(J)}\}$$

where:

$$[\tilde{K}] = \left(\frac{1}{8\ abc}\right)^2
\begin{bmatrix}
E_{11}[I_{xx}] + E_{44}[I_{yy}] + E_{66}[I_{zz}], & & \text{Symmetric} \\[4pt]
E_{12}[I_{xy}]^T + E_{44}[I_{xy}], & E_{22}[I_{yy}] + E_{44}[I_{xx}] + E_{55}[I_{zz}], & \\[4pt]
E_{13}[I_{zx}]^T, & E_{23}[I_{yz}]^T + E_{55}[I_{yz}], & E_{33}[I_{zz}] + E_{55}[I_{yy}] + E_{66}[I_{xx}]
\end{bmatrix}$$

$$\tag{47}$$

19

$$[I_{xx}] = \int_V \{D_x\} \lfloor D_x \rfloor \, dV$$

$$[I_{yy}] = \int_V \{D_y\} \lfloor D_y \rfloor \, dV$$

$$[I_{zz}] = \int_V \{D_z\} \lfloor D_z \rfloor \, dV$$

$$[I_{xy}] = \int_V \{D_x\} \lfloor D_y \rfloor \, dV$$

$$[I_{yz}] = \int_V \{D_y\} \lfloor D_z \rfloor \, dV$$

$$[I_{zx}] = \int_V \{D_z\} \lfloor D_x \rfloor \, dV$$

(48)

20

variation of the potential energy function with respect to
displacement degrees of freedom (as shown by the first term
of Equation (1)), yields the element stiffness matrix $[\tilde{K}]$
referenced to local grid point displacements. This matrix
is depicted in Equation (47).

The matrix products appearing as integrands in
Equation (48) lead to integrations of the following general
form,

$$I_{ij} = \int_{-a}^{a}\int_{-b}^{b}\int_{-c}^{c} (x+a)^m (x-a)^n (y+b)^p (y-b)^q (z+c)^r (z-c)^s \, dz \, dy \, dx$$

(49)

Since the limits of integration are constants, Equation
(49) can be written equivalently as

$$I_{ij} = \left[\int_{-a}^{a} (x+a)^m (x-a)^n \, dx\right]\left[\int_{-b}^{b} (y+b)^p (y-b)^q \, dy\right]$$

$$\left[\int_{-c}^{c} (z+c)^r (z-c)^s \, dz\right]$$

(50)

These definite integrals are readily evaluated by integra-
tion by parts and the $[I_{ij}]$ matrices are expressed in
Equations (51) - (56).

21

$$\frac{32}{9}\, a\, b^3 c^3 \begin{bmatrix} 4 & & & & & & & \\ 2 & 4 & & & & & & \\ 1 & 2 & 4 & & \text{-SYM.-} & & & \\ 2 & 1 & 2 & 4 & & & & \\ -4 & -2 & -1 & -2 & 4 & & & \\ -2 & -4 & -2 & -1 & 2 & 4 & & \\ -1 & -2 & -4 & -2 & 1 & 2 & 4 & \\ -2 & -1 & -2 & -4 & 2 & 1 & 2 & 4 \end{bmatrix} = [I_{xx}] \tag{51}$$

$$\frac{32}{9}\, a^3 b c^3 \begin{bmatrix} 4 & & & & & & & \\ -4 & 4 & & & & & & \\ -2 & 2 & 4 & & \text{-SYM.-} & & & \\ 2 & -2 & -4 & 4 & & & & \\ 2 & -2 & -1 & 1 & 4 & & & \\ -2 & 2 & 1 & -1 & -4 & 4 & & \\ -1 & 1 & 2 & -2 & -2 & 2 & 4 & \\ 1 & -1 & -2 & 2 & 2 & -2 & -4 & 4 \end{bmatrix} = [I_{yy}] \tag{52}$$

$$\frac{32}{9}\, a^3 b^3 c \begin{bmatrix} 4 & & & & & & & \\ 2 & 4 & & & & & & \\ -2 & -4 & 4 & & \text{-SYM.-} & & & \\ -4 & 2 & 2 & 4 & & & & \\ +2 & -1 & -1 & -2 & 4 & & & \\ 1 & +2 & 2 & -1 & 2 & 4 & & \\ -1 & -2 & 2 & 1 & -2 & -4 & 4 & \\ -2 & -1 & -1 & 2 & -4 & -2 & 2 & 4 \end{bmatrix} = [I_{zz}] \tag{53}$$

$$\frac{16}{3} a^2 b^2 c^3 \begin{bmatrix} -2 & 2 & 1 & -1 & -2 & 2 & 1 & -1 \\ -2 & 2 & 1 & -1 & -2 & 2 & 1 & -1 \\ -1 & 1 & 2 & -2 & -1 & 1 & 2 & -2 \\ -1 & 1 & 2 & -2 & -1 & 1 & 2 & -2 \\ 2 & -2 & -1 & 1 & 2 & -2 & -1 & 1 \\ 2 & -2 & -1 & 1 & 2 & -2 & -1 & 1 \\ 1 & -1 & -2 & 2 & 1 & -1 & -2 & 2 \\ 1 & -1 & -2 & 2 & 1 & -1 & -2 & 2 \end{bmatrix} = [I_{xy}] \tag{54}$$

$$\frac{16}{3} a^3 b^2 c^2 \begin{bmatrix} -2 & -2 & 2 & 2 & -1 & -1 & 1 & 1 \\ 2 & 2 & -2 & -2 & 1 & 1 & -1 & -1 \\ 2 & 2 & -2 & -2 & 1 & 1 & -1 & -1 \\ -2 & -2 & 2 & 2 & -1 & -1 & 1 & 1 \\ -1 & -1 & 1 & 1 & -2 & -2 & 2 & 2 \\ 1 & 1 & -1 & -1 & 2 & 2 & -2 & -2 \\ 1 & 1 & -1 & -1 & 2 & 2 & -2 & -2 \\ -1 & -1 & 1 & 1 & -2 & -2 & 2 & 2 \end{bmatrix} = [I_{yz}] \tag{55}$$

$$\frac{16}{3} a^2 b^3 c^2 \begin{bmatrix} 2 & 1 & 1 & 2 & -2 & -1 & -1 & -2 \\ 1 & 2 & 2 & 1 & -1 & -2 & -2 & -1 \\ -1 & -2 & -2 & -1 & 1 & 2 & 2 & 1 \\ -2 & -1 & -1 & -2 & 2 & 1 & 1 & 2 \\ 2 & 1 & 1 & 2 & -2 & -1 & -1 & -2 \\ 1 & 2 & 2 & 1 & -1 & -2 & -2 & -1 \\ -1 & -2 & -2 & -1 & 1 & 2 & 2 & 1 \\ -2 & -1 & -1 & -2 & 2 & 1 & 1 & 2 \end{bmatrix} = [I_{zx}] \tag{56}$$

The potential energy function given by
Equation (46) is referenced to local gridpoint displacements.
These displacements must first be reordered to be compatible
with the MAGIC III ordering system and then be transformed to
global displacements. The former is accomplished through use of
the transformation given below:

$$\{\delta^{(j)}\} = [T] \{\bar{\delta}^{(j)}\} \qquad (57)$$

where

$$\{\bar{\delta}^{(j)}\}^T = \lfloor \delta_1{}^{(1)}, \delta_2{}^{(2)}, \delta_1{}^{(3)}, \delta_2{}^{(1)}, \delta_2{}^{(2)}, \delta_2{}^{(3)} \cdots$$

$$\delta_8{}^{(1)}, \delta_8{}^{(2)}, \delta_8{}^{(3)} \rfloor$$

$$[T] = \begin{bmatrix}
1 & & & & & & & & & & & & & & & & & & & & & & & \\
& 1 & & & & & & & & & & & & & & & & & & & & & & \\
& & 1 & & & & & & & & & & & & & & & & & & & & & \\
& & & 1 & & & & & & & & & & & & & & & & & & & & \\
& & & & 1 & & & & & & & & & & & & & & & & & & & \\
& & & & & 1 & & & & & & & & & & & & & & & & & & \\
& & & & & & 1 & & & & & & & & & & & & & & & & & \\
& & & & & & & 1 & & & & & & & & & & & & & & & & \\
1 & & & & & & & & & & & & & & & & & & & & & & & \\
& 1 & & & & & & & & & & & & & & & & & & & & & & \\
& & 1 & & & & & & & & & & & & & & & & & & & & & \\
& & & 1 & & & & & & & & & & & & & & & & & & & & \\
& & & & 1 & & & & & & & & & & & & & & & & & & & \\
& & & & & 1 & & & & & & & & & & & & & & & & & & \\
& & & & & & 1 & & & & & & & & & & & & & & & & & \\
& & & & & & & 1 & & & & & & & & & & & & & & & & \\
1 & & & & & & & & & & & & & & & & & & & & & & & \\
& 1 & & & & & & & & & & & & & & & & & & & & & & \\
& & 1 & & & & & & & & & & & & & & & & & & & & & \\
& & & 1 & & & & & & & & & & & & & & & & & & & & \\
& & & & 1 & & & & & & & & & & & & & & & & & & & \\
& & & & & 1 & & & & & & & & & & & & & & & & & & \\
& & & & & & 1 & & & & & & & & & & & & & & & & & \\
& & & & & & & & & & & & & & & & & & & & & & & 1 \\
\end{bmatrix}$$

The transformation from local to global deformation is derived through the use of Equation (8), thus

$$\{\bar{\delta}^{(j)}\} = [T_{g\ell}] \{\Delta\} \tag{58}$$

where

$$\{\Delta\}^T = \lfloor U_1, V_1, W_1, U_2, V_2, W_2, \ldots, U_8, V_8, W_8 \rfloor.$$

The U, V, W   deformations are defined in Figure II-1. Also,

$$[T_{g\ell}] = \begin{bmatrix} [\tilde{T}_{g\ell}] & & & & & & & \\ & [\tilde{T}_{g\ell}] & & & & & & \\ & & [\tilde{T}_{g\ell}] & & & & & \\ & & & [\tilde{T}_{g\ell}] & & & & \\ & & & & [\tilde{T}_{g\ell}] & & & \\ & & & & & [\tilde{T}_{g\ell}] & & \\ & & & & & & [\tilde{T}_{g\ell}] & \\ & & & & & & & [\tilde{T}_{g\ell}] \end{bmatrix}$$

The $[\tilde{T}_{g\ell}]$ matrix is defined by Equation (8).

25

Use of Equations (57) and (58) in the potential energy equation, Equation (46), yields

$$\Phi_P = \frac{1}{2} \left(\frac{1}{8 \ abc} \right)^2 \lfloor \Delta \rfloor [T_{g\ell}]^T [T]^T [\tilde{K}] [T][T_{g\ell}] \{\Delta\}. \tag{59}$$

Taking the first variation of the potential energy with respect to the displacement degrees of freedom $\{\Delta\}$ (as shown by the first term in Equation (1))yields the element stiffness matrix [K]referenced to global gridpoint displacements. This matrix is depicted by Equation (60).

$$[K] = \left(\frac{1}{8 \ abc} \right)^2 [T_{g\ell}]^T [T]^T [\tilde{K}] [T] [T_{g\ell}] . \tag{60}$$

5.3 Stress Matrices

The element stress matrix follows as a direct consequence of the strain-displacement and stress-strain relationships. Recalling that

$$\{\sigma\} = [E]\left\{\{\epsilon\} - \{\bar{\epsilon}\}\right\} \tag{39}$$

where $\{\bar{\epsilon}\}$ is a column of either mechanical prestrain or thermal prestrain or both. Also recalling that

$$\{\epsilon\} = \left(\frac{1}{8 \ abc} \right) [D] \{\delta^{(J)}\} \tag{30}$$

it follows that

$$\{\sigma\} = \left(\frac{1}{8 \ abc} \right) [E] [D] \{\delta^{(J)}\} - [E] \{\bar{\epsilon}\} - [E]\{\epsilon^{\alpha}\} . \tag{61}$$

Use of Equations (57) and (58) in Equation (61) yields:

$$\{\sigma\} = \left(\frac{1}{8 \ abc} \right) [E] [D] [T] [T_{g\ell}] \{\Delta\} - [E] \{\bar{\epsilon}\} -[E]\{\vec{\epsilon}^{\alpha}\} \tag{62}$$

26

The distribution of prestrain throughout the element is assumed to be of the same functional form as the displacement mode shapes; i.e., an interpolation between grid point prestrain components. Thus,

$$\bar{\varepsilon}^{(j)} = (\frac{1}{8\ abc})\ \lfloor \check{B} \rfloor\ \{\bar{\varepsilon}^{(j)}\}, k = 1,\ 2,\ \ldots,\ 8 \tag{63}$$

with j = 1, 2, ... 6 corresponding to $\bar{\varepsilon}_x$, $\bar{\varepsilon}_y$, $\bar{\varepsilon}_z$, $\bar{\varepsilon}_{xy}$,

$\bar{\varepsilon}_{yz}$, $\bar{\varepsilon}_{zx}$.

The vector $\{\bar{\varepsilon}\}$ now becomes

$$\{\bar{\varepsilon}\} = (\frac{1}{8\ abc})\ [B]\ \{\bar{\varepsilon}^{(j)}\} \tag{64}$$

where

$$[B] = \begin{bmatrix} \lfloor \check{B} \rfloor & & & & & \\ & \lfloor \tilde{B} \rfloor & & & & \\ & & \lfloor \check{B} \rfloor & & & \\ & & & \lfloor \check{B} \rfloor & & \\ & & & & \lfloor \tilde{B} \rfloor & \\ & & & & & \lfloor \tilde{B} \rfloor \end{bmatrix}$$

$$\{\bar{\varepsilon}^{(j)}\}^T = \lfloor \bar{\varepsilon}_x,\ \bar{\varepsilon}_y,\ \bar{\varepsilon}_z,\ \bar{\varepsilon}_{xy},\ \bar{\varepsilon}_{yz},\ \bar{\varepsilon}_{zx} \rfloor$$

$$\{\bar{\varepsilon}^{(j)}\}^T = \lfloor \lfloor \varepsilon_k^{(1)} \rfloor,\ \lfloor \varepsilon_k^{(2)} \rfloor,\ \lfloor \varepsilon_k^{(3)} \rfloor,\ \lfloor \varepsilon_k^{(4)} \rfloor,\ \lfloor \varepsilon_k^{(5)} \rfloor,\ \lfloor \varepsilon_k^{(6)} \rfloor \rfloor\ .$$

27

The vector $\{\bar{\varepsilon}^\alpha\}$, the prestrain due to thermal effects, can be written as

$$\{\bar{\varepsilon}^\alpha\} = (\frac{1}{8 \, abc}) \, [B] \, [\tilde{\alpha}] \, \{\Delta T_k\} \tag{65}$$

where

$$[\tilde{\alpha}] = \begin{bmatrix} \alpha_x & [I] \\ \\ \alpha_y & [I] \\ \\ \alpha_z & [I] \end{bmatrix}$$

[I] is an (8 x 8) identity matrix and α_x, α_y, α_z are coefficients of thermal expansion,

$$\{\Delta T_k\}^T = \lfloor T_k - T_o \rfloor, \quad k = 1, 2, 3 \, .., \, 8$$

T_k is the temperature at the kth grid point and T_o is the element reference temperature.

Equation (62) can now be rewritten as follows:

$$\{\sigma\} = [S] \, \{\Delta\} - \{s\} - \{\overset{\shortmid}{s}\} \tag{66}$$

Each term in Equation (66) has a particular significance. The matrix

$$[S] = (\frac{1}{8 \, abc}) \, [E] \, [D] \, [T] \, [T_{g\ell}] \tag{67}$$

yields the element apparent stresses due to displacements of the element and is referred to as the element stress matrix. The matrix

$$\{s\} = (\frac{1}{8 \, abc}) \, [E] \, [B] \, \{\tilde{\varepsilon}_\kappa^{(J)}\} \tag{68}$$

yields stresses due to the prestrain state within the element
and is referred to as the element stress matrix due to pre-
strain. The matrix

$$\{s^1\} = (\frac{1}{8 \ abc}) \ [E] \ [B] \ [\overset{\sim}{\alpha}] \ \{\Delta T_k\} \tag{69}$$

yields stresses due to a temperature gradient within the
element and is referred to as the element thermal stress
matrix.

It is noted that the assumption made in
Equation (63) is invalid for a constant temperature and prestrain
distribution throughout the element since this assumption pro-
duces zero prestrain and zero thermal forces. Thus for a
constant prestrain and temperature distribution, the following
equations replace Equations (68) and (69).

$$\{s\} = [E] \ \{\overline{\epsilon}\} \tag{68A}$$

$$\{s'\} = \Delta T_{ave.} \ [E] \ \{\alpha\} \tag{68B}$$

where

$$\Delta T_{ave.} = T_{ave.} - T_o; \ T_{ave.} = \frac{T_1 + T_2 + \ \dots \ T_8}{8}$$

$$\{\alpha\}^T = \lfloor \alpha_x, \ \alpha_y, \ \alpha_z \rfloor \ .$$

5.4 Prestrain Load Matrix

The prestrain contribution to the potential
energy function is

$$\Phi_{\overline{\epsilon}} = \int_V \lfloor \epsilon \rfloor \ [E] \ \{\overline{\epsilon}\} \ dV \tag{67}$$

Substitution of Equations (30) and (64) into the above yields

$$\Phi_{\overline{\epsilon}} = (\frac{1}{8 \ abc})^2 \int_V \lfloor \delta^{(J)} \rfloor \ [D]^T \ [E] \ [B] \ \{\overline{\epsilon}_k^{(J)}\} \ dV \tag{68}$$

29

Performing the multiplication and integration gives

$$\Phi_{\tilde{\varepsilon}} = \lfloor \delta^{(J)} \rfloor \{\tilde{F}_{\tilde{\varepsilon}}\} \tag{69}$$

where

$$\{\tilde{F}_{\tilde{\varepsilon}}\} = (\frac{1}{8 \ abc})^2 [P] \{\bar{\varepsilon}_{\kappa}^{(J)}\}$$

$$[P] = \begin{bmatrix} E_{11} [I_{XB}], & E_{12} [I_{XB}], & E_{13} [I_{YB}], & E_{44} [I_{YB}], & 0, & E_{66} [I_{ZB}] \\ E_{12} [I_{YB}], & E_{22} [I_{YB}], & E_{23} [I_{YB}], & E_{44} [I_{XB}], & E_{55} [I_{ZB}], & 0 \\ E_{13} [I_{ZB}], & E_{23} [I_{ZB}], & E_{33} [I_{ZB}], & 0, & E_{55} [I_{YB}], & E_{66} [I_{XB}] \end{bmatrix} \tag{69A}$$

$$[I_{XB}] = \int_V \{D_X\} \lfloor \tilde{B} \rfloor \ dV = a [I_{XX}]$$

$$[I_{YB}] = \int_V \{D_Y\} \lfloor \tilde{B} \rfloor \ dV = b [I_{YY}]$$

$$[I_{ZB}] = \int_V \{D_Z\} \lfloor \tilde{B} \rfloor \ dV = c [I_{ZZ}]$$

Transformation of $\lfloor \delta^{(J)} \rfloor$ to global gridpoint deformations through use of Equations (57) and (58) and differentiation of the result with respect to the gridpoint deformations yields the prestrain load vector

$$\{F_{\tilde{\varepsilon}}\} = [T_{g\ell}]^T [T]^T \{\tilde{F}_{\tilde{\varepsilon}}\}. \tag{70}$$

30

For a constant prestrain throughout the element

$$\Phi_{\overline{\epsilon}} = (\frac{1}{8\ abc}) \int_V \lfloor \delta^{(j)} \rfloor [D]^T [E] \{\overline{\epsilon}\}\ dV \qquad (71)$$

Thus:

$$\{\tilde{F}_\epsilon\} = [\tilde{P}]\ \{\tilde{\epsilon}\} \qquad (72)$$

where $[\tilde{P}]$ is given by Equation (69B) and the load vector is given by Equation (70).

5.5 Thermal Load Matrix

The thermal load matrix is a special case of the prestrain load matrix. Substitution of the thermal strain

$$\{\epsilon_K^{(j)}\}^\alpha = [\tilde{\alpha}]\{\Delta T_k\} \qquad (73)$$

into Equation (69) defines a load matrix

$$\{\tilde{F}_\alpha\} = (\frac{1}{8\ abc})^2\ [P']\ [\tilde{\alpha}]\ \{\Delta T_k\} \qquad (74)$$

where

$$[P'] = \begin{bmatrix} E_{11}\ [I_{XB}], & E_{12}\ [I_{XB}], & E_{13}\ [I_{XB}] \\ \\ E_{12}\ [I_{YB}], & E_{22}\ [I_{YB}], & E_{23}\ [I_{YB}] \\ \\ E_{13}\ [I_{ZB}], & E_{23}\ [I_{ZB}], & E_{33}\ (I_{ZB}] \end{bmatrix}$$

31

$$
[\tilde{P}] =
\begin{bmatrix}
E_{66}^{ab} & E_{66}^{bc} & \cdots \\
E_{44}^{ac} & E_{55}^{ab} & E_{55}^{ac} \\
E_{13}^{bc} & E_{44}^{bc} & \\
E_{12}^{bc} & E_{23}^{ac} & E_{33}^{ab} \\
E_{11}^{bc} & E_{22}^{ac} & E_{23}^{ab} \\
& E_{12}^{ac} & E_{13}^{ab}
\end{bmatrix}
$$

The final thermal load matrix is given by

$$\{F_a\} = [T_{g\ell}]^T \; [T]^T \; \{\overset{\backsim}{F}_\alpha\} \tag{75}$$

For a constant temperature distribution throughout the element, the thermal strains are given by

$$\{\epsilon\}^\alpha = \Delta T_{ave.} \; \{\alpha\} \tag{76}$$

where

$$\Delta T_{ave.} = T_{ave.} - T_o$$

$$T_{ave.} = \frac{T_1 + T_2 + \ldots + T_8}{8}$$

Thus, substitution of Equation (76) into Equation (71) defines a load matrix

$$\{\overset{\backsim}{F}_\alpha\} = \Delta T_{ave.} \; [\overset{\backsim}{P}'] \; \{\alpha\} \tag{77}$$

The $[\overset{\backsim}{P}']$ matrix is obtained by taking only the first three columns of the $[\overset{\thicksim}{P}]$ matrix.

33

5.6 Pressure Load Matrix

The pressure load matrix is derived on the basis of constant pressure on each face of the rectangular prism element. Thus, the total work W_p due to the pressure loads is the sum of the work done on each face.

$$W_p = W_{1234} + W_{5678} + \cdots + W_{3478} \tag{78}$$

The subscripts denote a face of the prism (see Figure II-1).

Now

$$W_{1234} = \int_A p_{1234} \, \delta^{(1)} \, dA \tag{79}$$

Recalling Equation (11), Equation (79) can be written as

$$W_{1234} = \int_{-a}^{a} \int_{-b}^{b} \frac{1}{8\,abc} \lfloor \tilde{B} \rfloor \, \{\delta_\kappa^{(1)}\} \, dxdy \tag{80}$$

Performing the indicated integration yields

$$W_{1234} = p_{1234} \, bc \lfloor \delta_1{}^{(3)}, \; \delta_2{}^{(1)}, \; \delta_3{}^{(1)}, \; \delta_4{}^{(1)} \rfloor \{1\} \tag{81}$$

Additional integrations of the form shown by Equations (79) and (80) for the remaining faces yields

$$W_{3478} = p_{3478} \, a \, b \lfloor \delta_3{}^{(3)}, \; \delta_4{}^{(3)}, \; \delta_7{}^{(3)}, \; \delta_8{}^{(3)} \rfloor \{1\} \tag{82}$$

$$W_{2367} = p_{2367} \, a \, c \lfloor \delta_2{}^{(2)}, \; \delta_3{}^{(2)}, \; \delta_6{}^{(2)}, \; \delta_7{}^{(2)} \rfloor \{1\} \tag{83}$$

$$W_{1458} = p_{1458} \, a \, c \lfloor \delta_1{}^{(2)}, \; \delta_4{}^{(2)}, \; \delta_5{}^{(2)}, \; \delta_8{}^{(2)} \rfloor \{1\} \tag{84}$$

$$W_{1256} = p_{1256} \, ab \, \lfloor \delta_1^{(3)}, \, \delta_2^{(3)}, \delta_3^{(3)}, \, \delta_4^{(3)} \rfloor \, \{1\} \qquad (85)$$

$$W_{5678} = p_{5678} \, bc \, \lfloor \delta_5^{(1)}, \, \delta_6^{(1)} \, \delta_7^{(1)} \, \delta_8^{(1)} \rfloor \, \{1\} \qquad (86)$$

Equations (81) to (86) are combined to yield total work

$$W_p = \lfloor \delta_K^{(J)} \rfloor \, \{\tilde{F}_P\} = \lfloor \Delta \rfloor \, [T_{g\ell}]^T \, [T]^T \, \{\tilde{F}_P\} \qquad (87)$$

through use of Equations (57) and (58) and

$$\{\tilde{F}_P\}^T = \lfloor F_1, \, F_1, \, F_1, \, F_1, \, F_2, \, F_2, \, F_2, \, F_2, \, F_3, \, F_4, \, F_4, \, F_3,$$

$$F_3, \, F_4, \, F_4, \, F_3, \, F_5, \, F_5, \, F_6, \, F_6, \, F_5, \, F_5, \, F_6, \, F_6 \rfloor$$

Where:

$$F_1 = p_{1234} \, bc, \quad F_2 = p_{5678} \, bc, \quad F_3 = p_{1458} \, ac$$

$$F_4 = p_{2367} \, ac, \quad F_5 = p_{1256} \, ab, \quad F_6 = p_{3478} \, ab \, .$$

Taking the first variation of W_p in accordance with Equation (1) yields the pressure load matrix

$$\{F_p\} = [T_{g\ell}]^T \, [T]^T \, \{\tilde{F}_P\} \qquad (88)$$

VI.   Kinetic Energy - Mass Matrix

The kinetic energy for a discrete mechanical system, assuming a constant mass density ρ, can be written

$$\Phi_K = \rho/2 \int_V \lfloor \dot{q} \rfloor \; [1] \; \{\dot{q}\} \; dV \tag{89}$$

where $[1]$ is an identity matrix and where $\{\dot{q}\}$ are generalized velocities which, from the assumed displacement modes, are:

$$\{\dot{q}\}^T = \lfloor \dot{\delta}^{(1)}, \; \dot{\delta}^{(2)}, \; \dot{\delta}^{(3)} \rfloor \tag{90}$$

Substituting Equation (90) into Equation (89) yields

$$\Phi_K = \rho/2 \int_V \lfloor \dot{\delta}^{(1)}, \; \dot{\delta}^{(2)}, \; \dot{\delta}^{(3)} \rfloor \; [1] \begin{bmatrix} \dot{\delta}^{(1)} \\ \dot{\delta}^{(2)} \\ \dot{\delta}^{(3)} \end{bmatrix} \; dV \tag{91}$$

or

$$\Phi_K = \rho/2 \int_V [(\dot{\delta}^{(1)})^2 + (\dot{\delta}^{(2)})^2 + (\dot{\delta}^{(3)})^2] \; dV \; . \tag{92}$$

Recalling the displacement mode shapes

$$\delta^{(j)} = \frac{1}{8 \; abc} \; \lfloor \tilde{B} \rfloor \; \{\delta_k^{(j)}\} \tag{11}$$

and differentiating gives

$$\dot{\delta}^{(j)} = \frac{1}{8 \; abc} \; \lfloor B \rfloor \; \{\dot{\delta}_k^{(j)}\} \tag{93}$$

36

Thence,

$$(\dot{\delta}^{(j)})^2 = (\frac{1}{8\ abc})^2 \lfloor \dot{\delta}_k^{(j)} \rfloor\ [\tilde{m}]\ \{\dot{\delta}_k^{(j)}\} \qquad (94)$$

where

$$[\tilde{m}] = \{\tilde{B}\}\ \lfloor \tilde{B} \rfloor .$$

Substituting Equation (94) into Equation (92), for
j = 1, 2, 3, yields

$$\Phi_K = (\frac{1}{8\ abc})^2\ \rho/2 \int_V \lfloor \dot{\delta}^{(1)},\ \dot{\delta}^{(2)},\ \dot{\delta}^{(3)} \rfloor \begin{bmatrix} [\tilde{m}] & & \\ & [\tilde{m}] & \\ & & [\tilde{m}] \end{bmatrix} \begin{bmatrix} \dot{\delta}^{(1)} \\ \dot{\delta}^{(2)} \\ \dot{\delta}^{(3)} \end{bmatrix} dV \qquad (95)$$

or

$$\Phi_K = \frac{\rho}{2}\ \lfloor \dot{\delta}^{(j)} \rfloor\ [\tilde{M}]\ \{\dot{\delta}^{(j)}\} \qquad (96)$$

where

$$[\tilde{M}] = (\frac{1}{8\ abc})^2\ \rho \int_V \begin{bmatrix} [\tilde{m}] & & \\ & [\tilde{m}] & \\ & & [\tilde{m}] \end{bmatrix} dV \qquad (97)$$

Performing, as previously, the integration indicated in Equation (97) gives

$$[m] = \rho \left(\frac{1}{8\ abc}\right)^2 \int_v [\tilde{m}]\ dv = \left(\frac{8\ abc}{27}\right)\rho \begin{bmatrix} 1 & & & & & & & \\ 1/2 & 1 & & & & & & \\ 1/4 & 1/2 & 1 & & \text{SYMM.} & & & \\ 1/2 & 1/4 & 1/2 & 1 & & & & \\ 1/2 & 1/4 & 1/8 & 1/4 & 1 & & & \\ 1/4 & 1/2 & 1/4 & 1/8 & 1/2 & 1 & & \\ 1/8 & 1/4 & 1/2 & 1/4 & 1/4 & 1/2 & 1 & \\ 1/4 & 1/8 & 1/4 & 1/2 & 1/2 & 1/4 & 1/2 & 1 \end{bmatrix}$$

(98)

hence

$$[\tilde{M}] = \begin{bmatrix} [m], & 0, & 0 \\ 0, & [m], & 0 \\ 0, & 0, & [m] \end{bmatrix} \cdot$$

(99)

Reordering and transforming to global deformations through use of Equations (57) and (58) permits the kinetic energy to be written as:

$$\Phi_K = \frac{\lfloor\dot{\Delta}\rfloor}{2} [T_{g\ell}]^T [T]^T [\tilde{M}] [T] [T_{g\ell}] \{\dot{\Delta}\}$$

(100)

Taking the first variation of Φ_K with respect to velocities and differentiating once with respect to time, as shown in Equation (1), yields the desired consistent mass matrix referenced to global gridpoint displacements. Thus,

$$[M] = [T_{g\ell}]^T [T]^T [\tilde{M}] [T] [T_{g\ell}] .$$

(101)

38

C.   TETRAHEDRON ELEMENT

I.   Introduction

        The stiffness matrix for the tetrahedron element was
first derived and presented in References 10 and 11 respectively.
Later these relationships were reviewed and a consistent
mass matrix was reported in Reference 12. These formulations
have been extended in MAGIC III to include stress $[S]$,
prestrain load $\{F\}$, thermal load $\{F_T\}$, and pressure load $\{F_P\}$
matrices. These matrices were formulated on the basis of the
variational principles of continuum mechanics. The material that
follows summarizes the derivation of all the element matrices
mentioned above.

        A linear polynomial is assumed for each of the
three displacement modes. These mode shapes lead to a total of
twelve undetermined coefficients for the element which are chosen
to correspond to three translational displacement degrees of
freedom at each of the four vertices of the element. The nature
of the assumed displacement modes is such that the strains
throughout the element are constant.

        The tetrahedron element can be used to analyze
solid structures such as thick plates and beams. It can also be
used in conjunction with the rectangular prism and triangular
prism solid elements and in fact is used to generate the
triangular prism element.

II. Geometry

        Figure II-2 depicts the geometry of the tetrahedron
element. The local axes system x, y, z, and global system X, Y, Z
are also shown. The local axes are fixed at element gridpoint one
with the positive x axis directed along side one-three as shown.
The global coordinates of each grid point are given as

39
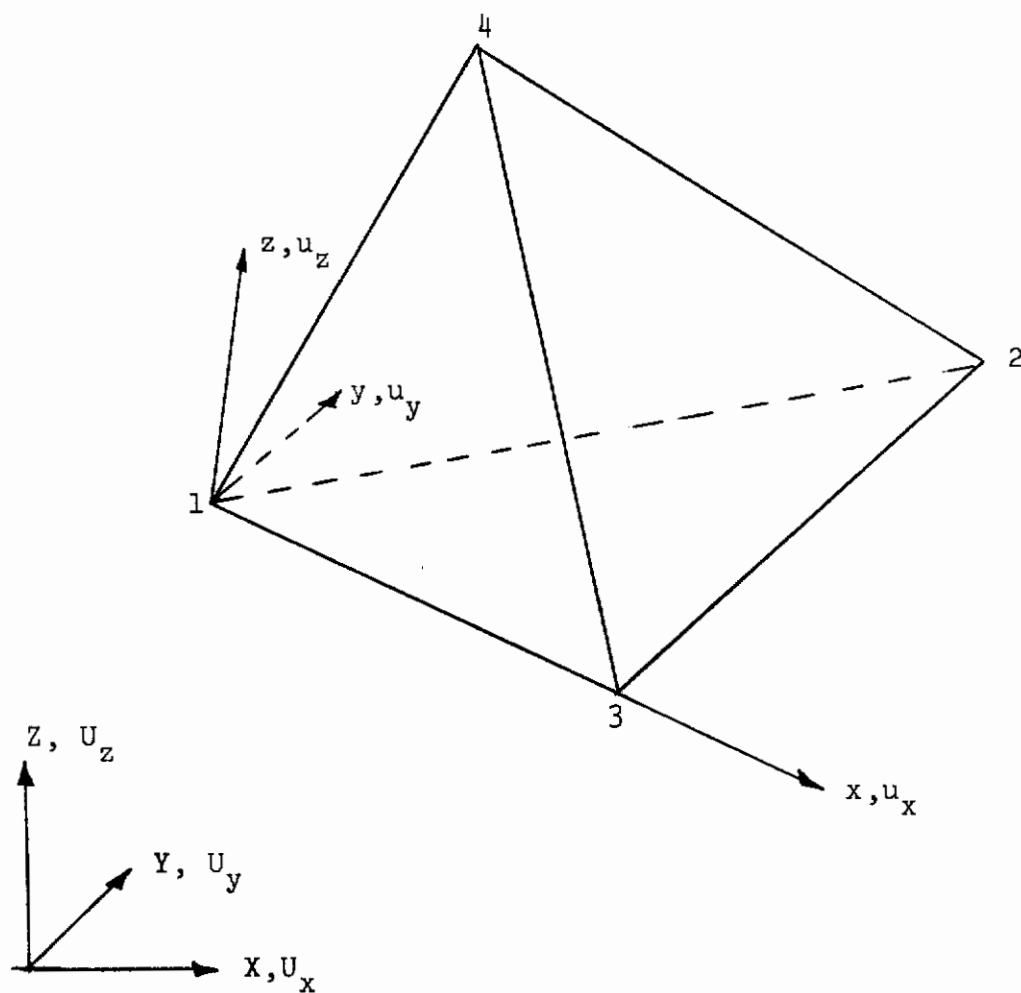
FIGURE II-2   TETRAHEDRON GEOMETRY

40

input from which the volume of the element is obtained

$$V = \frac{1}{6} \begin{vmatrix} 1 & X_1 & Y_1 & Z_1 \\ 1 & X_2 & Y_2 & Z_2 \\ 1 & X_3 & Y_3 & Z_3 \\ 1 & X_4 & Y_4 & Z_4 \end{vmatrix} . \tag{1}$$

The face areas of the element are given by

$$A_{431} = [(A_{431}^{YZ})^2 + (A_{431}^{XZ})^2 + (A_{431}^{XY})^2]^{1/2} \tag{2}$$

$$A_{432} = [(A_{432}^{YZ})^2 + (A_{432}^{XZ})^2 + (A_{432}^{XY})^2]^{1/2} \tag{3}$$

$$A_{421} = [(A_{421}^{YZ})^2 + (A_{421}^{XZ})^2 + (A_{421}^{XY})^2]^{1/2} \tag{4}$$

$$A_{321} = [(A_{321}^{YZ})^2 + (A_{321}^{XZ})^2 + (A_{321}^{XY})^2]^{1/2} . \tag{5}$$

The subscripts refer to an element face and the superscripts refer to area projection on a global plane. The components of the face area are given by:

$$A_{432}^{YZ} = 3V|B_{1,1}|, A_{432}^{XZ} = 3V|B_{4,1}|, A_{432}^{XY} = 3V|B_{6,1}| \tag{6}$$

$$A_{431}^{YZ} = 3V|B_{1,2}|, A_{431}^{XZ} = 3V|B_{4,2}|, A_{431}^{XY} = 3V|B_{6,2}| \tag{7}$$

$$A_{421}^{YZ} = 3V|B_{1,3}|, A_{421}^{XZ} = 3V|B_{4,3}|, A_{421}^{XY} = 3V|B_{6,3}| \tag{8}$$

$$A_{321}^{YZ} = 3V|B_{1,4}|, A_{321}^{XZ} = 3V|B_{4,4}|, A_{321}^{XY} = 3V|B_{6,4}| \tag{9}$$

41

The terms $|B_{1,1}|$, $|B_{1,2}|$, etc. represent the absolute value of elements (1,1) and (1,2), etc. in the [B] matrix which relates strains to displacements as shown in Equation (19) of this Section.

A rotational and translational transformation matrix from global to local coordinates is formed thru definition of position vectors emanating from the origin of the global axes system to element grid points 1, 2 and 3. This transformation matrix is

$$\{x^{(\ell)}\} = [\tilde{T}_{g\ell}] \left\{ \{X^{(g)}\} - \{X_1^{(g)}\} \right\} \tag{10}$$

where

$$\{x^{(\ell)}\}^T = \lfloor x^{(\ell)}, y^{(\ell)}, z^{(\ell)} \rfloor \text{ are the local coordinates.}$$

$$\{X^{(g)}\}^T = \lfloor X^{(g)}, Y^{(g)}, Z^{(g)} \rfloor \text{ are the global coordinates.}$$

$$\{X_1^{(g)}\}^T = \lfloor X_1^{(g)}, Y_1^{(g)}, Z_1^{(g)} \rfloor \text{ are the global coordinates of gridpoint one.}$$

$$[\tilde{T}_{g\ell}] = \begin{bmatrix} \dfrac{e_{11}}{|\bar{e}_1|} & , & \dfrac{e_{12}}{|\bar{e}_1|} & , & \dfrac{e_{13}}{|\bar{e}_1|} \\[2em] \dfrac{e_{21}}{|\bar{e}_2|} & , & \dfrac{e_{22}}{|\bar{e}_2|} & , & \dfrac{e_{23}}{|\bar{e}_2|} \\[2em] \dfrac{e_{31}}{|\bar{e}_3|} & , & \dfrac{e_{32}}{|\bar{e}_3|} & , & \dfrac{e_{33}}{|\bar{e}_3|} \end{bmatrix}$$

$$e_{11} = X_3 - X_1, \quad e_{12} = Y_3 - Y_1, \quad e_{13} = Z_3 - Z_1$$

$$e_{21} = e_{32}e_{13} - e_{12}e_{33}, \quad e_{22} = e_{11}e_{33} - e_{31}e_{13}, \quad e_{23} = e_{31}e_{12} - e_{11}e_{32}$$

$$e_{31} = (Y_3 - Y_1)(Z_2 - Z_1) - (Y_2 - Y_1)(Z_3 - Z_1)$$

$$e_{32} = (X_2 - X_1)(Z_3 - Z_1) - (X_3 - X_1)(Z_2 - Z_1)$$

$$e_{33} = (X_3 - X_1)(Y_2 - Y_1) - (X_2 - X_1)(Y_3 - Y_1)$$

$$|\bar{e}_1| = [e_{11}^2 + e_{12}^2 + e_{13}^2]^{1/2}$$

$$|\bar{e}_2| = [e_{21}^2 + e_{22}^2 + e_{23}^2]^{1/2}$$

$$|\bar{e}_3| = [e_{31}^2 + e_{32}^2 + e_{33}^2]^{1/2} \qquad .$$

III. Assumed Displacement Functions, Strain-Displacement

The assumed displacement functions in the global coordinate system are

$$U_x = C_1 X + C_2 Y + C_3 Z + C_4 \tag{11}$$

$$U_y = C_5 X + C_6 Y + C_7 Z + C_8 \tag{12}$$

$$U_z = C_9 X + C_{10} Y + C_{11} Z + C_{12} \tag{13}$$

where U_x, U_y, U_z are the deformations of the element along the global X, Y, and Z axes.

Evaluation of Equation (11) at the four gridpoints yields:

$$\{U_{x_1}\} = [\Gamma] \{C\} \tag{14}$$

where

$$\{U_{x_1}\}^T = \lfloor U_{x_1}, U_{x_2}, U_{x_3}, U_{x_4} \rfloor$$

$$\{C\}^T = \lfloor C_1, C_2, C_3, C_4 \rfloor$$

$$[\Gamma] = \begin{bmatrix} 1 & X_1 & Y_1 & Z_1 \\ 1 & X_2 & Y_2 & Z_2 \\ 1 & X_3 & Y_3 & Z_3 \\ 1 & X_4 & Y_4 & Y_4 \end{bmatrix}$$

Thus $\{C\} = [\Gamma]^{-1} \{U_{x_1}\}$ & $U_x = \lfloor 1, X, Y, Z \rfloor [\Gamma]^{-1} \{U_{x_1}\}$ (15)

Likewise, $U_y = \lfloor 1, X, Y, Z \rfloor [\Gamma]^{-1} \{U_{y_1}\}$ (16)

$$U_Z = \lfloor 1, X, Y, Z \rfloor [\Gamma]^{-1} \{U_{z_1}\} \ . \tag{17}$$

Equations (15) to (17) are used to derive element matrices. Note that the displacements functions are written in terms of global coordinates and displacements.

44

Definition of the assumed displacement functions permits derivation of the strain-displacement relations. The element strain components are

$$\{\varepsilon\} = \begin{bmatrix} \varepsilon_x \\ \varepsilon_y \\ \varepsilon_z \\ \gamma_{xy} \\ \gamma_{yz} \\ \gamma_{xz} \end{bmatrix} = \begin{bmatrix} \partial U_x/\partial x \\ \partial U_y/\partial y \\ \partial U_z/\partial z \\ \partial U_x/\partial y + \partial U_y/\partial x \\ \partial U_y/\partial z + \partial U_z/\partial y \\ \partial U_z/\partial x + \partial U_x/\partial z \end{bmatrix} = [B]\{U\} \qquad (18)$$

where

$$\{U\}^T = \lfloor U_{x_1}, \; U_{x_2}, \; U_{x_3}, \; U_{x_4}, \; U_{y_1}, \; U_{y_2}, \; U_{y_3}, \; U_{y_4},$$

$$U_{z_1}, \; U_{z_2}, \; U_{z_3}, \; U_{z_4} \rfloor$$

The [B] matrix is constructed from the $[\Gamma]^{-1}$ matrix as follows:

$$[B] = \begin{bmatrix} \text{Row 2 of } [\Gamma]^{-1}, \longleftarrow \text{Zeroes} \longrightarrow \\ \longleftarrow \text{Zeroes} \longrightarrow \text{Row 3 of } [\Gamma]^{-1}, \longleftarrow \text{Zeroes} \longrightarrow \\ \longleftarrow \text{Zeroes} \longrightarrow \text{Row 4 of } [\Gamma]^{-1} \\ \text{Row 3 of } [\Gamma]^{-1}, \quad \text{Row 2 of } [\Gamma]^{-1} \quad , \text{Row 3 of } [\Gamma]^{-1} \\ \text{Row 4 of } [\Gamma]^{-1}, \longleftarrow \text{Zeroes} \longrightarrow \text{Row 2 of } [\Gamma]^{-1} \end{bmatrix} \qquad (19)$$

45

IV   Potential Energy

The desired form of the potential energy is

$$U = \int_V (\frac{1}{2} \lfloor \varepsilon \rfloor [E] \{\varepsilon\} - \lfloor \varepsilon \rfloor [E] \{\bar{\varepsilon}\})\ dV \qquad (20)$$

which was derived in Section II-B.IV of this report. The matrix [E] is defined in that section also.

V   Element Matrices

5.1 Introduction

To effect the discretization of the element the assumed displacement functions are introduced into the potential energy function which in turn is substituted into the Lagrange equations to yield element matrices with respect to gridpoint displacement degrees of freedom. An exception is the element stress matrix which is derived from strain-displacement and stress-strain relationships.

5.2 Stiffness Matrix

The energy contribution to the linear elastic stiffness is given by

$$\Phi_P = \frac{1}{2} \int_V \lfloor \varepsilon \rfloor [E] \{\varepsilon\}\ dV. \qquad (21)$$

Substitution of the strain-displacement relationship, Equation (18), in this energy contribution yields

$$\Phi_P = \frac{1}{2} \int_V \lfloor U \rfloor [B]^T [E] [B] \{U\}\ dV. \qquad (22)$$

Since matrix [B] is not a function of the global coordinates the integration can be performed directly and

$$\Phi_P = \frac{V}{2} \lfloor U \rfloor [B]^T [E] [B] \{U\} \qquad (23)$$

The displacements {U} must be reordered to be compatible with the MAGIC III ordering system. Thus, the following transformation is defined:

$$\{U\} = [T] \{\overline{U}\} \tag{24}$$

where

$$\{\overline{U}\}^T = \lfloor U_{x_1}, \ U_{y_1}, \ U_{z_1}, \ U_{x_2}, \ U_{y_2}, \ U_{z_2}, \ \cdots \ U_{x_4}, \ U_{y_4}, \ U_{z_4} \rfloor \ .$$

The [T] matrix is defined by Equation (24A). Substitution of Equation (24) into Equation (23) yields Equation (25).

$$[T] = \begin{bmatrix} 1 & & & & & & & & & & & \\ & & & 1 & & & & & & & & \\ & & & & & & 1 & & & & & \\ & & & & & & & & 1 & & & \\ & 1 & & & & & & & & & & \\ & & & & 1 & & & & & & & \\ & & & & & & & 1 & & & & \\ & & 1 & & & & & & & & & \\ & & & & & 1 & & & & & & \\ & & & & & & & & & 1 & & \end{bmatrix} \tag{24A}$$

$$\dot{\Phi}_P = \frac{V}{2} \ \lfloor \overline{U} \rfloor \ [T]^T \ [B]^T \ [E] \ [B] \ [T] \ \{\overline{U}\} \tag{25}$$

47

Taking the first variation of the potential energy with respect to the displacement degrees of freedom $\{\bar{U}\}$ yields the element stiffness matrix $[K]$ referenced to global grid point displacements. This matrix is given below:

$$[K] = V [T]^T [B]^T [E] [B] [T] . \qquad (26)$$

5.3 Stress Matrices

The element stress matrix follows as a direct consequence of the strain-displacement and stress-strain relationships. Recalling that

$$\{\sigma\} = [E] \left\{ \{\epsilon\} - \{\bar{\epsilon}\} \right\} \qquad (27)$$

where $\{\bar{\epsilon}\}$ is a column of either mechanical prestrain or thermal prestrain or both. Also recalling that

$$\{\epsilon\} = [B] \{U\} = [B] [T] \{\bar{U}\} \qquad (28)$$

it follows that

$$\{\sigma\} = [E] [B] [T] \{\bar{U}\} - [E] \{\bar{\epsilon}\} - [E] \{\bar{\epsilon}\}^{\alpha} . \qquad (29)$$

The vector $\{\bar{\epsilon}^{\alpha}\}$, the prestrain due to thermal effects, can be written as

$$\{\bar{\epsilon}^{\alpha}\} = \Delta T \{\alpha\}; \quad \{\alpha\}^T = \lfloor \alpha_x, \ \alpha_y, \ \alpha_z, \ o, \ o, \ o \rfloor \qquad (30)$$

where

$$\Delta T = T_{ave.} - T_o, \ T_{ave.} = \frac{T_1 + T_2 + T_3 + T_4}{4}$$

and T_o is a reference temperature.

Equation (29) can now be rewritten

$$\{\sigma\} = [S] \{\bar{U}\} - \{s\} - \{s^1\} \qquad (31)$$

48

where:

$$[S] = [E] [B] [T]$$
$$\{s\} = [E] \{\bar{\epsilon}\}$$
$$\{s'\} = \Delta T [E] \{\alpha\}$$

5.4 Prestrain Load Matrix

The prestrain contribution to the potential energy function is

$$\Phi_{\bar{\epsilon}} = \lfloor \epsilon \rfloor [E] \{\bar{\epsilon}\} \, dV . \tag{32}$$

Substitution of Equations (18) and (24) into this equation yields

$$\Phi_{\bar{\epsilon}} = \int_V \lfloor \bar{U} \rfloor [T]^T [B]^T [E] \{\bar{\epsilon}\} \, dV$$

or

$$\Phi_{\bar{\epsilon}} = V \lfloor \bar{U} \rfloor [T]^T [B]^T [E] \{\bar{\epsilon}\} = \lfloor \bar{U} \rfloor \{F_{\bar{\epsilon}}\} . \tag{33}$$

Differentiation of Equation (33) with respect to the global gridpoint deformation yields the prestrain load vector

$$\{F_{\bar{\epsilon}}\} = V [T]^T [B]^T [E] \{\bar{\epsilon}\} . \tag{34}$$

5.5 Thermal Load Matrix

The thermal load matrix is a special case of the prestrain load matrix. Substitution of the thermal strain, Equation (30), into Equation (34) yields:

$$\{F_\alpha\} = \Delta T V [T]^T [B]^T [E] \{\alpha\} . \tag{35}$$

5.6 Pressure Load Matrix

The pressure load matrix is derived on the basis of constant pressure on each face of the tetrahedron element. Thus the total work, W_p, due to the pressure loads is the sum of the work done on each face.

$$W_p = W_{321} + W_{431} + W_{432} + W_{421} \tag{36}$$

49

The subscripts denote a face of the tetrahedron (see Figure II-2). Each work term is initially derived in a special set of local coordinates placed in a face of the tetrahedron. The resulting work term is then transformed to the global coordinate system. Thus

$$W_{321} = -\int_{A_{321}} \kappa \, p_{321} \, \mu_z \, dA \qquad (37)$$

where the negative sign accounts for direction of the pressure P_{321} and $\kappa = \text{sgn } z_4$.

The deformation μ_z can be expressed in terms of the assumed displacement functions and local coordinates x, y as

$$\mu_z = \frac{1}{|\gamma|} \lfloor \mu_{z_1}, \mu_{z_2}, \mu_{z_3}, \mu_{z_4} \rfloor \begin{bmatrix} A_1 \\ A_2 \\ A_3 \\ A_4 \end{bmatrix} \qquad (38)$$

where $|\gamma| = |x_2 y_3 z_4|$

$$A_1 = (-y_2 z_4 \, x + (x_2 - x_3) z_4 y + (x_3 y_4 - x_2 y_4 + x_4 y_2 - x_3 y_2) z$$
$$+ x_3 y_2 z_4) \div |\gamma|$$

$$A_2 = (x_3 z_4 y - x_3 y_4 z) \div |\gamma|$$

$$A_3 = (y_2 z_4 \, x - x_2 z_4 y + (x_2 y_4 - x_4 y_2) z) \div |\gamma|$$

$$A_4 = (x_3 y_2 z) \div |\gamma|$$

50

For purposes of integration, a triangular coordinate system
is defined as shown in Figure II-3 below:
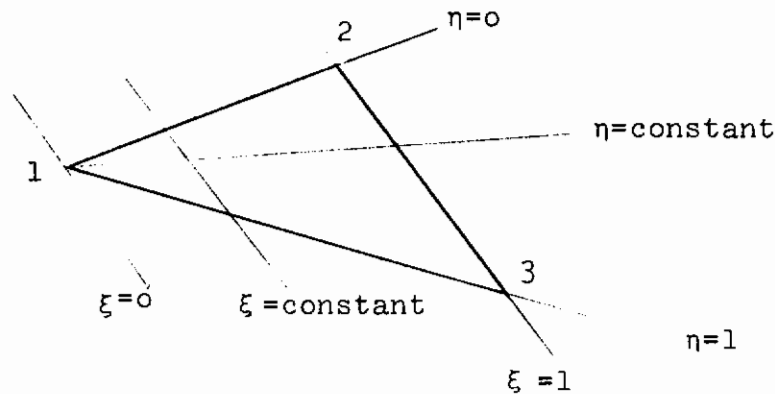
FIGURE II-3 TRIANGULAR COORDINATE SYSTEM

The transformation from (x,y) to (ξ, η) coordinates is
accomplished by using the following:

$$x = x_2 \xi - (x_2 - x_3) \xi \eta$$

$$y = y_2 (1-\eta) \xi$$

$$dxdy = |J(x,y)| d\xi d\eta \tag{39}$$

$$|J(x,y)| = \left| \frac{\partial x}{\partial \xi} \frac{\partial y}{\partial \eta} - \frac{\partial x}{\partial \eta} \frac{\partial y}{\partial s} \right| = \left| -x_3 y_2 \xi \right|$$

Substitutions of Equations (39) and setting $z = 0$ into
Equations (38) yields

$$\mu_z = \lfloor \mu_{z1}, \mu_{z_2}, \mu_{z_3}, \mu_{z_4} \rfloor \begin{bmatrix} 1 - \xi \\ (1-\eta) \xi \\ \xi \eta \\ 0 \end{bmatrix} \tag{40}$$

51

Use of this relationship in Equation (37) and performing the integration yields the result

$$W_{321} = -\frac{1}{3}\mathcal{K}\, p_{321}\, A_{321}\, \lfloor \mu_{z_1}, \mu_{z_2}, \mu_{z_3}, \mu_{z_4} \rfloor \begin{bmatrix} 1 \\ 1 \\ 1 \\ 0 \end{bmatrix}. \qquad (41)$$

The work due to pressure on face 431 is given by

$$W_{431} = -\int_{A_{431}} p_{431}\, \mu_{\bar{y}}\, dA \qquad (42)$$

where $\mu_{\bar{y}}$ is the deformation parallel to the pressure vector. (See Figure II-4 below.)
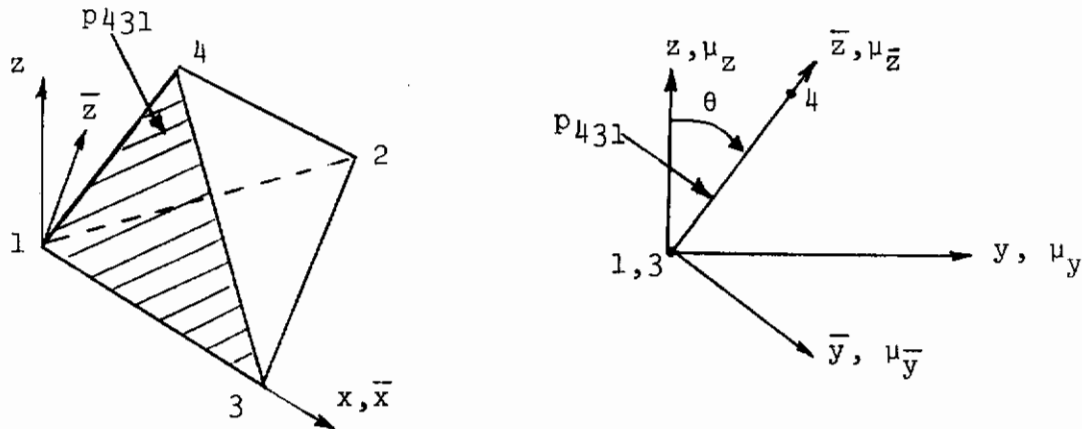
FIGURE II-4   PRESSURE LOAD - FACE 431

As above, the deformation $\mu_{\bar{y}}$ can be expressed as

$$\mu_{\bar{y}} = \lfloor \mu_{\bar{y}_1}, \mu_{\bar{y}_2}, \mu_{\bar{y}_3}, \mu_{\bar{y}_4} \rfloor \begin{bmatrix} 1-\xi \\ 0 \\ \xi\eta \\ (1-\eta)\xi \end{bmatrix} \qquad (43)$$

which is valid for $\bar{y} = 0$. Thus, substitution of Equation (43) into Equation (42) and integrating yields

52

$$W_{431} = -\frac{1}{3} p_{431} A_{431} \lfloor \mu_{\bar{y}_1}, \mu_{\bar{y}_2}, \mu_{\bar{y}_3}, \mu_{\bar{y}_4} \rfloor \begin{bmatrix} 1 \\ 0 \\ 1 \\ 1 \end{bmatrix} \cdot \tag{44}$$

The $\mu_{\bar{y}_i}$, $i = 1, 2, 3, 4$ deformations are transformed into tetrahedron local deformations using

$$\mu_{\bar{y}_i} = \mu_{y_i} \cos \theta - \mu_{z_i} \sin \theta \tag{45}$$

where

$$\theta = \tan^{-1} \left(\frac{y_4}{z_4} \right)$$

$$\begin{bmatrix} x_4 \\ y_4 \\ z_4 \end{bmatrix} = [\tilde{T}_{g\ell}] \left(\begin{bmatrix} X_4 \\ Y_4 \\ Z_4 \end{bmatrix} - \begin{bmatrix} X_1 \\ Y_1 \\ Z_1 \end{bmatrix} \right) \cdot$$

Use of Equation (45) in Equation (44) yields

$$W_{431} = -\frac{1}{3} p_{431} \cos \theta \lfloor \mu_{y_1}, \mu_{y_2}, \mu_{y_3}, \mu_{y_4} \rfloor \begin{bmatrix} 1 \\ 0 \\ 1 \\ 1 \end{bmatrix} \tag{46}$$

$$+ \frac{1}{3} p_{431} \sin \theta \lfloor \mu_{z_1}, \mu_{z_2}, \mu_{z_3}, \mu_{z_4} \rfloor \begin{bmatrix} 1 \\ 0 \\ 1 \\ 1 \end{bmatrix} \cdot$$

53

The work due to pressure on face 432 is given by

$$W_{432} = - \int_{A_{432}} p_{432} \; \mu_{y}^{\sim} \; dA \qquad (47)$$

where $\mu_{y}^{\sim}$ is the deformation parallel to the pressure vector. (See Figure II-5 below).
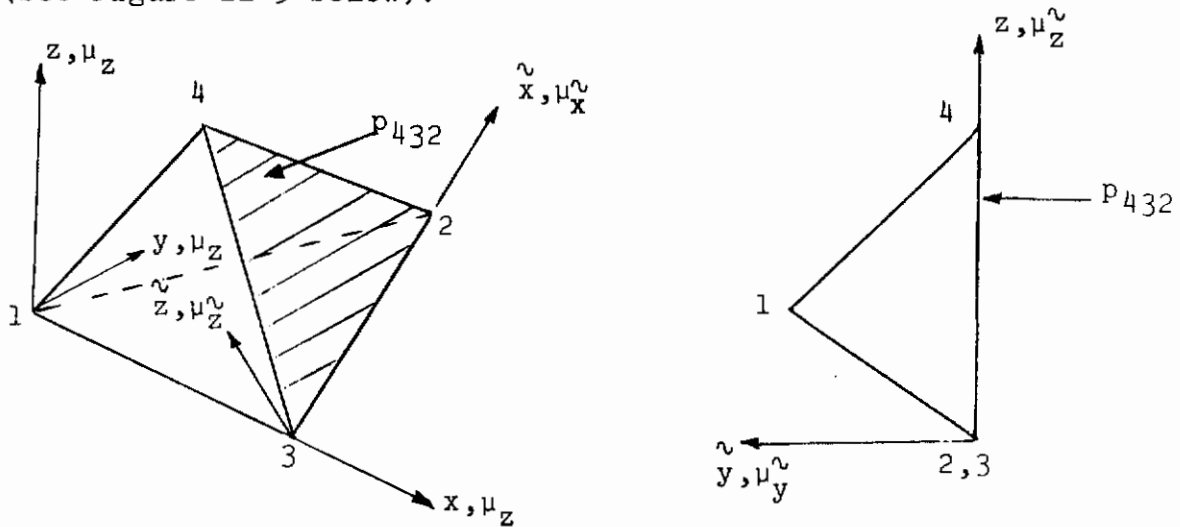
FIGURE II-5   PRESSURE LOAD-FACE 432

The deformation $\mu_{y}^{\sim}$ can be expressed again as

$$\mu_{y}^{\sim} = \lfloor \mu_{y_1}^{\sim}, \; \mu_{y_2}^{\sim}, \; \mu_{y_3}^{\sim}, \; \mu_{y_4}^{\sim} \rfloor \begin{bmatrix} 0 \\ \xi\eta \\ 1-\xi \\ (1-\eta)\xi \end{bmatrix} \qquad (48)$$

which is valid for $\tilde{y} = 0$. Substitution of this expression into Equation (47) yields

$$W_{432} = - \frac{1}{3} p_{432} \; A_{432} \lfloor \mu_{\tilde{y}_1}, \; \mu_{\tilde{y}_2}, \; \mu_{\tilde{y}_3}, \; \mu_{\tilde{y}_4} \rfloor \begin{bmatrix} 0 \\ 1 \\ 1 \\ 1 \end{bmatrix} \cdot \qquad (49)$$

54

The $\mu_{\tilde{y}i}$, $i = 1, 2, 3, 4$ deformations are transformed into tetrahedron local deformations using

$$\{\mu_{\tilde{y}}\} = [T_1] \{\bar{\mu}\} \qquad (50)$$

where

$$\{\mu_{\tilde{y}}\}^T = \lfloor \mu_{\tilde{y}_1}, \mu_{\tilde{y}_2}, \mu_{\tilde{y}_3}, \mu_{\tilde{y}_4} \rfloor$$

$$\{\bar{\mu}\}^T = \lfloor \mu_{x_1}, \mu_{y_1}, \mu_{z_1}, \mu_{x_2}, \mu_{y_2}, \mu_{z_2}, \mu_{x_3}, \mu_{y_3}, \mu_{z_3},$$

$$\mu_{x_4}, \mu_{y_4}, \mu_{z_4} \rfloor$$

$$[T_1] = \frac{1}{|\tilde{e}_2|} \begin{bmatrix} \tilde{e}_{21}, \tilde{e}_{22}, \tilde{e}_{23}, 0, 0, 0, 0, 0, 0, 0, 0, 0 \\ 0, 0, 0, \tilde{e}_{21}, \tilde{e}_{22}, \tilde{e}_{23}, 0, 0, 0, 0, 0, 0 \\ 0, 0, 0, 0, 0, 0, \tilde{e}_{21}, \tilde{e}_{22}, \tilde{e}_{23}, 0, 0, 0 \\ 0, 0, 0, 0, 0, 0, 0, 0, 0, \tilde{e}_{21}, \tilde{e}_{22}, \tilde{e}_{23} \end{bmatrix}$$

$$\tilde{e}_{21} = -y_2 z_4$$

$$\tilde{e}_{22} = z_4 (x_3 - x_2)$$

$$\tilde{e}_{23} = y_2 (x_4 - x_3) - y_4 (x_2 - x_3)$$

$$|\tilde{e}_2| = [(\tilde{e}_{21})^2 + (\tilde{e}_{22})^2 + (\tilde{e}_{23})^2]^{1/2}$$

The local coordinates are obtained from the transformation

$$
\begin{bmatrix} x_i \\ y_i \\ z_i \end{bmatrix} = [\tilde{T}_{g\ell}] \left[\begin{bmatrix} X_i \\ Y_i \\ Z_i \end{bmatrix} - \begin{bmatrix} X_1 \\ Y_1 \\ Z_1 \end{bmatrix} \right] \tag{50A}
$$

$$i = 1,2,3,4$$

Use of Equation (50) in Equation (49) gives

$$
W_{432} = - \frac{1}{3} p_{432} A_{432} \lfloor \bar{\mu} \rfloor [T_1]^T \begin{bmatrix} 0 \\ 1 \\ 1 \\ 1 \end{bmatrix} \cdot \tag{51}
$$

The work due to pressure on face 421 is given

by

$$
W_{421} = - \int_{A_{421}} p_{421}\, \mu_{y^\circ}\, dA \tag{52}
$$

where $\mu_y{}^\circ$ is the deformation parallel to the pressure vector. (See Figure II-6 below).
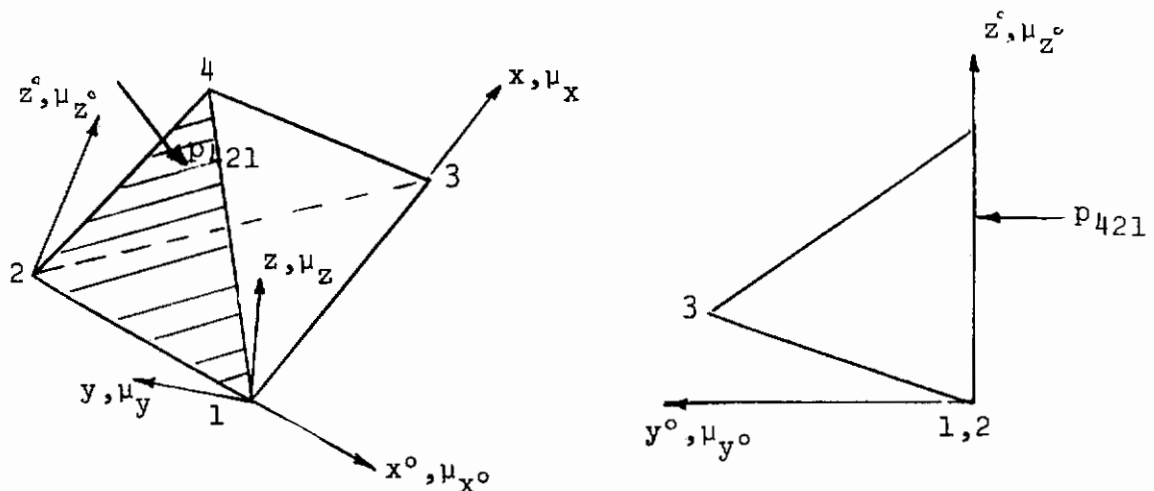
FIGURE II-6   PRESSURE LOAD - FACE 421

56

The deformation $\mu_y{}^o$ can be written as

$$\mu_y^o = \lfloor \mu_{y_1}^o, \ \mu_{y_2}^o, \ \mu_{y_3}^o, \ \mu_{y_4}^o \rfloor \begin{bmatrix} \xi\eta \\ 1-\xi \\ 0 \\ (1-\eta)\xi \end{bmatrix} \tag{53}$$

which is valid for $y^o = 0$. Substitution of Equation (53) into Equation (52) and integrating yields:

$$W_{421} = -\frac{1}{3} \ p_{431} \ A_{431} \ \lfloor \mu_{y_1}^o, \ \mu_{y_2}^o, \ \mu_{y_3}^o, \ \mu_{y_4}^o \rfloor \begin{bmatrix} 1 \\ 1 \\ 0 \\ 1 \end{bmatrix} \cdot \tag{54}$$

the $\mu_y{}^o{}_i$, $i = 1,2,3,4$ deformations are transformed into

tetrahedron local deformations using

$$\{\mu_y o\} = [T_2] \ \{\bar\mu\} \tag{55}$$

where $\quad \{\mu_y o\}^T = \lfloor \mu_{y^o 1}, \ \mu_{y^o 2}, \ \mu_{y^o 3}, \ \mu_{y^o 4} \rfloor$

$$[T_2] = \frac{1}{|e_2^o|} \begin{bmatrix} e_{21}^o, & e_{22}^o, & e_{23}^o, & 0, & 0, & 0, & 0, & 0, & 0, & 0, & 0, & 0 \\ 0, & 0, & 0, & e_{21}^o, & e_{22}^o, & e_{23}^o, & 0, & 0, & 0, & 0, & 0, & 0 \\ 0, & 0, & 0, & 0, & 0, & 0, & e_{21}^o, & e_{22}^o, & e_{23}^o, & 0, & 0, & 0 \\ 0, & 0, & 0, & 0, & 0, & 0, & 0, & 0, & 0, & e_{21}^o, & e_{22}^o, & e_{23}^o \end{bmatrix}$$

$$e_{21}^o = y_2 z_4, \ e_{22}^o = -x_2 z_4, \ e_{23}^o = x_2 y_4 - x_4 y_2$$

$$|e_2^o| = [(e_{21}^o)^2 + (e_{22}^o)^2 + (e_{23}^o)^2]^{1/2}$$

Use of Equation (55) in Equation (54) yields

$$W_{421} = -\frac{1}{3} \ p_{421} \ A_{421} \ \lfloor \bar\mu \rfloor \ [T_2]^T \begin{bmatrix} 1 \\ 1 \\ 0 \\ 1 \end{bmatrix} \cdot \tag{56}$$

The total work done by a uniform normal pressure on all sides of the tetrahedron is obtained by substituting Equations (41), (46), (51) and (56) into Equation (36). Thus:

$$
W_p = \left\lfloor \lfloor \mu_{x_1} \rfloor, \ \lfloor \mu_{y_1} \rfloor, \ \lfloor \mu_{z_1} \rfloor \right\rfloor \left[\begin{bmatrix} 0 \\ 0 \\ 0 \\ 0 \end{bmatrix} - \frac{1}{3} p_{431} A_{431} \cos \theta \begin{bmatrix} 1 \\ 0 \\ 1 \\ 1 \end{bmatrix} - \frac{1}{3} p_{321} A_{321} \kappa \begin{bmatrix} 1 \\ 1 \\ 1 \\ 0 \end{bmatrix} + \frac{1}{3} p_{431} A_{431} \sin \theta \begin{bmatrix} 1 \\ 0 \\ 1 \\ 1 \end{bmatrix} \right]
$$

$$
- 1/3 \, p_{432} A_{432} \lfloor \bar{\mu} \rfloor [T_1]^T \begin{bmatrix} 0 \\ 1 \\ 1 \\ 1 \end{bmatrix} - 1/3 \, p_{421} A_{421} \lfloor \bar{\mu} \rfloor [T_2]^T \begin{bmatrix} 1 \\ 1 \\ 0 \\ 1 \end{bmatrix} . \tag{57}
$$

The local deformations μ_{x_1}, μ_{y_1}, μ_{z_1}

must first be reordered to correspond to the MAGIC III ordering system. Thus:

$$
\left\lfloor \lfloor \mu_{x_1} \rfloor, \ \lfloor \mu_{y_1} \rfloor, \ \lfloor \mu_{z_1} \rfloor \right\rfloor = \lfloor \bar{\mu} \rfloor [T]^T \tag{58}
$$

In addition, these local deformations are transformed to global deformations through use of

$$
\lfloor \bar{\mu} \rfloor = \lfloor U \rfloor [\tilde{T}_{g\ell}]^T \tag{59}
$$

58

Substitution of Equations (58) and (59) into Equation (57) and taking the first variation of the result with respect to global deformations yields the final result:

$$\{F_p\} = [T_{g\ell}]^T \left\{ [T]^T \{\tilde{F}_p\} + [T_1]^T \{\tilde{F}_{p_1}\} + [T_2]^T \{\tilde{F}_{p_2}\} \right\} \qquad (60)$$

where:
$$[T_{g\ell}] = \begin{bmatrix} [\tilde{T}_{g\ell}] & & & \\ & [\tilde{T}_{g\ell}] & & \\ & & [\tilde{T}_{g\ell}] & \\ & & & [\tilde{T}_{g\ell}] \end{bmatrix}$$

$$\{\tilde{F}_p\} = \begin{bmatrix} \begin{bmatrix} 0 \\ 0 \\ 0 \\ 0 \end{bmatrix} \\[2em] - \frac{1}{3} p_{431} A_{431} \cos\theta \begin{bmatrix} 1 \\ 0 \\ 1 \\ 1 \end{bmatrix} \\[2em] - \frac{1}{3} p_{321} A_{321}\kappa \begin{bmatrix} 1 \\ 1 \\ 1 \\ 0 \end{bmatrix} + \frac{1}{3} p_{431} A_{431} \sin\theta \begin{bmatrix} 1 \\ 0 \\ 1 \\ 1 \end{bmatrix} \end{bmatrix}$$

$$\{\tilde{F}_{p_1}\} = - \frac{1}{3} p_{432} A_{432} \begin{bmatrix} 0 \\ 1 \\ 1 \\ 1 \end{bmatrix} \quad ; \quad \{\tilde{F}_{p_2}\} = -\frac{1}{3} p_{421} A_{421} \begin{bmatrix} 1 \\ 1 \\ 0 \\ 1 \end{bmatrix}$$

VI   Kinetic Energy – Mass Matrix

The kinetic energy for a discrete mechanical system assuming a constant mass density, ρ, can be written:

$$\Phi_K = \frac{\rho}{2} \int_V \lfloor \dot{\mu} \rfloor \; [1] \; \{\dot{\mu}\} \; dV \tag{61}$$

where $[1]$ is an identity matrix and $\{\dot{\mu}\}$ are local velocities of any point in the element.

$$\lfloor \dot{\mu} \rfloor = \lfloor \dot{\mu}_x, \; \dot{\mu}_y, \; \dot{\mu}_z \rfloor \; . \tag{62}$$

Thus

$$\Phi_K = \frac{\rho}{2} \int_V [(\dot{\mu}_x)^2 + (\dot{\mu}_y)^2 + (\dot{\mu}_z)^2] \; dV \; . \tag{63}$$

The velocities $\dot{\mu}_x$, $\dot{\mu}_y$ and $\dot{\mu}_z$ can be expressed in terms of local grid point velocities through the use of the assumed displacement functions. Thus

$$\dot{\mu}_x = \frac{\lfloor A \rfloor}{6V} \begin{bmatrix} \dot{\mu}_{x_1} \\ \dot{\mu}_{x_2} \\ \dot{\mu}_{x_3} \\ \dot{\mu}_{x_4} \end{bmatrix} \quad ; \quad \dot{\mu}_y = \frac{\lfloor A \rfloor}{6V} \begin{bmatrix} \dot{\mu}_{y_1} \\ \dot{\mu}_{y_2} \\ \dot{\mu}_{y_3} \\ \dot{\mu}_{y_4} \end{bmatrix} \tag{64}$$

$$\dot{\mu}_z = \frac{\lfloor A \rfloor}{6V} \begin{bmatrix} \dot{\mu}_{z_1} \\ \dot{\mu}_{z_2} \\ \dot{\mu}_{z_3} \\ \dot{\mu}_{z_4} \end{bmatrix} \quad ; \quad \lfloor A \rfloor = \lfloor A_1, \; A_2, \; A_3, \; A_4 \rfloor \tag{65}$$

60

where:

$$A_1 = y_{32}z_4 \, x + x_{23} \, z_4 \, y + (x_3y_4 - x_4y_3 - x_2y_4 + x_4y_2$$

$$+ \; x_2y_3 - x_3y_2) \; z + 6V$$

$$A_2 = -y_3z_4 x + x \, z_4 \, y + (x_4y_3 - x_3y_4) \; z$$

$$A_3 = y_2z_4 \, x - x_2z_4 y + (x_2y_4 - y_2x_4)$$

$$A_4 = (y_2x_3 - x_2y_3) \; z$$

and $\quad y_{32} = y_3 - y_2 \quad , \quad x_{23} = x_2 - x_3 \; .$

Thus the products in Equations (63) are given by

$$(\dot{\mu}_x)^2 = \lfloor \dot{\mu}_{x_i} \rfloor \; \{A\} \; \lfloor A \rfloor \; \{\dot{\mu}_{x_i}\}$$

$$(\dot{\mu}_y)^2 = \lfloor \dot{\mu}_{y_i} \rfloor \; \{A\} \; \lfloor A \rfloor \; \{\dot{\mu}_{y_i}\} \qquad\qquad (66)$$

$$(\dot{\mu}_z)^2 = \lfloor \dot{\mu}_{z_i} \rfloor \; \{A\} \; \lfloor A \rfloor \; \{\dot{\mu}_{z_i}\} \qquad , \; i = 1,2,3,4 \; .$$

The kinetic energy now becomes

$$\Phi_K = \frac{\rho}{2} \lfloor \lfloor \dot{\mu}_{x_i} \rfloor , \; \lfloor \dot{\mu}_{y_i} \rfloor , \; \lfloor \dot{\mu}_{z_i} \rfloor \rfloor \begin{bmatrix} \int_V \{A\} \lfloor A \rfloor \; dV, & 0 & , & 0 \\ 0 & , \int_V \{A\} \lfloor A \rfloor dV, & 0 \\ 0 & , & 0 & , \int_V \{A\} \lfloor A \rfloor dV \end{bmatrix} \begin{bmatrix} \{\dot{\mu}_{x_i}\} \\ \{\dot{\mu}_{y_i}\} \\ \{\dot{\mu}_{z_i}\} \end{bmatrix}$$

$$(67)$$

61

or

$$\Phi_K = \frac{1}{2} \lfloor \dot{\mu}_1 \rfloor [M] \{\dot{\mu}_1\} \tag{68}$$

where

$$[M] = \begin{bmatrix} [\tilde{m}], & 0, & 0 \\ 0, & [\tilde{m}], & 0 \\ 0, & 0, & [\tilde{m}] \end{bmatrix}; [\tilde{m}] = \rho \int_V \{A\} \lfloor A \rfloor dV . \tag{69}$$

The local grid point velocities in Equation (68) must be reordered for use in MAGIC III. This is accomplished using Equation (58) in Equation (68). Thus

$$\Phi_K = \frac{1}{2} \lfloor \dot{\mu} \rfloor [T]^T [\tilde{M}] [T] \{\dot{\mu}\} \tag{70}$$

where

$$\lfloor \dot{\mu} \rfloor = \lfloor \dot{\mu}_{x_1}, \dot{\mu}_{y_1}, \dot{\mu}_{z_1}, \dot{\mu}_{x_2}, \dots \dot{\mu}_{z_4} \rfloor .$$

In addition, these local grid point velocities must be transformed to global grid point velocities. Equation (58) in Section B of this report is used. Thus the kinetic energy is

$$\Phi_K = \frac{1}{2} \lfloor \dot{U} \rfloor [T_{g\ell}]^T [T]^T [\tilde{M}] [T] [T_{g\ell}] \{\dot{U}\} . \tag{71}$$

Taking the first variation of Φ_K with respect to velocities and differentiating the result once with respect to time yields the desired mass matrix referenced to global grid point velocities.

$$[M] = [T_{g\ell}]^T [T]^T [\tilde{M}] [T] [T_{g\ell}] \ . \tag{72}$$

It now remains to evaluate the matrix $[\tilde{m}]$ of Equation (69). For purposes of integration, a tetrahedral coordinate system will be used. Let local coordinates x, y, z be defined by the transformations

$$x = x_4(1-\zeta) + x_3\xi\zeta - (x_3-x_2)\xi\eta\zeta$$

$$y = y_4(1-\zeta) + x_4\xi\zeta - (x_3-y_2)\xi\eta\zeta \tag{73}$$

$$z = z_4 (1-\zeta)$$

$$dV = dxdydz = \left|J(\tfrac{x,y,z}{\xi,\eta,\zeta})\right|d\xi d\eta d\zeta = 6V\,\xi\zeta^2\,d\xi d\eta d\zeta \ .$$

Using these relationships, the A terms in Equation (69) become

$$A_1 = (1-\xi)\zeta, \quad A_2 = \xi\eta\zeta, \quad A_3 = (1-\eta)\xi\zeta, \quad A_4 = 1-\zeta \ . \tag{74}$$

Thus the integrations are performed simply and the $[\tilde{m}]$ matrix is

$$[\tilde{m}] = \frac{\rho V}{20} \begin{bmatrix} 2 & 1 & 1 & 1 \\ 1 & 2 & 1 & 1 \\ 1 & 1 & 2 & 1 \\ 1 & 1 & 1 & 2 \end{bmatrix} \ . \tag{75}$$

D.   TRIANGULAR PRISM ELEMENT

I.   Introduction

Three tetrahedrons are assembled as shown in Figure II-7 to form a triangular prism element. When this approach is taken, element matrices for three tetrahedrons are computed and assembled automatically within the MAGIC III System. A considerable reduction in input is realized which leads to a corresponding reduction in the possibility of input error when large scale analyses are performed. The input required for one triangular prism is identical to that for one tetrahedron except that six node points define the prism instead of four which would define the tetrahedron.

II.   Element Static Matrices

2.1   Stiffness Matrix

The stiffness matrix for each tetrahedron which makes up the triangular prism element is computed in accordance with Equation (26) of Section C of this report. Recalling that

$$\Phi_P = 1/2 \, \lfloor \tilde{U} \rfloor \, [K] \, \{\bar{U}\} \tag{1}$$

or for each of the tetrahedrons:

$$\Phi_P^I = 1/2 \, \lfloor \Delta_6, \ \Delta_2, \ \Delta_3, \ \Delta_1 \rfloor
\begin{bmatrix}
K_{11}^I & K_{12}^I & K_{13}^I & K_{14}^I \\
 & K_{22}^I & K_{23}^I & K_{24}^I \\
 & & K_{33}^I & K_{34}^I \\
 & \text{(Symm.)} & & K_{44}^I
\end{bmatrix}
\begin{bmatrix}
\Delta_6 \\
\Delta_2 \\
\Delta_3 \\
\Delta_1
\end{bmatrix} \tag{2}$$

Where $\quad \Delta_6 = \begin{bmatrix} U_{x_6} \\ U_{y_6} \\ U_{z_6} \end{bmatrix} \qquad$ for example. The superscript I

64
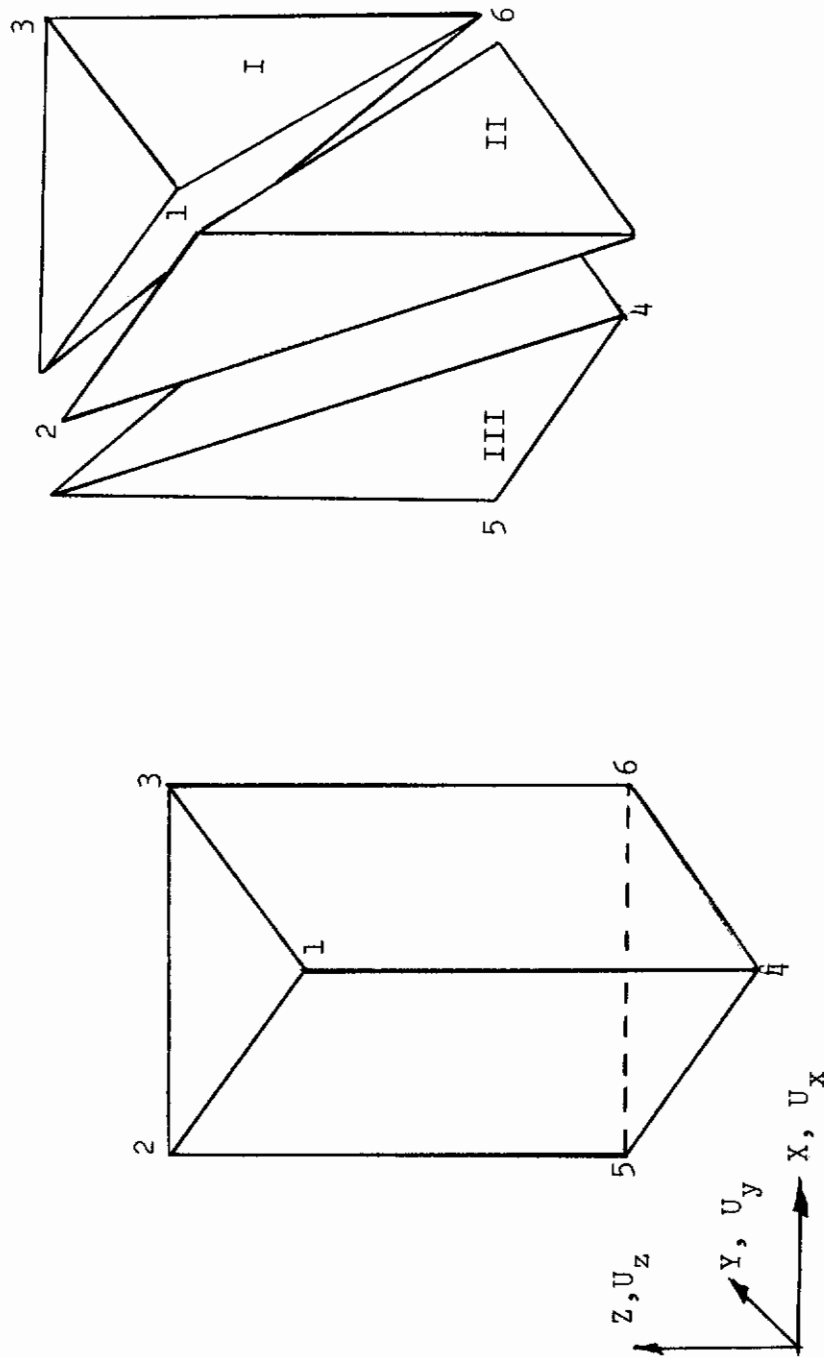
FIGURE II-7   TRIANGULAR PRISM ELEMENT

refers to tetrahedron number one. Also

$$\Phi_P^{II} = 1/2 \lfloor \Delta_6, \ \Delta_2, \ \Delta_1, \ \Delta_4 \rfloor \begin{bmatrix} K_{11}^{II} & K_{12}^{II} & K_{13}^{II} & K_{14}^{II} \\ & K_{22}^{II} & K_{23}^{II} & K_{24}^{II} \\ & & K_{33}^{II} & K_{34}^{II} \\ \text{(Symm.)} & & & K_{44}^{II} \end{bmatrix} \begin{bmatrix} \Delta_6 \\ \Delta_2 \\ \Delta_1 \\ \Delta_4 \end{bmatrix} \qquad (3)$$

$$\Phi_P^{III} = 1/2 \lfloor \Delta_2, \ \Delta_6, \ \Delta_5, \ \Delta_4 \rfloor \begin{bmatrix} K_{11}^{III} & K_{12}^{III} & K_{13}^{III} & K_{14}^{III} \\ & K_{22}^{III} & K_{23}^{III} & K_{24}^{III} \\ & & K_{33}^{III} & K_{34}^{III} \\ \text{(Symm.)} & & & K_{44}^{III} \end{bmatrix} \begin{bmatrix} \Delta_2 \\ \Delta_6 \\ \Delta_5 \\ \Delta_4 \end{bmatrix} \qquad (4)$$

The total strain energy of the prism will be the sum of the energies of the tetrahedrons. Thus, assembly of Equations (2) to (4) yields:

$$\Phi_P^P = 1/2 \lfloor \Delta^P \rfloor [K^P] \{\Delta^P\} \qquad (5)$$

where $\{\Delta^P\}^T = \lfloor \Delta_1, \ \Delta_2, \ \Delta_3, \ \Delta_4, \ \Delta_5, \ \Delta_6 \rfloor$

and the superscript P refers to prism quantities.

$[K^P]$ is the desired stiffness matrix shown in Equation (6).

66

$$[K^P]=\begin{bmatrix}
K_{44}^I+K_{33}^{II}, & K_{24}^I+K_{23}^{II}, & K_{34}^I & K_{34}^{II} & 0 & K_{14}^I+K_{13}^{II}\\[4pt]
 & K_{22}^I+K_{22}^{II}+K_{11}^{III} & K_{23}^I & K_{24}^{II}+K_{14}^{III} & K_{13}^{III} & K_{12}^I+K_{12}^{II}+K_{12}^{III}\\[4pt]
 & & K_{33}^I & 0 & 0 & K_{13}^I\\[4pt]
 & & & K_{44}^{II}+K_{44}^{III} & K_{34}^{III} & K_{14}^{II}+K_{24}^{III}\\[4pt]
 & & & & K_{33}^{III} & K_{23}^{III}\\[4pt]
\text{(Symmetric)} & & & & & K_{11}^I+K_{11}^{II}+K_{22}^{III}
\end{bmatrix}\qquad(6)$$

2.2 Stress Matrices

Recalling that

$$\{\sigma\}=[S]\,\{\bar{U}\}-[E]\,\{\bar{\epsilon}\}-\Delta T\,[E]\,\{\alpha\}\tag{7}$$

Equation (7) can be used for each tetrahedron to give

$$\{\sigma^I\}=[S^I]\,\{\bar{U}\}-[E]\,\{\bar{\epsilon}^{\,I}\}-\Delta T^I[E]\,\{\alpha\}\tag{8}$$

$$\{\sigma^{II}\}=[S^{II}]\,\{U^{II}-[E]\,\{\bar{\epsilon}^{II}\}-\Delta T^{II}\,[E]\{\alpha^{II}\}\tag{9}$$

$$\{\sigma^{III}\}=[S^{III}]\,\{U^{III}\}-[E]\,\{\bar{\epsilon}^{III}\}-\Delta T^{III}\,[E]\{\alpha^{III}\}\tag{10}$$

Neglecting the prestrain and thermal strain for the moment, Equations (8) to (10) can be rewritten as:

$$\{\sigma_o^{\,I}\} = [S_1^{\,I},\ S_2^{\,I},\ S_3^{\,I},\ S_3^{\,I}] \begin{bmatrix} \Delta_6 \\ \Delta_2 \\ \Delta_3 \\ \Delta_1 \end{bmatrix} \tag{11}$$

$$\{\sigma_o^{\,II}\} = [S_1^{\,II},\ S_2^{\,II},\ S_3^{\,II},\ S_4^{\,II}] \begin{bmatrix} \Delta_6 \\ \Delta_2 \\ \Delta_1 \\ \Delta_4 \end{bmatrix} \tag{12}$$

$$\{\sigma_o^{\,III}\} = [S_1^{\,III},\ S_2^{\,III},\ S_3^{\,III},\ S_4^{\,III}] \begin{bmatrix} \Delta_2 \\ \Delta_6 \\ \Delta_5 \\ \Delta_4 \end{bmatrix} . \tag{13}$$

Assemblying Equations (11) to (13) yields the desired relationship

$$\begin{bmatrix} \sigma_o^{\,I} \\ \sigma_o^{\,II} \\ \sigma_o^{\,III} \end{bmatrix} = \begin{bmatrix} S_4^{\,I} & S_2^{\,I} & S_3^{\,I} & 0 & 0 & S_1^{\,I} \\ S_3^{\,II} & S_2^{\,II} & 0 & S_4^{\,II} & 0 & S_1^{\,II} \\ 0 & S_1^{\,III} & 0 & S_4^{\,III} & S_3^{\,III} & S_2^{\,III} \end{bmatrix} \begin{bmatrix} \Delta_1 \\ \Delta_2 \\ \Delta_3 \\ \Delta_4 \\ \Delta_5 \\ \Delta_6 \end{bmatrix} \tag{14}$$

or, more compactly;

$$\{\sigma_o^{\,P}\} = [S^P]\, \{\Delta^P\} . \tag{15}$$

68

The contribution to the stresses from prestrain and thermal loads can be written as follows:

$$\{\sigma_{\bar{\epsilon}}{}^{I}\} = [E]\ \{\bar{\epsilon}^{I}\},\ \{\sigma_{\bar{\epsilon}}{}^{II}\} = [E]\{\bar{\epsilon}^{II}\},\ \{\sigma_{\bar{\epsilon}}{}^{III}\} = [E]\ \{\bar{\epsilon}^{III}\} \qquad (16)$$

or

$$
\begin{bmatrix}
\{\sigma_{\bar{\epsilon}}{}^{I}\} \\
\{\sigma_{\bar{\epsilon}}{}^{II}\} \\
\{\sigma_{\bar{\epsilon}}{}^{III}\}
\end{bmatrix}
=
\begin{bmatrix}
[E] & 0 & 0 \\
0 & [E] & 0 \\
0 & 0 & [E]
\end{bmatrix}
\begin{bmatrix}
\{\bar{\epsilon}^{I}\} \\
\{\bar{\epsilon}^{II}\} \\
\{\bar{\epsilon}^{III}\}
\end{bmatrix}
\qquad (17)
$$

or

$$\{\sigma_{\bar{\epsilon}}{}^{P}\} = [E_{\bar{\epsilon}}{}^{P}]\ \{\bar{\epsilon}^{P}\}\ . \qquad (18)$$

Likewise

$$\{\sigma_{\alpha}{}^{I}\} = \Delta T^{I}\ [E]\ \{\alpha^{I}\},\ \{c_{\alpha}{}^{II}\} = \Delta T^{II}\ [E]\ \{\alpha^{II}\}, \qquad (19)$$
$$\{\sigma_{\alpha}{}^{III}\} = \Delta T^{III}\ [E]\ \{\alpha^{III}\}$$

or

$$
\begin{bmatrix}
\sigma_{\alpha}^{I} \\
\sigma_{\alpha}^{II} \\
\sigma_{\alpha}^{III}
\end{bmatrix}
=
\begin{bmatrix}
\Delta T^{I}\ [E] & 0 & 0 \\
0 & \Delta T^{II}[E] & 0 \\
0 & 0 & \Delta T^{III}[E]
\end{bmatrix}
\begin{bmatrix}
\{\alpha^{I}\} \\
\{\alpha^{II}\} \\
\{\alpha^{III}\}
\end{bmatrix}
\qquad (20)
$$

or

$$\{\sigma_{\alpha}{}^{P}\} = [E_{\alpha}{}^{P}]\ \{\alpha^{P}\}\ . \qquad (21)$$

Combining equations (15), (18), and (21) yields:

$$\{\sigma^P\} = [S^P]\{\Delta^P\} - [E_{\bar{\varepsilon}}^P]\{\bar{\varepsilon}^P\} - [E_\alpha^P]\{\alpha^P\} \ . \tag{22}$$

2.3 Pre-Strain Load

The work energy is

$$\Phi_{\bar{\varepsilon}} = V \lfloor\bar{U}\rfloor [T]^T [B]^T [E]\{\bar{\varepsilon}\} = \lfloor\bar{U}\rfloor\{F_{\bar{\varepsilon}}\} \tag{23}$$

where

$$\{F_{\bar{\varepsilon}}\} = V [T]^T [B]^T [E]\{\bar{\varepsilon}\} \ .$$

Equation (23) can be rewritten as

$$\Phi_\varepsilon = \lfloor\bar{U}_1, \ \bar{U}_2, \ \bar{U}_3, \ \bar{U}_4\rfloor \begin{bmatrix} F_{1,1} \\ F_{2,1} \\ F_{3,1} \\ \cdot \\ \cdot \\ \cdot \\ F_{12,1} \end{bmatrix} \tag{24}$$

where, for example:

$$\lfloor\bar{U}_1\rfloor = \lfloor U_{x1}, \ U_{y1}, \ U_{z1}\rfloor \ .$$

Then for each tetrahedron

$$\Phi_{\bar{\varepsilon}}^{(I)} = \lfloor\Delta_6, \ \Delta_2, \ \Delta_3, \ \Delta_1\rfloor \begin{bmatrix} F_{1,1} \\ F_{2,1} \\ F_{3,1} \\ \cdot \\ \cdot \\ \cdot \\ F_{12,1} \end{bmatrix}^{(I)} \tag{25}$$

70

$$\Phi_{\bar{\varepsilon}}^{(II)} = \lfloor \Delta_6, \ \Delta_2, \ \Delta_1, \ \Delta_4 \rfloor \begin{bmatrix} F_{1,1} \\ F_{2,1} \\ F_{3,1} \\ \cdot \\ \cdot \\ \cdot \\ F_{12,1} \end{bmatrix}^{(II)} \tag{26}$$

$$\Phi_{\bar{\varepsilon}}^{(III)} = \lfloor \Delta_2, \ \Delta_6, \ \Delta_5, \ \Delta_4 \rfloor \begin{bmatrix} F_{1,1} \\ F_{2,1} \\ F_{3,1} \\ \cdot \\ \cdot \\ \cdot \\ F_{12,1} \end{bmatrix}^{(III)} \tag{27}$$

Assembly of Equations (25) to (27) yields the desired matrix:

$$\Phi_{\bar{\varepsilon}} = \lfloor \Delta^P \rfloor \ \{F_{\bar{\varepsilon}}^P\} \tag{28}$$

where the prestrain load matrix is given by:

$$\{F_{\bar{\varepsilon}}^P\} = \begin{bmatrix} F_{10,1}^{(I)} \ + \ F_{7,1}^{(II)} \\[6pt] F_{11,1}^{(I)} \ + \ F_{8,1}^{(II)} \\[6pt] F_{12,1}^{(I)} \ + \ F_{9,1}^{(II)} \\[6pt] F_{4,1}^{(I)} \ + \ F_{4,1}^{(II)} \ + \ F_{1,1}^{(III)} \\[6pt] F_{5,1}^{(I)} \ + \ F_{4,1}^{(II)} \ + \ F_{2,1}^{(III)} \\[6pt] F_{6,1}^{(I)} \ + \ F_{5,1}^{(II)} \ + \ F_{3,1}^{(III)} \\[6pt] F_{7,1}^{(I)} \end{bmatrix}$$

(Continued on next page)

71

$$
\begin{Bmatrix}
F_{8,1}^{(I)} \\
F_{9,1}^{(I)} \\
F_{10,1}^{(II)} + F_{10,1}^{(III)} \\
F_{11,1}^{(II)} + F_{11,1}^{(III)} \\
F_{12,1}^{(II)} + F_{12,1}^{(III)} \\
F_{7,1}^{(III)} \\
F_{8,1}^{(III)} \\
F_{9,1}^{(III)} \\
F_{1,1}^{(I)} + F_{1,1}^{(II)} + F_{4,1}^{(II)} \\
F_{2,1}^{(I)} + F_{2,1}^{(II)} + F_{5,1}^{(III)} \\
F_{3,1}^{(3)} + F_{3,1}^{(II)} + F_{6,1}^{(III)}
\end{Bmatrix}
\qquad (29)
$$

2.4 Thermal Load Matrix

The prism thermal load matrix $\{F_\alpha^P\}$ will be of the same form as $\{F_\varepsilon^P\}$ in Equation (29). The force entries in this vector are given by:

$$
\{F_\alpha\} = V\Delta T \, [T]^T \, [B]^T \, [E] \, \{\alpha\} \cdot \qquad (30)
$$

Equation (30) is evaluated for each tetrahedron.

72

2.5 Pressure Load Matrix

The prism pressure load matrix $\{F_P^P\}$ will be of the same form as $\{F_{\bar{\varepsilon}}^P\}$ in Equation (29). The force entries in this vector are given by:

$$\{F_P\} = [T_m]^T\left\{[[T]^T \{\tilde{F}_P\} + [T_1]^T \{\tilde{F}_{P_1}\} + [T_2]^T\{\tilde{F}_{P_2}\}\right\} \cdot (31)$$

Equation (31) is evaluated for each tetrahedron.

III. Kinetic Energy and Mass Matrix

The kinetic energy for each tetrahedron is given by:

$$\Phi_K^{(I)} = 1/2 \lfloor \dot{\Delta}_6, \dot{\Delta}_2, \dot{\Delta}_3, \dot{\Delta}_1 \rfloor [M^{(I)}]\lfloor \dot{\Delta}_6, \dot{\Delta}_2, \dot{\Delta}_3, \dot{\Delta}_1 \rfloor^T \quad (32)$$

$$\Phi_K^{(II)} = 1/2 \lfloor \dot{\Delta}_6, \dot{\Delta}_2, \dot{\Delta}_1, \dot{\Delta}_4 \rfloor [M^{(II)}] \lfloor \dot{\Delta}_6, \dot{\Delta}_2, \dot{\Delta}_1, \dot{\Delta}_4 \rfloor^T \quad (33)$$

$$\Phi_K^{(III)} = 1/2 \lfloor \dot{\Delta}_2, \dot{\Delta}_6, \dot{\Delta}_5, \dot{\Delta}_4 \rfloor [M^{(III)}]\lfloor \dot{\Delta}_2, \dot{\Delta}_6, \dot{\Delta}_5, \dot{\Delta}_4 \rfloor^T \quad (34)$$

The mass matrix for the ith tetrahedron can be written as:

$$[M^{(i)}] = \begin{bmatrix} M_{1,1} & M_{1,2} & M_{1,3} & M_{1,4} \\ M_{2,1} & M_{2,2} & M_{2,3} & M_{2,4} \\ M_{3,1} & M_{2,3} & M_{3,3} & M_{3,4} \\ M_{4,1} & M_{2,4} & M_{3,4} & M_{4,4} \end{bmatrix} \cdot \quad (35)$$

The total kinetic energy of the prism will be the sum of the kinetic energies of each tetrahedron. Assembly of Equations (32) to (34) yields:

$$\Phi_K^P = 1/2 \lfloor \dot{\Delta}^P \rfloor [M^P] \{\dot{\Delta}^P\} \quad (36)$$

where

$$\{\dot{\Delta}^P\}^T = \lfloor \dot{\Delta}_1, \dot{\Delta}_2, \dot{\Delta}_3, \dot{\Delta}_4, \dot{\Delta}_5, \dot{\Delta}_6 \rfloor$$

[M^P] is the desired mass matrix shown in Equation (37).

$$[M^P] = \begin{bmatrix}
M^I_{4,4}+M^{II}_{3,3} & & & & & \\[4pt]
M^I_{2,4}+M^{II}_{2,3} & M^I_{2,2}+M^{II}_{2,2}+M^{III}_{1,1} & & & & \\[4pt]
M^I_{3,4} & M^I_{2,3} & M^I_{3,3} & & & \\[4pt]
M^{II}_{3,4} & M^{II}_{2,4}+M^{III}_{1,4} & 0 & M^{II}_{4,4}+M^{III}_{4,4} & & \\[4pt]
0 & M^{III}_{1,3} & 0 & M^{III}_{3,4} & M^{III}_{33} & \\[4pt]
M^I_{1,4}+M^{II}_{1,3} & M^I_{1,2}+M^{II}_{1,2}+M^{III}_{1,2} & M^I_{1,3} & M^{II}_{1,4}+M^{III}_{2,4} & M^{III}_{23} & M^I_{1,1}+M^{II}_{1,1}+M^{II}_{2,2}
\end{bmatrix}$$

(Symmetric)

(37)

74

E. **SYMMETRIC TRIANGULAR PRISM ELEMENT**

I. Introduction

The symmetric triangular prism finite element shown in Figure II-8 is a special case of the full, triangular prism element discussed in Section D. This element was developed to eliminate conditioning problems inherent in the analysis of thin symmetric sections. As an example, in the analysis of aircraft wing or tail sections, the element can be used very effectively to model full-depth honeycomb core constructions which are used for shear transfer between the top and bottom skins. The use of this element allows the analysis to be performed using either the top or bottom symmetric half of the structure.

Appropriate boundary conditions are applied at the element level which specialize the full-depth prism into the symmetric element. The procedure employed in the reduction is as follows. Six tetrahedron elements are automatically assembled within the program with the three on the lower side of the plane of symmetry being the mirror images of the corresponding three tetrahedrons on the upper side. This approach assures that symmetric and antisymmetric modes will uncouple when the element is specialized to a symmetric representation. Appropriate symmetric and antisymmetric boundary conditions are imposed on the plane of symmetry at the element level. Based on these conditions, the degrees-of-freedom associated with the bottom symmetric half of the structure are expressed in terms of the remaining degrees-of-freedom. Thus, a transformation between deformations on the full prism and symmetric prism is derived which is used in a simple fashion to generate the desired matrices.

II. Element Matrices

The transformation discussed above is

(1)

$$\{\Delta^P\} = [\hat{T}] \{\Delta^{SP}\}$$
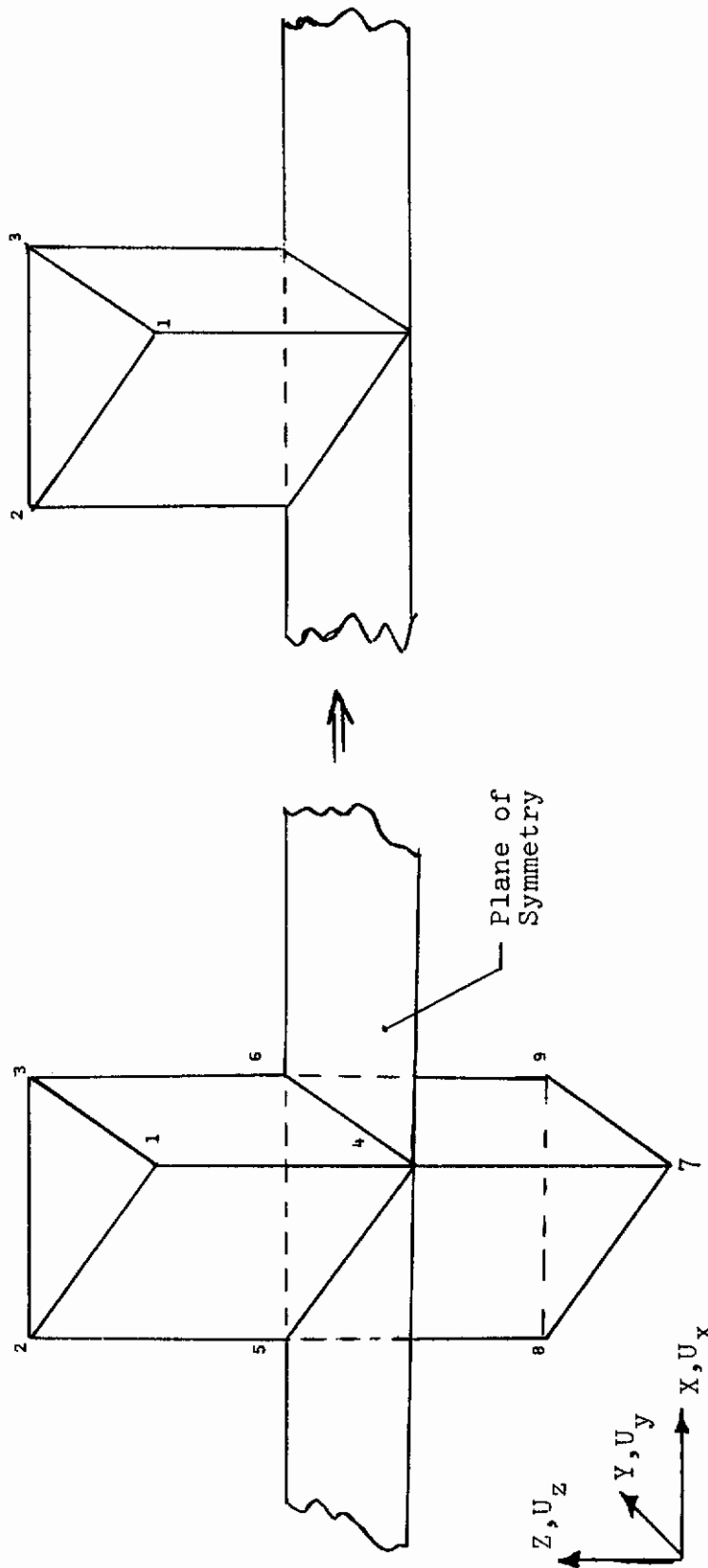
FIGURE II-8   SYMMETRIC TRIANGULAR PRISM ELEMENT

where
$$\{\Delta^P\}^T = \lfloor \Delta_1, \Delta_2, \Delta_3, \Delta_4, \Delta_5, \Delta_6 \rfloor$$

$$\Delta_i = \lfloor U_{x_i}, U_{y_i}, U_{z_i} \rfloor, \quad i = 1,2,3$$

$$\{\Delta^{SP}\}^T = \lfloor \Delta_1, \Delta_2, \Delta_3 \rfloor$$

$$[\hat{T}] = \begin{bmatrix} 1 & & & & & & & \\ & 1 & & & & & & \\ & & 1 & & & & & \\ & & & 1 & & & & \\ & & & & 1 & & & \\ & & & & & 1 & & \\ & & & & & & 1 & \\ & & & & & & & 1 \\ & 1 & & & & & & \\ & & & & & & & \\ & & 1 & & & & & \\ & & & & & & & \\ & & & & & & & 1 \end{bmatrix}$$

The superscripts P and SP refer to prism and symmetric prism respectively.

2.1 Stiffness Matrix

Use of Equation (1) in the strain energy, Equation (5) of Section D yields the stiffness matrix for the symmetric prism.

$$[K]^{SP} = [\hat{T}]^T [K^P] [\hat{T}] \cdot \tag{2}$$

2.2 Stress Matrix

The stress matrix for the symmetric prism is given by use of Equation (1) in Equation (22) of Section D.

$$\{\sigma^{SP}\} = [S^P] [\hat{T}] \{\Delta^{SP}\} - [E^P_{\bar{\varepsilon}}] \{\bar{\varepsilon}^P\} - [E^P_{\alpha}] \{\alpha^P\} \tag{3}$$

77

2.3 Prestrain, Thermal and Presssure Load Matrices

Symmetric prism prestrain, thermal and pressure load matrices are given by use of the transformation equation in Equations (28), (30), and (31) of Section D. Thus

$$\{F_{\varepsilon}^{SP}\} = [\hat{T}]^T \{F_{\varepsilon}^{P}\} \tag{4}$$

$$\{F_{\alpha}^{SP}\} = [\hat{T}]^T \{F_{\alpha}^{P}\} \tag{5}$$

$$\{F_{P}^{SP}\} = [\hat{T}]^T \{F_{P}^{P}\} \quad . \tag{6}$$

2.4 Consistent Mass Matrix

The mass matrix for the symmetric prism is obtained simply by substitution of the transformation equation in Equation (36) of Section D. Thus

$$[M^{SP}] = [\hat{T}]^T [M^{P}] [\hat{T}] \quad . \tag{7}$$

F. SYMMETRIC SHEAR WEB ELEMENT

I. Introduction

The symmetric shear web element shown in Figure II-9 was developed to conduct analyses of the type discussed in Section E. Appropriate symmetric and antisymmetric boundary conditions are imposed on the centerline of symmetry at the element level. Based on these conditions, element matrices can be readily derived only using the two upper gridpoints as reference points. The assumed displacement method is utilized to derive the stiffness and stress of the subject element.

II. Geometry

Figure II-9 depicts the geometry of the shear web element. Also shown are the local (x,y,z) and global (X,Y,Z) axes systems. The local axes are fixed in the xz plane of the element as shown in the figure. Element length, L, is given by the simple expression

$$L = [(X_2-X_1)^2 + (Y_2-Y_1)^2]^{1/2} \tag{1}$$

78
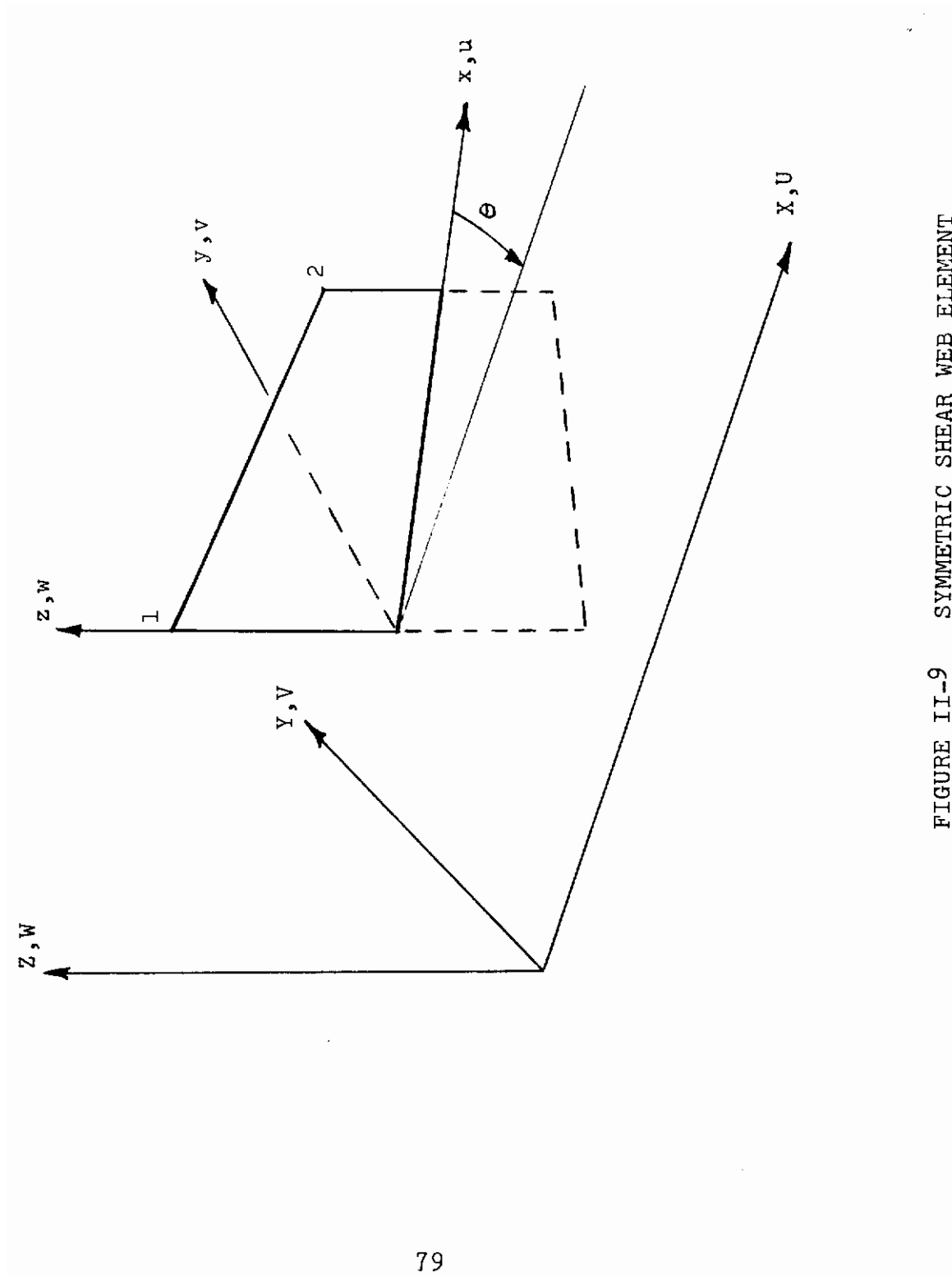
FIGURE II-9   SYMMETRIC SHEAR WEB ELEMENT

where X_1, Y_1, X_2 and Y_2 are the global coordinates of the two grid points which define the element.

The transformation from local deformations μ, w to global deformations U, V, W is given by the following:

$$\{\bar{\mu}\} = [T_{g\ell}] \, \{\bar{U}\} \tag{2}$$

where

$$\{\bar{\bar{\mu}}\}^T = \lfloor \mu_1, \; w_1, \; u_2, \; w_2 \rfloor$$

$$\{\bar{U}\}^T = \lfloor U_1, \; V_1, \; W_1, \; U_2, \; V_2, \; W_2 \rfloor$$

$$[T_{g\ell}] = \begin{bmatrix} \cos\theta & \sin\theta & 0 & 0 & 0 & 0 \\ 0 & 0 & 1 & 0 & 0 & 0 \\ 0 & 0 & 0 & \cos\theta & \sin\theta & 0 \\ 0 & 0 & 0 & 0 & 0 & 1 \end{bmatrix}$$

$$\cos\theta = \frac{x_2 - x_1}{L} \; , \quad \sin\theta = \frac{y_2 - y_1}{L} \; .$$

III. Assumed Displacement Functions

The assumed displacement functions in the local coordinate system are:

$$u = (a_1 + a_{2x}) \, z$$

$$w = b_1 + b_2 \, x + b_3 \, x^2 + b_4 \, x^3 \tag{3}$$

$$\frac{dw}{dx} = w_x = b_2 + 2b_3 x + 3b_4 x^2$$

Evaluation of Equation (3) at gridpoints 1 and 2 yields:

$$
\begin{bmatrix} u_1 \\ w_1 \\ w_{x_1} \\ u_2 \\ w_2 \\ w_{x_2} \end{bmatrix}
=
\begin{bmatrix}
z_1 & 0 & 0 & 0 & 0 & 0 \\
0 & 0 & 1 & 0 & 0 & 0 \\
0 & 0 & 0 & 1 & 0 & 0 \\
z_2 & x_2 z_2 & 0 & 0 & 0 & 0 \\
0 & 0 & 1 & x_2 & x_2^2 & x_2^3 \\
0 & 0 & 0 & 1 & 2x_2 & 3x_2
\end{bmatrix}
\begin{bmatrix} a_1 \\ a_2 \\ b_1 \\ b_2 \\ b_3 \\ b_4 \end{bmatrix}
$$

or

$$\{u\} = [\Gamma]\ \{A\} \qquad\qquad (4)$$

where

$$\{u\}^T = \lfloor u_1,\ w_1,\ w_{x_1},\ u_2,\ w_2,\ w_{x2} \rfloor$$

$$\{A\}^T = \lfloor a_1,\ a_2,\ b_1,\ b_2,\ b_3,\ b_4 \rfloor$$

$$
[\Gamma] =
\begin{bmatrix}
z_1 & 0 & 0 & 0 & 0 & 0 \\
0 & 0 & 1 & 0 & 0 & 0 \\
0 & 0 & 0 & 1 & 0 & 0 \\
z_2 & x_2 z_2 & 0 & 0 & 0 & 0 \\
0 & 0 & 1 & x_2 & x_2^2 & x_2^3 \\
0 & 0 & 0 & 1 & 2x_2 & 3x_2^2
\end{bmatrix}
$$

Thus
$$\{A\} = [\Gamma]^{-1}\ \{u\} \qquad\qquad (5)$$

where:

$$
[\Gamma]^{-1} = \begin{bmatrix}
\dfrac{1}{z_1} & 0 & 0 & 0 & 0 & 0 \\[2em]
\dfrac{-1}{x_2 z_1} & 0 & 0 & \dfrac{1}{x_2 z_2} & 0 & 0 \\[2em]
0 & 1 & 0 & 0 & 0 & 0 \\[1em]
0 & 0 & 1 & 0 & 0 & 0 \\[1em]
0 & \dfrac{-3}{x_2^2} & \dfrac{-2}{x_2} & 0 & \dfrac{3}{x_2^2} & \dfrac{-1}{x_2} \\[2em]
0 & \dfrac{2}{x_2^3} & \dfrac{1}{x_2^2} & 0 & \dfrac{-2}{x_2^3} & \dfrac{1}{x_2^2}
\end{bmatrix}
$$

Definition of the assumed displacement functions permits derivation of the strain-displacement relationships. The element strain components are:

$$
\{\varepsilon\} = \begin{bmatrix} \varepsilon_x \\ \varepsilon_z \\ \varepsilon_{xz} \end{bmatrix} = \begin{bmatrix} \partial \mu / \partial x \\ \partial w / \partial z \\ \partial \mu / \partial z + \partial w / \partial x \end{bmatrix} = \begin{bmatrix} 0 & z & 0 & 0 & 0 & 0 \\ 0 & 0 & 0 & 0 & 0 & 0 \\ 1 & x & 0 & 1 & 2x & 3x^2 \end{bmatrix} \begin{bmatrix} a_1 \\ a_2 \\ b_1 \\ b_2 \\ b_3 \\ b_4 \end{bmatrix} \qquad (6)
$$

or

$$\{\varepsilon\} = [B]\{A\} \qquad (7)$$

where

$$
[B] = \begin{bmatrix} 0 & z & 0 & 0 & 0 & 0 \\ 0 & 0 & 0 & 0 & 0 & 0 \\ 1 & x & 0 & 1 & 2x & 3x^2 \end{bmatrix} \cdot \qquad (8)
$$

82

IV.   Potential Energy, Stiffness Matrix

The potential energy is

$$\Phi_P = \frac{1}{2} \int_V \lfloor \sigma \rfloor \ \{\varepsilon\} \ dV \qquad (9)$$

Now:

$$\{\sigma\} = [E] \ \{\varepsilon\} \qquad (10)$$

where

$$\{\sigma\}^T = \lfloor \sigma_x, \ \sigma_y, \ \sigma_{xz} \rfloor$$

$$[E] = \begin{bmatrix} E_x & E_{xz} & 0 \\ E_{zx} & E_z & 0 \\ 0 & 0 & G_{xz} \end{bmatrix} \ .$$

Use of Equations (5), (7), and (10) in Equation (9) yields

$$\Phi_P = 1/2 \int_V \lfloor u \rfloor \ [\Gamma^{-1}]^T \ [B]^T \ [E] \ [B] \ [\Gamma^{-1}] \ \{u\} \ dV \qquad (11)$$

$$\Phi_P = 1/2 \lfloor u \rfloor \ [\tilde{K}] \ \{u\} \qquad (12)$$

where

$$[\tilde{K}] = \int_V [\Gamma^{-1}]^T \ [B]^T \ [E] \ [B] \ [\Gamma]^{-1} \ dV \ .$$

Substituting for the $[\Gamma]$, $[B]$ and $[E]$ matrices from above and dropping the bending terms E_x, E_z, E_{xz} in the triple product $[B]^T \ [E] \ [B]$ yields Equation (13) after integration.

83

$$[K] = \frac{tG_{xz}}{60}
\begin{bmatrix}
\dfrac{5L}{z_1^2}(3z_1+z_2) & & & & & \text{Symmetric} \\[2ex]
-\dfrac{6}{z_1}(3z_1+2z_2) & \dfrac{36}{L}(z_1+z_2) & & & & \\[2ex]
\dfrac{5L}{z_1 z_2}(z_1+z_2) & -\dfrac{6}{z_2}(2z_1+3z_2) & \dfrac{5L}{z_2^2}(z_1+3z_2) & & & \\[2ex]
\dfrac{6}{z_1}(3z_1+2z_2) & -\dfrac{36}{L}(z_1+z_2) & \dfrac{6}{z_2}(2z_1+3z_2) & \dfrac{36}{L}(z_1+z_2) & & \\[2ex]
\dfrac{L}{z_1}(6z_1-z_2) & 6z_2 & -\dfrac{L}{z_2}(z_1+4z_2) & -6z_2 & 2L(3z_1+z_2) & \\[2ex]
-\dfrac{L}{z_1}(4z_1+z_2) & 6z_1 & -\dfrac{L}{z_2}(z_1-6z_2) & -6z_1 & -L(z_1+z_2) & 2L(z_1+3z_2)
\end{bmatrix}$$

(13)

Note that this stiffness matrix is written in terms of global coordinates since z = Z at each grid point.

The deformations {u} and element stiffness matrix are now rearranged to give:

$$\Phi_P = \frac{1}{2} \lfloor \bar{u} \rfloor [\tilde{K}_1] \{\bar{u}\} \tag{14}$$

where

$$\{\bar{u}\}^T = \lfloor u_1, \; w_1, \; u_2, \; w_2, \; w_{x_1}, \; w_{x_2} \rfloor$$

$$[\tilde{K}_1] = \begin{bmatrix} K_{11} & K_{12} \\ K_{21} & K_{22} \end{bmatrix}$$

$$[K_{11}] = \frac{tGxz}{60} \begin{bmatrix} \frac{5L}{Z_1^2}(3Z_1+Z_2) & & & \text{Symmetric} \\ \frac{-6}{Z_1}(3Z_1+2Z_2) & \frac{36}{L}(Z_1+Z_2) & & \\ \frac{5L}{Z_1 Z_2}(Z_1+Z_2) & \frac{-6}{Z_2}(2Z_1+3Z_2) & \frac{5L}{Z_2^2}(Z_1+3Z_2) & \\ \frac{6}{Z_1}(3Z_1+2Z_2) & \frac{-36}{L}(Z_1+Z_2) & \frac{6}{Z_2}(2Z_1+3Z_2) & \frac{36}{L}(Z_1+Z_2) \end{bmatrix}$$

$$[K_{21}] = [K_{12}]^T = \frac{tGxz}{60} \begin{bmatrix} \frac{L}{Z_1}(6Z_1-Z_2) & 6Z_2 & \frac{-L}{Z_2}(Z_1+4Z_2) & -6Z_2 \\ \frac{-L}{Z_1}(4Z_1+Z_2) & 6Z_1 & \frac{-L}{Z_2}(Z_1-6Z_2) & -6Z_1 \end{bmatrix}$$

$$[K_{22}] = \frac{tGxz}{60} \begin{bmatrix} 2L(3Z_1+Z_2) & -L(Z_1+Z_2) \\ -L(Z_1+Z_2) & 2L(Z_1+3Z_2) \end{bmatrix} .$$

85

The transformation matrix $[\gamma]$ is formed which eliminates the w_{x_1} and w_{x_2} degrees of freedom

$$\{\bar{u}\} = [\gamma] \{\bar{\bar{u}}\} \tag{15}$$

where $\quad [\gamma] = \begin{array}{c} [I] \\[6pt] [K_{22}]^{-1} [K_{21}] \end{array}$

$\{\bar{\bar{u}}\}^T = \lfloor u_1, w_1, u_2, w_2 \rfloor$ and $[I]$ is an identity matrix.

Substitution of Equation (15) into Equation (14) yields:

$$\Phi_P = \frac{1}{2} \lfloor \bar{\bar{u}} \rfloor^T [K_R] \{\bar{\bar{u}}\} \tag{16}$$

The reduced stiffness matrix $[K_R]$ is given by Equation (17).

$$[K_R] = [\gamma]^T [\tilde{K}_1] [\gamma] = AC_1 \begin{bmatrix} 1 & & & & \text{Symmetric} \\[6pt] \dfrac{-2Z_1}{L} & 4\left(\dfrac{Z_1}{L}\right)^2 & & & \\[10pt] \dfrac{Z_1}{Z_2} & \dfrac{-2Z_1^2}{LZ_2} & \left(\dfrac{Z_1}{Z_2}\right)^2 & & \\[10pt] \dfrac{+2Z_1}{L} & -4\left(\dfrac{Z_1}{L}\right)^2 & \dfrac{2Z_1^2}{LZ_2} & 4\left(\dfrac{Z_1}{L}\right)^2 \end{bmatrix} \tag{17}$$

where

$$C_1 = \frac{t\,G_{xz}}{60(11Z_1^2 + 38Z_1 Z_2 + 11Z_2^2)}$$

$$A = \frac{45L}{Z_1^2} (Z_1 + Z_2)(Z_1^2 + 8Z_1 Z_2 + Z_2^2)$$

86

It is now necessary to transform the local deformation $\{\bar{\bar{u}}\}$ to global deformations. This is accomplished by using Equation (2) in Equation (16). Thus

$$\Phi_P = \frac{1}{2} \lfloor \bar{U} \rfloor [K] \{U\} \tag{18}$$

where the final desired stiffness matrix for the symmetric shear web is

$$[K] = [T_{g\ell}]^T [K_R] [T_{g\ell}] \quad . \tag{19}$$

V.   STRESS MATRIX

In the absence of prestrain and thermal strain, the stresses are given simply by Equation (10).

$$\{\sigma\} = [E] \{\varepsilon\} \tag{10}$$

Use of Equations (5) and (7) yields:

$$\{\sigma\} = [E] [B] [\Gamma]^{-1} \{u\} \quad . \tag{20}$$

The deformation vector $\{u\}$ is reordered to be compatible with Equation (14) through the transformation

$$\{u\} = [T_1] \{\bar{u}\} \tag{21}$$

where

$$[T_1] = \begin{bmatrix} 1 & 0 & 0 & 0 & 0 & 0 \\ 0 & 1 & 0 & 0 & 0 & 0 \\ 0 & 0 & 0 & 0 & 1 & 0 \\ 0 & 0 & 1 & 0 & 0 & 0 \\ 0 & 0 & 0 & 1 & 0 & 0 \\ 0 & 0 & 0 & 0 & 0 & 1 \end{bmatrix}$$

Use of Equations (21), (15) and (2) in Equation (20) yields:

$$\{\sigma\} = [\tilde{S}] \, [T_{g\ell}] \, \{\bar{U}\} \tag{22}$$

where for $x = L/2$ and dropping the bending terms gives:

$$[\tilde{S}] = \frac{G_{xz} \, (6Z_1{}^2 + 48Z_1 Z_2 + 6Z_2{}^2)}{(11Z_1{}^2 + 38Z_1 Z_2 + 11Z_2{}^2)} \begin{bmatrix} 0 & 0 & 0 & 0 \\ 0 & 0 & 0 & 0 \\ \dfrac{1}{2Z_1} & \dfrac{-1}{L} & \dfrac{1}{2Z_2} & \dfrac{1}{L} \end{bmatrix} \cdot \tag{23}$$

G. TRIANGULAR RING ELEMENT (Asymmetric Loading)

I. Introduction

The formulation of the triangular cross-section ring element described herein is derived from, and is mathematically consistent with, the formulation described in References 13, 14, and 15. This ring element provides a powerful tool for the analysis of thick-walled and solid axisymmetric structures of finite length. It may be used to idealize any axisymmetric structure taking into account:

1. arbitrary axial variations in geometry,
2. axial variation in orientation of material axes of orthotropy,
3. radial and axial variations in material properties,
4. any asymmetric loading system including pressure and temperature, and
5. degradation of material properties due to temperature.

88

The discrete element technique was first applied to the analysis of axisymmetric solids by Clough and Rashid[16]. The formulation of the triangular cross-section ring was extended by Wilson[17] to include nonaxisymmetric as well as axisymmetric loads.

Wilson's formulation for the asymmetric case was extended in Reference [18] to include orthotropic material properties with variable orientation axes. This extended development is presented here as well as a more precise means of effecting the integration of the strain energy over the volume of the ring. Thermal and pressure load vectors and mass matrices are also developed.

Thus, the discrete element representation presented consists of algebraic expression for the following matrices:

1. Stiffness , $[K]$

2. Pressure Load , $\{F_p\}$

3. Thermal Load , $\{F_T\}$

4. Gravity Load , $\{F_G\}$

5. Centrifugal Load , $\{C_G\}$

6. Stress , $[S]$

7. Mass , $[M]$

The matrices arise as coefficient matrices in the Lagrange equations for the element. The appropriate generalized form of the Lagrange equation is

$$\frac{\partial \Phi_1}{\partial q_r} + \frac{d}{dt}\left(\frac{\partial \Phi_2}{\partial q_r}\right) = 0$$

where

q_r = r^{th} generalized displacement coordinate

Φ_1 = total potential energy

Φ_2 = kinetic energy

q_r = r^{th} generalized velocity coordinate

89

Various quantities in the following development will be expanded in terms of Fourier series. The set of unbarred amplitudes which make up these series are referred to as the A series coefficients and the barred quantities are referred to as the B series coefficients.

II. Displacement Functions for the Triangular Element

The element generalized displacements (see Figure II-10), can be expressed in Fourier series form.

$$u(r,z,\theta) = u_o(r,z) + \sum_{j=1}^{\infty} u_j(r,z) \cos j\theta + \sum_{j=1}^{\infty} \bar{u}_j(r,z) \sin j\theta \quad (1)$$

$$V(r,z,\theta) = v_o(r,z) + \sum_{j=1}^{\infty} V_j(r,z) \sin j\theta + \sum_{j=1}^{\infty} \bar{V}_j(r,z) \cos j\theta \quad (2)$$

$$w(r,z,\theta) = w_o(r,z) + \sum_{j=1}^{\infty} w_j(r,z) \cos j\theta + \sum_{j=1}^{\infty} \bar{w}_j(r,z) \sin j\theta \quad (3)$$

Linear displacement amplitudes (in the r and Z directions) are assumed.

$$u_j = \beta_{1j} + \beta_{2j} r + \beta_{3j} Z \quad (4)$$

$$V_j = \beta_{4j} + \beta_{5j} r + \beta_{6j} Z \quad (5)$$

$$W_j = \beta_{7j} + \beta_{8j} r + \beta_{9j} Z \quad (6)$$

Note that continuity of displacement across element boundaries is preserved. A transformation from generalized coordinates to grid point displacement coordinates is effected by writing

$$U_{ij} = \beta_{1j} + \beta_{2j} r_i + \beta_{3j} Z_i \quad (7)$$

$$V_{ij} = \beta_{4j} + \beta_{5j} r_i + \beta_{6j} Z_i$$

$$W_{ij} = \beta_{7j} + \beta_{8j} r_i + \beta_{9j} Z_i$$

90

The generalized coordinates, $\{\beta_i\}$, can be expressed (on the harmonic level) in terms of grid point coordinates $\{q_i\}$ as

$$\{\beta_j\} = [\Gamma_{\beta q}] \{q_j\} \tag{8}$$

where

$$\{q_j\}^T = \lfloor U_{1j}, \; V_{1j}, \; W_{1j}, \; U_{2j}, \; V_{2j}, \; W_{2j}, \; U_{3j}, \; V_{3j}, \; W_{3j} \rfloor \tag{9}$$

$$\{\beta_j\} = \lfloor \beta_{1j}, \; \beta_{2j}, \; \beta_{3j}, \; \beta_{4j}, \; \beta_{5j}, \; \beta_{6j}, \; \beta_{7j}, \; \beta_{8j}, \; \beta_{9j} \rfloor \tag{10}$$

From Equation (7), with reference to Figure (II-10)

$$[\Gamma_{\beta q}] = \begin{bmatrix} 1 & r_1 & Z_1 & 0 & 0 & 0 & 0 & 0 & 0 \\ 0 & 0 & 0 & 1 & r_1 & Z_1 & 0 & 0 & 0 \\ 0 & 0 & 0 & 0 & 0 & 0 & 1 & r_1 & Z_1 \\ 1 & r_2 & Z_2 & 0 & 0 & 0 & 0 & 0 & 0 \\ 0 & 0 & 0 & 1 & r_2 & Z_2 & 0 & 0 & 0 \\ 0 & 0 & 0 & 0 & 0 & 0 & 1 & r_2 & Z_2 \\ 1 & r_3 & Z_3 & 0 & 0 & 0 & 0 & 0 & 0 \\ 0 & 0 & 0 & 1 & r_3 & Z_3 & 0 & 0 & 0 \\ 0 & 0 & 0 & 0 & 0 & 0 & 1 & r_3 & Z_3 \end{bmatrix} \tag{11}$$

which is non-singular.

91
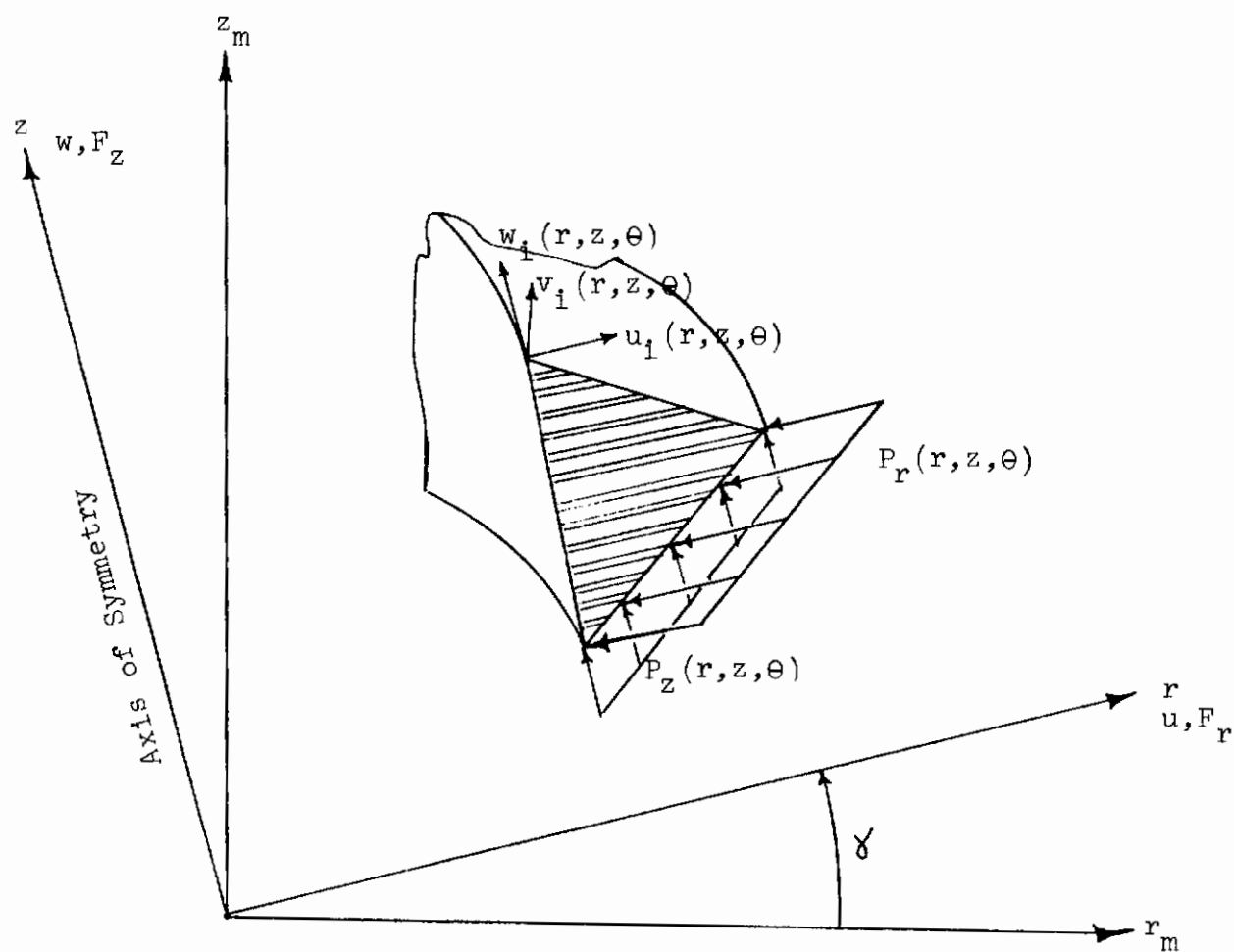
FIGURE II-10 TRIANGULAR RING ELEMENT (ASYMMETRIC LOADING)

Defining $\{q_j^*\}$ as follows,

$$\{q_j^*\} = \lfloor U_j, \ V_j, \ W_j \rfloor \tag{12}$$

Equations (4) thru (6) can be expressed in matrix form as shown below

$$\{q_j^*\} = [\beta(r,z)] \ \{\beta_j\} \ . \tag{13}$$

Substituting Equation (8) into Equation (13), an expression relating the generalized element displacements to the element nodal displacements (on the harmonic level) can be obtained. This relation is given by Equation (14)

$$\{q_j^*\} = [\lambda] \ \{q_j\} \tag{14}$$

where

$$[\lambda] = [\beta(r,z)] \ [\Gamma_{\beta q}] \ . \tag{15}$$

$[\lambda]$ can be expressed in explicit form as follows,

$$[\lambda] \quad \begin{bmatrix} \lambda_1 & 0 & 0 & \lambda_2 & 0 & 0 & \lambda_3 & 0 & 0 \\ 0 & \lambda_1 & 0 & 0 & \lambda_2 & 0 & 0 & \lambda_3 & 0 \\ 0 & 0 & \lambda_1 & 0 & 0 & \lambda_2 & 0 & 0 & \lambda_3 \end{bmatrix} \tag{16}$$

where

$$\lambda_1 = (r_2 z_3 - z_2 r_3 - (z_3 - z_2)r + (r_3 - r_2)Z)/|A|$$

$$\lambda_2 = (z_1 r_3 - r_1 z_3 + (z_3 - z_1)r - (r_3 - r_1)Z)/|A| \tag{17}$$

$$\lambda_3 = (r_1 z_2 - z_1 r_2 - (z_2 - z_1)r + (r_2 - r_1)Z)/|A|$$

$$|A| = |r \ z_3 + r_1 z_2 + z_1 r_3 - z_2 r_3 - r_1 z_3 - r_2 z_1|$$

93

III. <u>Potential Energy</u>

The total potential energy is derived as the sum of strain energy and external work contributions.

The strain energy density is defined as

$$U' = \int \lfloor d\epsilon \rfloor \{\sigma\} \tag{18}$$

where

$$\{\epsilon\}^T = \lfloor \epsilon_{rr}, \; \epsilon_{zz}, \; \epsilon_{\theta\theta}, \; \epsilon_{xz}, \; \epsilon_{r\theta}, \; \epsilon_{z\theta} \rfloor \tag{19}$$

$$\{\sigma\}^T = \lfloor \sigma_{rr}, \; \sigma_{zz}, \; \sigma_{\theta\theta}, \; \sigma_{xz}, \; \sigma_{r\theta}, \; \sigma_{z\theta} \rfloor \; . \tag{20}$$

Linear elastic material behavior is assumed from the initial state of strain $\{\epsilon_i\}$ to the final state of stress $\{\sigma\}$ and strain $\{\epsilon\}$,

$$\{\sigma^{(m)}\} = [E^{(m)}] \left\{ \{\epsilon^{(m)}\} - \{\epsilon_i^{(m)}\} \right\} \; , \tag{21}$$

where the superscript (m) is used to indicate that the elastic modulus matrix $[E^{(m)}]$ is evaluated in a coordinate system defined for the material that may be different than the r, z system (see Figure II-10).

The matrix of elastic constants for an orthotropic body with respect to cylindrical coordinate axes is

$$[E^{(m)}] = \frac{1}{\Delta} \begin{bmatrix} E_r(1-\nu_{\theta z}\nu_{z\theta}), & E_r(\nu_{zr} + \nu_{z\theta}\nu_{\theta r}), & E_r(\nu_{\theta r} + \nu_{zr}\,\nu_{\theta z}), & 0, & 0, & 0 \\ & E_z(1-\nu_{r\theta}\nu_{\theta r}), & E_\theta(\nu_{\theta z} + \nu_{r\theta}\,\nu_{zr}), & 0, & 0, & 0 \\ & & E_\theta(1-\nu_{rz}\,\nu_{zr}), & 0, & 0, & 0 \\ & & & \Delta G_{rz}, & 0, & 0 \\ & \text{Symmetric} & & & \Delta G_{r\theta}, & 0 \\ & & & & & \Delta G_{z\theta} \end{bmatrix} \tag{22}$$

94

where

$$\Delta = 1 - \nu_{r\theta}\nu_{\theta r} - \nu_{\theta z}\nu_{z\theta} - \nu_{zr}\nu_{rz} - \nu_{r\theta}\nu_{\theta z}\nu_{zr} - \nu_{rz}\nu_{\theta r}\nu_{z\theta} . \qquad (23)$$

From symmetry

$$E_r \nu_{\theta r} = E_\theta \nu_{r\theta}; \; E_r \nu_{zr} = E_z \nu_{rz}; \; E_z \nu_{\theta z} = E_\theta \nu_{z\theta} . \qquad (24)$$

Poisson's ratio, ν_{ij}, is defined as the ratio of the strain in the j direction to the strain in the i direction due to a stress in the i direction.

Equation (22) is more conveniently written in the following manner:

$$[E^{(m)}] = \begin{bmatrix} E_{11}^{(m)} & E_{12}^{(m)} & E_{13}^{(m)} & 0 & 0 & 0 \\ & E_{22}^{(m)} & E_{23}^{(m)} & 0 & 0 & 0 \\ & & E_{33}^{(m)} & 0 & 0 & 0 \\ & & & E_{44}^{(m)} & 0 & 0 \\ & & & & E_{55}^{(m)} & 0 \\ & & & & & E_{66}^{(m)} \end{bmatrix} . \qquad (25)$$

Substitution of the assumed constituitive relations into the strain energy density, and the integration, yields

$$U' = 1/2 \, \{\epsilon^{(m)}\}^T \, [E^{(m)}] \, \{\epsilon^{(m)}\} - \{\epsilon^{(m)}\}^T \, [E^{(m)}] \, \{\epsilon_i^{(m)}\} . \qquad (26)$$

If the material axes $\{r^{(m)}\}$ are oriented at an angle γ from the element geometric axes (see Figure II-10), a transformation must be introduced

$$\{\epsilon^{(m)}\} = [T_{\epsilon\sigma}] \, \{\epsilon\} \qquad (27)$$

$$\{\sigma^{(m)}\} = [T_{\epsilon\sigma}] \, \{\sigma\} \qquad (28)$$

95

$$[T_{\varepsilon\sigma}] = \begin{bmatrix} \cos^2\gamma & \sin^2\gamma & 0 & 2\sin\gamma\cos\gamma & 0 & 0 \\ \sin^2\gamma & \cos^2\gamma & 0 & -2\sin\gamma\cos\gamma & 0 & 0 \\ 0 & 0 & 1 & 0 & 0 & 0 \\ -\sin\gamma\cos\gamma & \sin\gamma\cos\gamma & 0 & \cos^2\gamma-\sin^2\gamma & 0 & 0 \\ 0 & 0 & 0 & 0 & \cos\gamma & \sin\gamma \\ 0 & 0 & 0 & 0 & -\sin\gamma & \cos\gamma \end{bmatrix} \quad (29)$$

Substituting back into Equation (26) and integrating over the volume of the element, we obtain

$$U' = \quad (1/2 \{\varepsilon\}^T [E] \{\varepsilon\} - \{\varepsilon\}^T [E] \{\varepsilon_1\}) \, dV \quad (30)$$

where

$$[E] = [T_{\varepsilon\sigma}]^T [E^{(m)}] [T_{\varepsilon\sigma}] \, . \quad (31)$$

Equation (30) is the desired form of the potential energy.

The strains, Equation (19) are related to displacements as follows in a cylindrical coordinate system.

$$\{\varepsilon\}^T = \lfloor U_r, \; W_z, \; U/r + V_\theta/r, \; U_z+W_r, \; 1/r(U_\theta-V)+V_r, V_z+1/rW_\theta \rfloor \quad (32)$$

where

$$U_r = \frac{\partial u}{\partial r} \; , \; \text{Etc.} \quad (33)$$

IV.   Stiffness Matrix for the Triangular Element

In order to effect the discretization of the element, the assumed displacement functions are introducted into the potential energy function. Substitution of the total potential energy function into the Lagrange equations yields the element matrices with respect to gridpoint displacements. Stiffness and mass matrices, as well as load vectors, are derived in this way. The element stress matrix is derived from the strain-displacement and stress-strain relations.

The energy contribution of linear elastic stiffness is, in terms of strains,

$$\Phi_K = 1/2 \quad \{\epsilon\}^T [E] \{\epsilon\} \, dv \tag{34}$$

In recognition of the fact that the generalized displacements were described in Fourier series form, the strains can be described as shown in Equation (35).

$$\{\epsilon\} = \{\epsilon_o\} + \sum_{j=1}^{\infty} \lceil C_j \rfloor \{\epsilon_j\} + \sum_{j=1}^{\infty} \lceil \bar{C}_j \rfloor \{\bar{\epsilon}_j\} \tag{35}$$

For the A series, j^{th} harmonic $\{\epsilon_j\}$ is expressed as follows,

$$\{\epsilon_j\}^T = \lfloor \epsilon_{rr_j}, \; \epsilon_{zz_j}, \; \epsilon_{\theta\theta_j}, \; \epsilon_{rz_j}, \; \epsilon_{r\theta_j}, \; \epsilon_{z\theta_j} \rfloor \tag{36}$$

and the Matrix $\lceil c_j \rfloor$ is a diagonal matrix which appears as given in Equation (37).

$$\lceil c_j \rfloor = \lceil \cos j\theta, \; \cos j\theta, \; \cos j\theta, \; \cos j\theta, \; \sin j\theta, \; \sin j\theta \rfloor \tag{37}$$

Matrix $\lceil \bar{C}_j \rfloor$ is given by Equation (38).

$$\lceil \bar{C}_j \rfloor = \lceil \sin j\theta, \; \sin j\theta, \; \sin j\theta, \; \sin j\theta, \; \cos j\theta, \; \cos j\theta \rfloor \tag{38}$$

Expressing the strains (on the harmonic level) in terms of the generalized coordinates using Equations 4, 5, 6, and 32 yields

$$\{\epsilon_j\} = [D_j] \{\beta_j\} \tag{39}$$

where

$$\{\beta_j\}^T = \lfloor \beta_{1_j} \; . \; . \; . \; \beta_{9_j} \rfloor$$

97

and

$$[D_j] = \begin{bmatrix} 0 & 1 & 0 & 0 & 0 & 0 & 0 & 0 & 0 \\ 0 & 0 & 0 & 0 & 0 & 0 & 0 & 0 & 1 \\ 1/r & 1 & Z/r & j/r & j & jZ/r & 0 & 0 & 0 \\ 0 & 0 & 1 & 0 & 0 & 0 & 0 & 1 & 0 \\ -j/r & -j & -jZ/r & -1/r & 0 & -Z/r & 0 & 0 & 0 \\ 0 & 0 & 0 & 0 & 0 & 1 & -j/r & -j & -jZ/r \end{bmatrix} \qquad (40)$$

where for the B series j assumes the value of $-j$ in Equation
(40). The differential volume is

$$dV = r \, d\theta \, dz \, dr . \qquad (41)$$

Substituting Equations (35) and (41) into Equation (34),
and integrating with respects to θ yields

$$\Phi_K = 2\pi \int_r \int_z \lfloor \varepsilon_0 \rfloor [E] \{\varepsilon_0\} \, r \, dz \, dr + \pi \sum_{j=1}^{\infty} \int_r \int_z \lfloor \varepsilon_j \rfloor [E] \{\varepsilon_j\} r \, dz \, dr$$

$$+ \pi \sum_{j=1}^{\infty} \int_r \int_z \lfloor \bar{\varepsilon}_j \rfloor [E] \{\bar{\varepsilon}_j\} \, r \, dz \, dr . \qquad (42)$$

It can be seen that the energy term represented by Equation (34)
uncouples harmonically (Equation 42) due to the orthogonality
conditions which exist mathematically for the triangular ring.
The energy component for the Ath series, j[th] harmonic is

$$\Phi_{kj} = \pi \int_r \int_z \lfloor \varepsilon_j \rfloor [E] \{\varepsilon_j\} \, r \, dz \, dr \qquad (43)$$

and by substituting Equation (39) into Equation (43)

$$\Phi_{kj} = \pi \int_r \int_z \lfloor \beta_j \rfloor [D_j]^T [E] [D_j] \{\beta_j\} \, r \, dz \, dr . \qquad (44)$$

98

Noting that the generalized coordinates are not variable functions of r and Z, we can write

$$\Phi_{kj} = \lfloor \beta_j \rfloor \left[\pi \int_r \int_z r[D_j]^T [E] [D_j] \, dzdr \right] \{\beta_j\} \tag{45}$$

where the triple matrix product $r[D_j]^T [E] [D_j]$ is given by Equation (46) on the following page.

By inspection of the matrix in Equation (46), we see that all the integrals in Equation (43) are the type

$$\delta_{ij} = \int r^i \, z^j \, dzdr . \tag{47}$$

The integration is carried out over the interior of the element, shown in Figure II-10. The integration is performed in two parts:

1) Between the lines 1-2 and 1-3, i.e. between

$z = k_{12} \, r + m_{12}$ and $z = k_{13} \, r + m_{13}$ from r_1 to r_3.

2) Between the lines 1-2 and 3-2, i.e., between $z = k_{12}$

$r + m_{12}$ and $z = k_{32} \, r + m_{32}$ from r_3 to r_2.

where

$$K_{12} = \frac{Z_2 - Z_1}{r_2 - r_1} \qquad\qquad M_{12} = - \frac{r_1 Z_2 - r_2 Z_1}{r_2 - r_1}$$

$$K_{13} = \frac{Z_3 - Z_1}{r_3 - r_1} \qquad\qquad M_{13} = - \frac{r_1 Z_3 - r_3 Z_1}{r_3 - r_1} \tag{48}$$

$$K_{32} = \frac{Z_2 - Z_3}{r_2 - r_3} \qquad\qquad M_{32} = - \frac{r_3 Z_2 - r_2 Z_3}{r_2 - r_3}$$

Triple Matrix product $r[D_j]^T[E][D_j] =$

$$r[D_j]^T[E][D_j] =
\begin{bmatrix}
[E_{33}+j^2E_{55}]\frac{1}{r} & [E_{13}+E_{33}+j^2E_{55}] & [E_{33}+j^2E_{55}]\frac{z}{r}+E_{34} & [E_{33}+E_{55}]\frac{1}{r} & jE_{33} & E_{23}+j^2\frac{z}{r}E_{56} \\[6pt]
 & [E_{11}+2E_{13}+E_{33}+j^2E_{55}]r & [E_{13}+E_{33}+j^2E_{55}]z+(E_{14}+E_{34})r & [E_{13}+E_{33}+E_{55}]j & [E_{13}+E_{33}]jr & [E_{12}+E_{23}]r+j^2zE_{56} \\[6pt]
 & & \{E_{33}+j^2E_{55}\}\frac{z^2}{r}+E_{44}r+2zE_{34}+E_{56} & \{E_{33}+E_{55}\}j\frac{z}{r}+jE_{34} & E_{33}jz+jrE_{34} & zE_{23}+E_{24}r+\frac{j^2z^2}{r}E_{56} \\[6pt]
 & & & (E_{55}+j^2E_{33})\frac{1}{r}-E_{56} & j^2E_{33} & jE_{23}+\frac{jz}{r}E_{56} \\[6pt]
 & \text{SYMMETRIC} & & & j^2rE_{33} & jrE_{23} \\[6pt]
 & & & & & E_{22}r+\frac{j^2z^2}{r}E_{66}
\end{bmatrix}
\qquad (46)$$

The potential energy component for the specified harmonic (A series, j^{th} harmonic) is related to the stiffness matrix for that harmonic, $[\widetilde{K}_j]$, referred to generalized coordinates as follows

$$\phi_{kj} = \{\beta_j\}^T [\widetilde{K}_j] \{\beta_j\} \ . \qquad (49)$$

$[\widetilde{K}_j]$ is recognized as the integral in Equation (45). Its terms are evaluated by substituting the appropriate δ_{ij} integrals (see Equation (47)) for the powers of r and Z in Equation (46) as well as the substitution of the appropriate harmonic number j. The result is presented on the following page in Equation (50).

Introducing the transformation to gridpoint displacements, Equation (8) of Section II, and taking the first variation with respect to the displacements, we obtain the element stiffness matrix

$$[K_j] = [\Gamma_{\beta q}]^T [K_j] [\Gamma_{\beta q}] \ . \qquad (51)$$

Through a judicious choice of displacement functions, the essentially three-dimensional character of the ring changes to one inherently two-dimensional in nature. Thus, an essentially three-dimensional problem (asymmetric loading on a solid of revolution) can be solved by undertaking a series of two-dimensional applications of the stiffness matrix given by Equation (51).

V.   Load Vectors for the Triangular Element

5.1 Distributed Load Vector

The external work potential for a system of distributed loads (see Figure II-10) acting on the element face can be represented in the most general form as follows:

101

$$[\bar{R}_j] = \tag{50}$$

$$
\begin{array}{l}
[E_{33}+J^2E_{55}]\delta_{-1,0} \quad [E_{13}+E_{33}+J^2E_{55}]\delta_{0,0} \quad [E_{33}+J^2E_{55}]\delta_{-1,1} \quad [E_{33}+E_{55}]\delta_{-1,0} \quad \delta_{0,0} \quad (E_{33}+E_{55})J\delta_{-1,1} \\[2pt]
\hspace{20em} +E_{34}\delta_{0,0} \hspace{10em} -JE_{56}\delta_{0,0} \\[10pt]

\{E_{11}+2E_{13}+E_{33}\} \quad \{E_{13}+E_{33}+J^2E_{55}\}\delta_{0,0} \quad [E_{13}+E_{33}+E_{55}]\delta_{0,0} \quad [E_{13}+E_{33}]J\delta_{0,1} \quad [E_{13}+E_{33}+J^2E_{55}]\delta_{0,1} \quad [E_{14}+E_{34}] \\[2pt]
+J^2E_{55}]\delta_{-1,0} \hspace{34em} +J^2E_{56}]\delta_{-1,0} \\[2pt]
+J^2E_{55}\delta_{-1,0} \hspace{34em} -JE_{56}\delta_{1,0} \\[10pt]

[E_{13}+E_{33}+J^2E_{55}]\delta_{0,1} \quad +(E_{14}+E_{34})\delta_{1,0} \quad JE_{33}\delta_{0,1} \quad J^2E_{56}\delta_{0,0} \quad E_{44}+ \\[10pt]

\{E_{33}+J^2E_{55}\}\delta_{-1,2} \quad [E_{33}+E_{55}]J\delta_{-1,1} \quad +JE_{34}\delta_{1,0} \quad J^2E_{56}\delta_{-1,1} \quad \{E_{34}+J^2E_{56}\}\delta_{0,1} \\[2pt]
+E_{44}\delta_{1,0} \quad +JE_{34}\delta_{0,0} \hspace{14em} +E_{24}\delta_{1,0} \\[2pt]
+2E_{34}\delta_{0,1} \hspace{28em} +J^2E_{56}\delta_{-1,2} \\[10pt]

\{E_{55}+J^2E_{33}\}\delta_{-1,0} \quad J^2\delta_{0,0}E_{33} \quad \{E_{55}+J^2E_{33}\}\delta_{-1,1} \quad -\delta_{0,0}E_{56} \quad J\delta_{0,0}E_{23} \\[2pt]
\hspace{26em} J\delta_{0,0}(E_{34}+E_{56}) \quad +J\delta_{-1,1}E_{56} \\[10pt]

J^2\delta_{1,0}E_{33} \quad J\delta_{-1,0}E_{56} \quad 0 \quad J\delta_{1,0}E_{34} \quad J\delta_{1,0}E_{23} \\[10pt]

\{E_{55}+J^2E_{33}\}\delta_{-1,2} \quad J\delta_{-1,1}E_{56} \quad -J\delta_{1,0}E_{66} \quad J\delta_{0,1}(E_{23}-E_{66}) \\[2pt]
+E_{66}\delta_{1,0} \hspace{10em} +J\delta_{0,0}E_{66} \quad +J\delta_{-1,2}E_{56} \\[2pt]
-2\delta_{0,1}E_{56} \\[10pt]

J^2\delta_{-1,0}E_{66} \quad J^2E_{66}\delta_{0,0} \quad J^2\delta_{-1,1}E_{66} \\[10pt]

\{E_{44}+J^2E_{66}\}\delta_{1,0} \quad J^2\delta_{0,1}E_{66} \\[10pt]

E_{22}\delta_{1,0} \\[2pt]
+E_{24}\delta_{1,0} \\[2pt]
+J^2\delta_{-1,2}E_{66}
\end{array}
$$

SYMMETRIC

102

$$V_d = \iint\limits_{s\ \theta} \lfloor q* \rfloor \ \{P\} \ r \ d\theta \ dS \ .$$
(52)

The most general distributed load system which could be applied to the element is expressed in the following Fourier series relationships:

$$P_r \ (r,z,\theta) = P_{ro} \ (r,z) + \sum_{j=1}^{\infty} P_{rj}(r,z) \cos j\theta$$

$$+ \sum_{j=1}^{\infty} \overline{P}_{rj} \ (r,z) \sin j\theta$$

$$P_\theta(r,z,\theta) = P_\theta(r,z) + \sum_{j=1}^{\infty} P_{\theta j}(r,z) \sin j\theta$$
(53)

$$+ \sum_{j=1}^{\infty} \overline{P}_{\theta j}(r,z) \cos j\theta$$

$$P_z(r,z,\theta) = P_{zo}(r,z) + \sum_{j=1}^{\infty} P_{zj}(r,z) \cos j\theta$$

$$+ \sum_{j=1}^{\infty} P_{zj}(r,z) \sin j\theta$$

If typically for the A series, j^{th} harmonic

$$\{P_j\}^T = \lfloor P_{rj}, \ P_{zj}, \ P_{\theta j} \rfloor$$
(54)

and

$$\lceil C_j^\circ \rfloor = \lceil \cos j\theta, \ \sin j\theta, \ \cos j\theta \rfloor$$
(55)

$$\lceil \bar{C}^\circ_j \rfloor = \lceil \sin j\theta, \ \cos j\theta, \ \sin j\theta \rfloor$$
(56)

103

Then {P} and {q*} (see Section II, Equation (13)) can be described as follows

$$\{P\} = \{P_o\} + \sum_{j=1}^{\infty} \lceil C^o_j \rfloor \{P_j\} + \sum_{j=1}^{\infty} \lceil \bar{C}_j{}^o \rfloor \{\bar{P}_j\} \qquad (57)$$

$$\{q*\} = \{q*_o\} + \sum_{J=1}^{\infty} \lceil C^o_J \rfloor \{q*_j\} + \sum_{j=1}^{\infty} \lceil \bar{C}_j{}^o \rfloor \{\bar{q}*_j\} \ . \qquad (58)$$

Substituting Equations (57) and (58) into Equation (52), the following result is obtained

$$V_d = 2\pi \int_s \lfloor q*_o \rfloor \{P_o\} \ r \ ds + \sum_{j=1}^{\infty} \int_s \lfloor q*_j \rfloor \{P_j\} r \ ds$$

$$\qquad (59)$$

$$+ \sum_{j=1}^{\infty} \pi \int_s \lfloor \bar{q}*_j \rfloor \{\bar{P}_j\} \ r \ ds \ .$$

It can be seen that the external work potential due to the applied distributed loads uncouples harmonically as did the internal energy term ϕ_k; in Section IV. For the Ath series, j^{th} harmonic

$$V_{d_j} = \pi \int_s \lfloor q*_j \rfloor \{P_j\} \ r \ ds \ . \qquad (60)$$

Relating generalized element displacements to element nodal displacements in Equation (60) via Equation 14 of Section II, Equation (60) can be written as follows:

$$V_{d_j} = \pi \int_s \lfloor q_j \rfloor [\lambda]^T \{P_j\} r \ ds \ . \qquad (61)$$

104

Noticing that the generalized nodal coordinates are not a function of ds, Equation (61) can be rewritten as follows:

$$V_{d_j} = \lfloor q_j \rfloor \, \Pi \int_s [\lambda]^T \{P_j\} \, r \, ds \ . \tag{62}$$

Substituting Equation (62) into the Lagrange Equation, it can be shown that generalized equivalent nodal loads $\{F_{p_j}\}$ can be defined which act on the generalized nodal coordinates and which represent the mathematical equivalent to the applied distributed load system.

$\{F_{p_j}\}$ can be defined as follows

$$\{F_{p_j}\} = \Pi \int_s [\lambda]^T \{P_j\} r \, ds \tag{63}$$

where

$$\{F_{p_j}\}^T = \lfloor F_{p_j}^{1r}, \ F_{p_j}^{1z}, \ F_{p_j}^{1\theta}, \ F_{p_j}^{2r}, \ F_{p_j}^{2z}, \ F_{p_j}^{2\theta}, \ F_{p_j}^{3r}, \ F_{p_j}^{3z}, \ F_{p_j}^{3\theta} \rfloor$$

expressing the following relationships,

$$Z = K_{12} \, r + M_{12} \tag{64}$$

where

$$K_{12} = \frac{z_2 - z_1}{r_2 - r_1} \tag{65}$$

$$M_{12} = \frac{r_2 z_1 - r_1 z_2}{r_2 - r_1} \tag{66}$$

and where

$$ds = \sqrt{dr^2 + dz^2} = \frac{dz}{\sin \alpha} \tag{67}$$

it can be shown that the matrix of equivalent nodal forces represented by Equation (63) can be expressed as follows

$$
\begin{Bmatrix}
F_{pj}^{1r} \\
F_{pj}^{1z} \\
F_{pj}^{1\theta} \\
F_{pj}^{2r} \\
F_{pj}^{2z} \\
F_{pj}^{2\theta} \\
F_{pj}^{3r} \\
F_{pj}^{3z} \\
F_{pj}^{3\theta}
\end{Bmatrix}
= \frac{K_{12}\Pi}{\sin \alpha}
\begin{bmatrix}
P_{rj}\{(A_1+C_1 M_{12})\delta_1 + (B_1 + C_1 K_{12})\delta_2\} \\
\\
P_{zj}\{(A_1+C_1 M_{12})\delta_1 + (B_1 + C_1 K_{12})\delta_2\} \\
\\
0 \\
\\
P_{rj}\{(A_2 + C_2 M_{12})\delta_1 + (B_2 + C_2 K_{12})\delta_2\} \\
\\
P_{zj}\{(A_2 + C_2 M_{12})\delta_1 + (B_2 + C_2 K_{12})\delta_2\} \\
\\
0 \\
\\
P_{rj}\{(A_3 + C_3 M_{12})\delta_1 + (B_3 + C_3 K_{12})\delta_2\} \\
\\
P_{zj}\{(A_3 + C_3 M_{12})\delta_1 + B_3 + C_3 K_{12})\delta_2\} \\
\\
0
\end{bmatrix}
\qquad (68)
$$

The constants A_1 and B_1 are defined as follows

$$
|A_1| = \frac{1}{|A|}(r_2 z_3 - z_2 r_3) \qquad B_1 = \frac{1}{|A|}(Z_2 - Z_3) \qquad (69)
$$

$$
A_2 = \frac{1}{|A|}(z_1 r_3 - r_1 z_3) \qquad B_2 = \frac{1}{|A|}(Z_3 - Z_1)
$$

$$
A_3 = \frac{1}{|A|}(r_1 z_2 - z_1 r_2) \qquad B_3 = \frac{1}{|A|}(z_1 - z_2)
$$

where

$$|A| = |r_2 z_3 + r_1 z_2 + z_1 r_3 - z_2 r_3 - r_1, z_3 - r_2 z_1| \quad . \tag{70}$$

δ_1 and δ_2 represent the following definite integrals $\qquad$ (71)

$$\delta_1 = \int_{r_1}^{r_2} r \, dr = \frac{r_2^2 - r_1^2}{2}$$

and

$$\delta_2 = \int_{r_1}^{r_2} r^2 \, dr = \frac{r_2^3 - r_1^3}{3} \quad . \tag{72}$$

A special case is obtained when $r_2 = r_1$. In this instance the formulation must be changed. For this special case, the equivalent nodal load vector $\{F_{p_j}\}$ can be shown to be equal to Equation (73).

$$\{F_{p_j}\} = \begin{Bmatrix} P_{r_j} (Z_2 - Z_1) r_1 \\ P_{z_j} (Z_2 - Z_1) r_1 \\ 0 \\ P_{r_j} (Z_2 - Z_1) r_1 \\ P_{z_j} (Z_2 - Z_1) r_1 \\ 0 \\ 0 \\ 0 \\ 0 \end{Bmatrix} \quad . \tag{73}$$

107

The load vectors represented by Equations (68) and (73) do not account for a distributed loading acting tangentially (P_θ) to the element face. The loading system has been specialized from the original complete representation (Equation (53) to account for varying distributed loads which act parallel to the r and Z axis (P_r and P_z) respectively. These can be combined to model a varying pressure load. Both these loading conditions can admit complete circumferential asymmetry.

5.2 Prestrain and Thermal Load Vectors

The prestrain load vector is constructed assuming uniform distribution of prestrain across the element. The prestrain contribution to the total potential energy is

$$\Phi_\epsilon = \int \{\epsilon\}^T [E] \{\epsilon_\iota\} \, dV \,. \tag{74}$$

It can be shown that Equation (52) when appropriate substitutions are made and an integration with respect to θ effected, takes the following form

$$\Phi_\epsilon = 2\Pi \iint_{r\,z} \lfloor \epsilon_o \rfloor [E] \{\epsilon_{\iota_o}\} r dz dr + \Pi \sum_{j=1}^{\infty} \iint_{r\,z} \lfloor \epsilon_j \rfloor [E] \{\epsilon_{\iota_j}\} r dz dr \tag{75}$$

$$+ \Pi \sum_{j=1}^{\infty} \iint_{y\,z} \lfloor \epsilon_j \rfloor [E] \{\epsilon_{\iota_j}\} r dz dr \,.$$

Typically, for the Ath series, j[th] harmonic we have

$$\Phi_{\epsilon_j} = \Pi \iint_{r\,z} \lfloor \epsilon_j \rfloor [E] \{\epsilon_{\iota_j}\} r dz dr \,. \tag{76}$$

108

Substituting Equation (39) of Section IV into Equation (76) yields

$$\Phi_{\epsilon_j} = \{\beta_j\}^T \ \Pi \iint\limits_{r \ z} [D_j]^T \ rdzdr \ [E] \ \{\epsilon_{1_j}\} \qquad (77)$$

Let

$$[\tilde{D}_j] = \Pi \iint\limits_{r \ z} [D_j]^T \ r \ dzdr \qquad (78)$$

Which may be written in terms of the δ_{1_j} integrals, as

$$[\tilde{D}_j] = \begin{bmatrix}
0 & 0 & \delta_{0,0} & 0 & -j\,\delta_{0,0} & 0 \\
\delta_{1,0} & 0 & \delta_{1,0} & 0 & -j\,\delta_{1,0} & 0 \\
0 & 0 & \delta_{0,1} & \delta_{1,0} & -j\,\delta_{0,1} & 0 \\
\tilde{0} & 0 & j\,\delta_{0,0} & 0 & -\delta_{0,0} & 0 \\
0 & 0 & j\,\delta_{1,0} & 0 & 0 & 0 \\
0 & 0 & j\,\delta_{0,1} & 0 & -\delta_{0,1} & \delta_{1,0} \\
0 & 0 & 0 & 0 & 0 & -j\,\delta_{0,0} \\
0 & 0 & 0 & \delta_{1,0} & 0 & -j\,\delta_{1,0} \\
0 & \delta_{1,0} & 0 & 0 & 0 & -j\,\delta_{0,1}
\end{bmatrix} \qquad (79)$$

Transformation of Equation (68) to gridpoint displacement coordinates and substitution into the Lagrange equation yields the prestrain load vector.

$$\{F_{\epsilon_j}\} = [\Gamma_{B_q}]^T \ [\tilde{D}_j] \ [E] \ \{\epsilon_{1_j}\} \qquad (80)$$

109

Where the load components are

$$\{F_{\epsilon_j}\}^T = \lfloor F_{\epsilon_j}^{1r}, \; F_{\epsilon_j}^{1z}, \; F_{\epsilon_j}^{1\theta}, \; F_{\epsilon_j}^{2r}, \; F_{\epsilon_j}^{2z}, \; F_{\epsilon_j}^{2\theta}, \; F_{\epsilon_j}^{3y}, \; F_{\epsilon_j}^{3z}, \; F_{\epsilon_j}^{3\theta} \rfloor \qquad (81)$$

and the prestrain components are

$$\{\epsilon_{ij}\}^T = \lfloor \epsilon_{1r_j}, \; \epsilon_{1\theta_j}, \; \epsilon_{1z_j}, \; 0 \rfloor \qquad (82)$$

The thermal load vector is a special case of the pre-strain load vector. Define a matrix of thermal expansion coefficients as

$$\{\alpha\}^T = \lfloor \alpha_r, \; \alpha_\theta, \; \alpha_z, \; 0 \rfloor \qquad (83)$$

ΔT is the asymmetric temperature rise above ambient to which the element is subjected and which represents the average of adjacent gridpoint temperatures. ΔT can be expressed in Fourier series form as follows:

$$\Delta T = \Delta T_o + \sum_{j=1}^{\infty} \Delta T_j \cos j\theta + \sum_{j=1}^{\infty} \Delta \overline{T}_j \sin j\theta \qquad (84)$$

The thermal load vector for the jth series, A^{th} harmonic appears as follows

$$\{F_{T_j}\} = \Pi \; [\Gamma_{B_q}]^T \; [\tilde{D}_j] \; [E] \; \{\alpha\} \; \Delta T_j \qquad (85)$$

5.3 Gravity and Centrifugal Load Vectors

The external work done by the force of gravity on the displacements can be written as follows:

$$V_g = \int \rho \; GW \; dv \qquad (86)$$

$$dV = r \; d\theta \; dr \; dz$$

$$G = \text{Acceleration of Gravity}$$

$$\rho = \text{Mass Density}$$

$$W = \text{Assumed Displacement Function in Z direction}$$

110

Substituting for W into Equation (86) and integrating with respect to θ

$$V_g = 2\Pi \; \rho G \int_y \int_z W_o \; r \; drdz \tag{87}$$

Express Equation (87) in matrix form as follows,

$$V_g = \lfloor \beta_{70}, \; \beta_{80}, \; \beta_{90} \rfloor \; 2\Pi\rho G \int_r \int_z \begin{Bmatrix} 1 \\ r \\ z \end{Bmatrix} rdrdz \tag{88}$$

The vector of forces on the generalized coordinate is in terms of the integrals defined by Equation (47) of Section IV. Then

$$\{F_{go}\}^T = 2\Pi\rho g \; \lfloor 0, \; 0, \; 0, \; 0, \; 0, \; 0, \; \delta_{10}, \; \delta_{20}, \; \delta_{11} \rfloor \tag{89}$$

This force is specifically a force which is present only in the zero[th] or axisymmetric harmonic. The vector of gravity forces on gridpoint coordinates is

$$\{F_{g_o}\} = [\Gamma_{\beta_q}]^T \; \{\overline{F}_{g_o}\} \tag{90}$$

The external work done by centrifugal force due to spin about the axis of symmetry can be written as follows

$$V_S = \int \rho \; \omega^2 \; r \; u \; dv \tag{91}$$

where ω is the spin rate and ρ is the mass density, assumed constant throughout the element. Substituting for u into Equation (91) and integrating with respect to θ gives

$$V_S = 2\Pi \; \rho\omega^2 \int_r \int_z U_o \; r^2 \; dzdr \tag{92}$$

111

Expressing Equation (92) in matrix form

$$V_S = \lfloor \beta_{10}, \beta_{20}, \beta_{30} \rfloor \ 2\Pi \ \rho\omega^2 \int_r \int_z \{ \frac{1}{r} \}r^2 \ dzdr \qquad (93)$$

The vector of forces as the generalized coordinates appears a

$$\{F_{so}\}^T = 2\Pi \ \rho\omega^2 \lfloor \delta_{20}, \delta_{30}, \delta_{21}, 0, 0, 0, 0, 0, 0 \rfloor \quad (94)$$

and the vector of centrigugal forces on gridpoint coordinates is

$$\{F_{so}\} = [\Gamma_{\beta q}]^T \ \{\bar{F}_{so}\} \qquad (95)$$

Again $\{F_{so}\}$ represents a force which acts only on the zeroth or axisymmetric harmonic.

VI. Stress Matrices For The Triangular Element

The element stresses on the harmonic level for the A series, j^{th} harmonic are given by

$$\{\sigma_j\} = [E] \ \{\varepsilon_j\} - [E] \ \{\varepsilon_{ij}\} \qquad (96)$$

The stresses are evaluated at the centroid of the cross-section, i.e. at

$$r_0 = 1/3 \ (r_1 + r_2 + r_3) \qquad (97)$$

$$z_0 = 1/3 \ (z_1 + z_2 + z_3)$$

112

In Equation (96), substitute for strains in terms of displacements

$$\{\sigma_j\} = [E]\ [D_{o_j}]\ [\Gamma_{\beta q}]\ \{q_j\} - [E]\ \{\epsilon_{i_j}\} \tag{98}$$

where, from Equation (40) of Section IV

$$[D_{o_j}] = \begin{bmatrix} 0 & 1 & 0 & 0 & 0 & 0 & 0 & 0 & 0 \\ 0 & 0 & 0 & 0 & 0 & 0 & 0 & 0 & 1 \\ 1/r_o & 1 & Z_o/r_o & j/r_o & j & jZ_o/r_o & 0 & 0 & 0 \\ 0 & 0 & 1 & 0 & 0 & 0 & 0 & 1 & 0 \\ -j/r_o & -j & -jZ_o/r_o & -1/r_o & 0 & -Z_o/r_o & 0 & 0 & 0 \\ 0 & 0 & 0 & 0 & 0 & 1 & -j/r_o & -j & -jZ_o/r_o \end{bmatrix} \tag{99}$$

Equation (98) is used to evaluate elastic stresses on the harmonic level. The matrix $\{\sigma_j\}$ represents a set of harmonic level stress amplitudes. To arrive at actual stresses for any circumferential position around the element, the various sets of amplitudes which arise during an analysis must be recombined in a set of appropriate Fourier series. Thermal stresses are obtained by multiplying thermal strains by the matrix of elastic coefficients, Equation (31) of Section III.

VII. Mass Matrix for the Triangular Element

The kinetic energy of the element is

$$\Phi_V = \tfrac{1}{2}\int \rho\ (\dot{u}^2 + \dot{v}^2 + \dot{w}^2)\ dV \tag{100}$$

Where $\dot{u}$, $\dot{v}$ and $\dot{w}$ are the components of radial, circumferential and axial velocity. Substituting for $\dot{u}$, $\dot{v}$ and $\dot{w}$, integrating with respect to θ and utilizing Equations (8) from Section II, Φ_V can be cast in the following form,

113

$$\Phi_V = \Pi \lfloor \dot{q}_o \rfloor \ [\Gamma_{\beta q}]^T \ [M^*] \ [\Gamma_{\beta q}] \ \{\dot{q}_o\}$$

$$+ \frac{\Pi}{2} \sum_{j=1}^{\infty} \lfloor \overset{\circ}{q}_j \rfloor \ [\Gamma_{\beta q}]^T \ [M^*] \ [\Gamma_{\beta q}] \ \{\overset{\circ}{q}_j\} \tag{101}$$

$$+ \frac{\Pi}{2} \sum_{j=1}^{\infty} \lfloor \dot{\bar{q}}_j \rfloor [\Gamma_{\beta q}]^T \ [M^*] \ [\Gamma_{\beta q}] \ \{\dot{\bar{q}}_j\}$$

Where for the A series, J^{th} harmonic

$$[M^*] = \rho \begin{bmatrix} [\tilde{m}] & & \\ & [\tilde{m}] & \\ & & [\tilde{m}] \end{bmatrix} \tag{102}$$

and

$$[\tilde{M}] = \begin{bmatrix} \delta_{10} & \delta_{20} & \delta_{11} \\ & \delta_{30} & \delta_{21} \\ \text{Symmetric} & & \delta_{12} \end{bmatrix} \tag{103}$$

Then the kinetic energy component for the A series, j^{th} harmonic can be written in the following Matrix form

$$\Phi_{V_j} = \lfloor \dot{q}_j \rfloor \ [\hat{M}] \ \{\dot{q}_j\} \tag{104}$$

where for the A series, j^{th} harmonic

$$[\hat{M}_j] = \Pi \ [M^*] \tag{105}$$

and for the zeroth harmonic

$$[\hat{M}_o] = 2\Pi \ [M^*] \tag{106}$$

The typical harmonic level mass matrix referred to gridpoint coordinates is

$$[M_j] = [\Gamma_{\beta q}]^T \ [\hat{M}_j] \ [\Gamma_{\beta q}] \tag{107}$$

114

H. MODIFIED QUADRILATERAL THIN SHELL ELEMENT

I. Introduction

The modified quadrilateral thin shell element (Entry number 38 in the library of finite element representations incorporated within the MAGIC III System) is described in this section. This finite element differs from the present finite element (number 21 of the MAGIC II System) only in the approximation of in-plane behavior. No difference other than the identification number is evident to the user.

This additional finite element representation, is included in the MAGIC III System for use in the idealization of membrances and plane-strain sections that require elongated finite element shapes. This circustance is frequently encountered. One important class of applications requiring high aspect ratio finite elements is the stress analysis of structural joints. A rule of thumb that may be applied to guide the choice of element type for such applications is to use the modified quadlateral thin shell element for those finite elements whose aspect ratio exceeds six. This guideline derives from experience with the IBM 360/65 computer.

The approximation of in-plane behavior embodied in the modified quadrilateral thin shell finite element differs from that in the original finite element in two respects. Firstly, the subdivision of the finite element into four triangular zones defined by the diagonals of the quadrilateral is avoided in generating the modified finite element. This avoids the integrations over triangular zones that were judged to be the principal constraint for accurate generation of finite element number 21 at high aspect ratio. The other distinguishing feature of the modified finite element is that it embodies a relatively simple discretization by direct interpolation of the displacement values of the eight gridpoints. The original finite element number 21 on the other hand involves the assumption of polynomials whose coefficients must be determined in terms of the gridpoint displacements by a matrix inversion. The accuracy of this operation which is carried out for each of the four triangular subdivision deteriorates with increasing aspect ratio.

115

The development and evaluation of the original finite element is presented in Pages 113 to 162 of Reference 1. The development of the modified finite element, number 38, parallels that of the original finite element except for the central portion of the representation of the in-plane behavior. Therefore, the development reported herein is confined to the representation of the in-plane behavior. The interface of this development with that of Reference 1 is clearly defined and a common notation is employed. All features of finite element number 21 such as material orthotropy, midpoint node suppression, etc., are maintained in modified finite element (number 38).

The implementation into the MAGIC III System leaves the program-analyst interface unchanged. The user documentation for finite element number 21 applies to the modified finite element which is designated finite element number 38. The interface between finite element library and the surrounding framework of the MAGIC III System is identical for finite element numbers 21 and 38. The new calculations are confined entirely within that portion of the finite element representation that generates the basic in-plane behavior representation.

Numerical results are presented that compare the original and the modified finite element representations at ordinary and at high aspect ratios. For ordinary aspect ratios, the performance of the modified finite element is found to be satisfactory although generally less accurate than the original finite element which is constructed as an assemblage of four subelements. However, for high aspect ratios the performance of finite element number 38 is shown to be superior to finite element number 21. This confirms the successful completion of the effort to provide, in the MAGIC III System, a quadrilateral membrane finite element with relaxed constraints upon permissible aspect ratio.

II. Basic Relationships

The geometry of the quadrilateral finite element is illustrated in Figure II-11(a). At the branch point from the original sequence of calculations to the modified computation, the following information is known:

a. (x_g, y_g) –   coordinates of each of the eight gridpoints.

b. t_m –   effective thickness of the membrane.

c. $[E^{(g)}]$ –   material stiffness matrix for either plane stress or plane strain as appropriate.

d. $\{\bar{e}^{(g)}\}$ –   prestress vector arising from prestrain, temperature load or direct prestress.

Using the foregoing information, the relations that underlie the formulation of a representation of the quadrilateral membrane are given below.

a. Strain-Displacement Relation (Eq. 285, Ref. 1)

$$\{e^{(g)}\}^T = \left\lfloor \frac{\partial u^{(g)}}{\partial x_g}, \; \frac{\partial v^{(g)}}{\partial y_g}, \; \frac{\partial u^{(g)}}{\partial y_g} + \frac{\partial v^{(g)}}{\partial x_g} \right\rfloor \tag{1}$$

b. Stress-Strain Relation (Eq. 280, Ref. 1)

$$\{\sigma^{(g)}\} = [E^{(g)}]\left\{\{e^{(g)}\} - \{\bar{e}^{(g)}\}\right\} \tag{2}$$

c. Potential Energy Functional (Eq. 279, Ref. 1)

$$\Phi_m = \int_A t_m \left(\frac{1}{2} \lfloor e^{(g)} \rfloor \; [E^{(g)}] \; \{e^{(g)}\} - \lfloor e^{(g)} \rfloor \; \{\bar{e}^{(g)}\} \right) dA \tag{3}$$

The construction of the desired finite element representation consists of the assumption of approximations for $u^{(g)}$ and $v^{(g)}$ and the substitution of these approximations into the above relations. Then, integration of Equation (3) yields the basic membrane finite element representations, as:

117
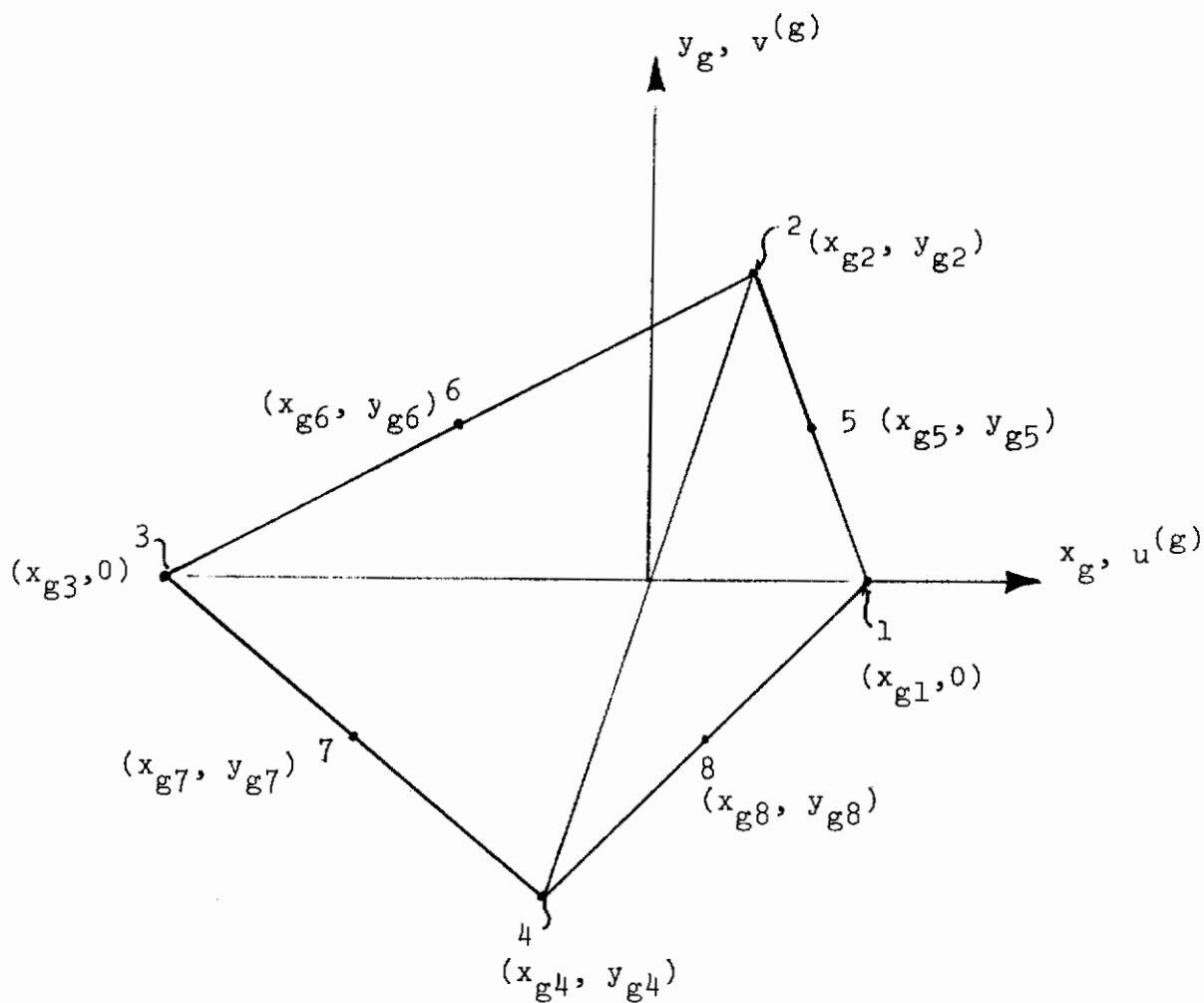
FIGURE II-11(a)   QUADRILATERAL ELEMENT IN PHYSICAL SPACE

118
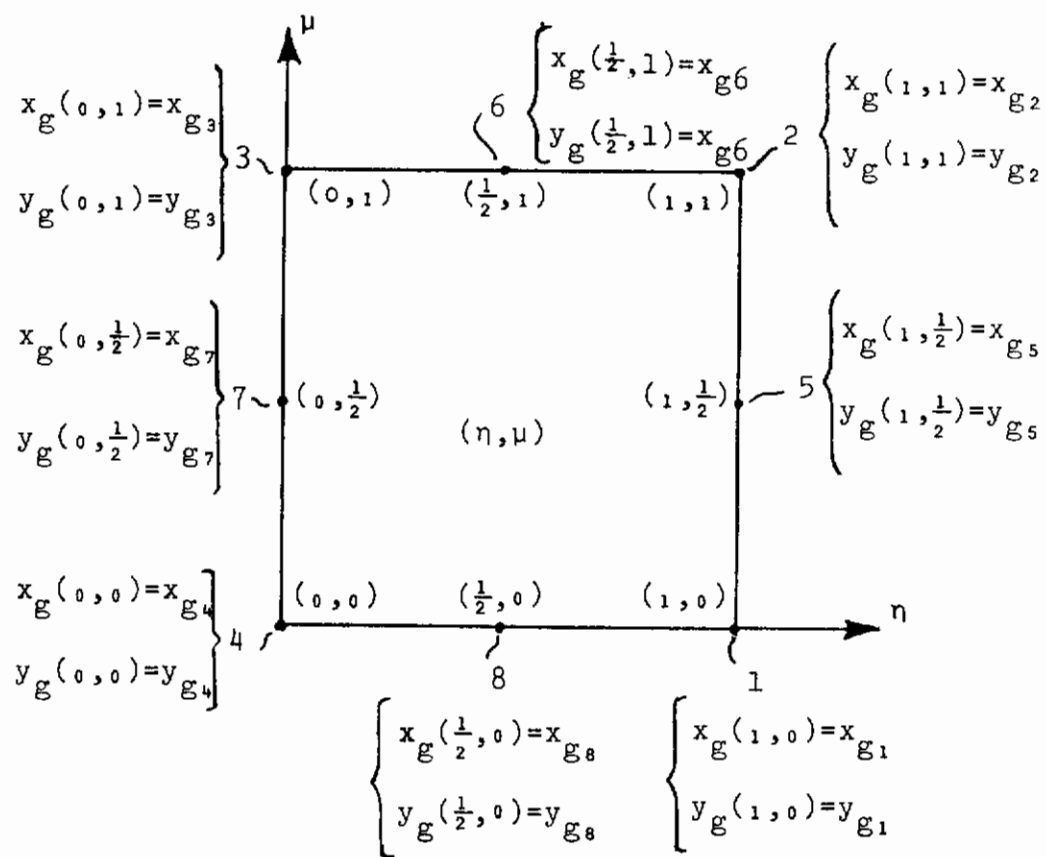
FIGURE II-11(b)   QUADRILATERAL ELEMENT IN TRANSFORMED SPACE

119

$$\Phi_m = 1/2 \lfloor \delta_{gm} \rfloor [K_m^{(g)}] \{\delta_{gm}\} - \lfloor \delta_{gm} \rfloor \{F_\epsilon\} \tag{4}$$

$$\{N^{(g)}\} = [S_N^{(g)}] \{\delta_{gm}\} - \{s_N^{(g)}\}$$

wherein,

$\{\delta_{gm}\}$ is the vector of in-plane gridpoint displacements in the (x_g, y_g) coordinate system (Eq. 255, Ref. 1)

$[K_m^{(g)}]$ is the element membrane stiffness matrix stated with respect to the $\{\delta_{gm}\}$ displacement degrees of freedom.

$\{F_\epsilon^{(g)}$ is the element membrane prestrain matrix stated with respect to the $\{\delta_{gm}\}$ displacement degrees of freedom.

$\{N^{(g)}\}$ is the vector of sets of membrane stress resultants aligned with the (x_g, y_g) coordinate axes.

$[S_N^{(g)}]$ is the element stress matrix stated with respect to the $\{\delta_{gm}\}$ displacement degrees of freedom.

$\{s_N^{(g)}\}$ is the vector of sets of membrane prestress resultants aligned with the (x_g, y_g) coordinate axes (Eq. 351, Ref. 1).

Equations (4) and (5) serve to define the information that the present development must provide at the point of return into the original sequence of calculations performed in generating finite element number 21. Specifically, the matrices $[K_m^{(g)}]$, $\{F_\epsilon^{(g)}\}$ and $[S_N^{(g)}]$ must be provided. The vector $\{s_N^{(g)}\}$ is unchanged by the modified calculations.

120

The present objective is to develop explicit definitions for the $[K_m^{(g)}]$, $\{F_\epsilon^{(g)}\}$ and $[S_N^{(g)}]$. Once these have been obtained, the original sequence of calculations is reentered and Equations 257, 261, 262, 263 and 265 of Reference 1 are employed to obtain the elemenet stiffness and load matrices in terms of the components of displacement employed for assembly. This sequence of transformations can be denoted symbolically by:

$$\{\delta_{gm}\} = [^\Gamma] \{q\} \qquad (5)$$

wherein $\{q\}$ is the final set of gridpoint displacement degrees of freedom. The final form of the finite element representation is obtained by substitution of Equation (6) into Equations (4) and (5) and adding to the corresponding representation of the flexural behavior in the manner described in Reference 1.

III.   Transformation of Coordinates

It is clear from Equation (3) that the construction of a finite element representation involves the integration of functions (usually polynomials) over the interior region of the finite element. Because the performance of such integrations is awkward for the quadrilateral shape defined in the (x_g, y_g) coordinates of Figure II-11(a) a coordinate transformation is introduced. Specifically, the quadrilateral element is mapped onto the unit square of Figure II-11b using mapping transformations defined by Reference 20:

$$x_g(\eta,\mu) = \lfloor H(\eta,\mu) \rfloor \, \{\hat{x}_g\} \qquad 0 \leq \eta,\mu \leq 1 \qquad (6)$$

$$y_g(\eta,\mu) = \lfloor H(\eta,\mu) \rfloor \, \{\hat{y}_g\} \qquad 0 \leq \eta,\mu \leq 1 \qquad (7)$$

121

wherein:

$$\{\hat{x}_g\}^T = \lfloor x_{g1}, \ x_{g2}, \ x_{g3}, \ x_{g4}, \ x_{g5}, \ x_{g6}, \ x_{g7}, \ x_{g8} \rfloor \qquad (8)$$

$$\{\hat{y}_g\}^T = \lfloor y_{g1}, \ y_{g2}, \ y_{g3}, \ y_{g4}, \ g_{g5}, \ y_{g6}, \ y_{g7}, \ y_{g8} \rfloor \qquad (9)$$

$$\{H\} = \begin{Bmatrix} \eta(1-\mu) \ (+2\eta - 2\mu - 1) \\[4pt] \eta\mu \ (+2\eta +2\mu -3) \\[4pt] (1-\eta) \ \mu \ (-2\eta + 2\mu - 1) \\[4pt] (1-\eta) \ (1-\mu) \ (-2\eta -2\mu + 1) \\[4pt] +4 \ \eta\mu \ (1-\mu) \\[4pt] +4 \ \eta\mu \ (1-\eta) \\[4pt] +4 \ (1-\eta) \ \mu \ (1-\mu) \\[4pt] +4\eta \ (1-\eta) \ (1-\mu) \end{Bmatrix} \qquad (10)$$

    Given the (x_g, y_g) coordinate values of the eight grid-points, these relations map the physical (x_g, y_g) space, point-by-point, onto a unit square in the transformed (η,μ) space. Functions defined in the physical space are expressible in the transformed space as explicit functions of the transformed coordinates, i.e.,

$$f \ (x_g, \ y_g) = f \ (x_g \ (\eta,\mu), \ y_g \ (\eta,\mu)) = f \ (\eta,\mu) \quad 0 \leq \eta,\mu \leq 1 \qquad (11)$$

For example, for the components of displacement aligned with the (x_g, y_g) - axes:

$$u^{(g)} = u^{(g)} \ (\eta,\mu), \quad v^{(g)} = v^{(g)} \ (\eta,\mu) \quad 0 \leq \eta,\mu \leq 1 \qquad (12)$$

Derivatives of functions in the (x_g, y_g) coordinates are expressible in terms of derivatives in terms of the transformed (η, μ) coordinates. Using the chain rule of differentiation obtain

$$\left\{ \begin{array}{c} \dfrac{\partial f}{\partial \eta} \\[2ex] \dfrac{\partial f}{\partial \mu} \end{array} \right\} = \left[\begin{array}{cc} \dfrac{\partial x_g}{\partial \eta} & , \quad \dfrac{\partial y_g}{\partial \eta} \\[2ex] \dfrac{\partial x_g}{\partial \mu} & , \quad \dfrac{\partial y_g}{\partial \mu} \end{array} \right] \left\{ \begin{array}{c} \dfrac{\partial f}{\partial x_g} \\[2ex] \dfrac{\partial f}{\partial y_g} \end{array} \right\} \tag{13}$$

The inverse relation follows by direct calculation, i.e.,

$$\left\{ \begin{array}{c} \dfrac{\partial f}{x_g} \\[2ex] \dfrac{\partial f}{\partial y_g} \end{array} \right\} = \frac{1}{J_o} \left[\begin{array}{cc} \dfrac{\partial Y_g}{\partial \mu} & \dfrac{\partial y_g}{\partial \eta} \\[2ex] \dfrac{\partial x_g}{\partial \mu} & \dfrac{\partial x_g}{\partial \eta} \end{array} \right] \left\{ \begin{array}{c} \dfrac{\partial f}{\partial \eta} \\[2ex] \dfrac{\partial f}{\partial \mu} \end{array} \right\} \tag{14}$$

in which the coefficient matrix is denoted by $[J]$ and

$$J_o = \det\,([J]) = \frac{\partial x_g}{\partial \eta} \; \frac{\partial y_g}{\partial \mu} - \frac{\partial x_g}{\partial \mu} \; \frac{\partial y_g}{\partial \eta} \tag{15}$$

The elemental area in the physical space is related to that of the transformed space by:

$$dA = dx_g\, dy_g = J_o\; d_\eta\, d_\mu \tag{16}$$

Equations (6) through (16) are sufficient to permit transformtion of the basic relations of Equations (1) through (3) Section II to expression in terms of the (η, μ) coordinates. The form of the strain-displacement relation becomes,

$$\{e^{(g)}\} = [T_u]\; \{\Delta_{mu}\} \tag{17}$$

wherein

$$\{\Delta_{mu}\} = \left\lfloor \frac{\partial u^{(g)}}{\partial \eta}\,,\; \frac{\partial u^{(g)}}{\partial \mu}\,,\; \frac{\partial v^{(g)}}{\partial \eta}\,,\frac{\partial v^{(g)}}{\partial \mu} \right\rfloor \tag{18}$$

123

and:

$$[T_u] = \frac{1}{J_o} \begin{bmatrix} J_{11} & , & J_{12}, & 0 & , & 0 \\ 0 & , & 0 & J_{21}, & J_{22} \\ J_{21} & , & J_{22}, & J_{11}, & J_{12} \end{bmatrix} \tag{19}$$

Equation (17) is a different mapping than that employed in deriving finite element number 21 but takes a symbolic form identical to Equation 299 of Reference 1.

As a direct consequence of Equation (17), the transformed stress-displacement relation of Equation (2), Section II is given by

$$\{\sigma^{(g)}\} = [E^{(g)}] [T_u] \{\Delta_{mu}\} - \{\bar{e}^{(g)}\} \tag{20}$$

The potential energy functional of Equation (3), Section II is transformed to expression as:

$$\Phi_m = \int_o^1 \int_o^1 \left(-\frac{1}{2} \lfloor \Delta_{mu} \rfloor [I_{mk}] \{\Delta_{mu}\} - \lfloor \Delta_{mu} \rfloor \{I_{me}\}\right) d\eta \, d\mu \tag{21}$$

wherein

$$[I_{mk}] = T_m J_o [T_u]^T [E^{(g)}] [T_u] \tag{22}$$

$$\{I_{me}\} = t_m J_o [T_u]^T \{\bar{e}^{(g)}\} \tag{23}$$

This result is the symbolic equivalent of Equation 305 of Reference 1 although the mapping employed is different.

The potential energy functional, as given in Equation (21), is now in a form that readily admits integration over the area of the element for the limits of integration on η and μ are constants.

124

IV. Discretization

The formulation of the finite element representation is carried forward by approximating the displacement functions $u^{(g)}$ and $v^{(g)}$ and integrating the potential energy over the interior region of the finite element. Polynomials, defined in the transformed space, are employed to approximate the displacement functions. The symbolic form of the approximations is given by:

$$u^{(g)}(\eta,\mu) = \lfloor H(\eta,\mu) \rfloor \{\hat{u}^{(g)}\} \tag{24}$$

$$v^{(g)}(\eta,\mu) = \lfloor H(\eta,\mu) \rfloor \{\hat{v}^{(g)}\} \tag{25}$$

The vector of mode shapes $\{H\}$ is the same as that employed to transform from (x_g, y_g) to (η,μ) coordinates. These mode shapes interpolate the displacement functions within the interior region of the element on the basis of the associated sets of gridpoint displacement values:

$$\{\hat{u}^{(g)}\}^T = \lfloor u_1^{(g)}, u_2^{(g)}, u_3^{(g)}, u_4^{(g)}, u_5^{(g)}, u_6^{(g)}, u_7^{(g)}, u_8^{(g)} \rfloor$$

$$\tag{25}$$

$$\{\hat{v}^{(g)}\}^T = \lfloor v_1^{(g)}, v_2^{(g)}, v_3^{(g)}, v_4^{(g)}, v_5^{(g)}, v_6^{(g)}, v_7^{(g)}, v_8^{(g)} \rfloor$$

$$\tag{26}$$

Discretization of the basic relations is accomplished in two steps. First, the displacement approximations are employed to obtain $\{\Delta_{mu}\}$ of Equation (18), Section III as:

$$\{\Delta_{mu}\} = [D_m] \{\delta_{gm}\} \tag{27}$$

wherein:

$$[D_m] = \begin{bmatrix} \dfrac{\partial}{\partial \eta} \lfloor H \rfloor & , & \lfloor 0 \rfloor \\[2mm] \dfrac{\partial}{\partial \mu} \lfloor H \rfloor & , & \lfloor 0 \rfloor \\[2mm] \lfloor 0 \rfloor & , & \dfrac{\partial}{\partial \eta} \lfloor H \rfloor \\[2mm] \lvert 0 \rvert & , & \dfrac{\partial}{\partial \mu} \lfloor H \rfloor \end{bmatrix} \qquad (28)$$

$$\{\delta_{gm}\}^T = \lfloor \lfloor \hat{u}^{(g)} \rfloor, \quad \lfloor \hat{v}^{(g)} \rfloor \rfloor \qquad (29)$$

Now, using this extended symbolic **notation**, the basic relations are discretized. The stress-displacement relation of Equation (20), Section III becomes:

$$\{\sigma^{(g)}\} = \left[E^{(g)} \right] \left[T_u \right] \left[D_m \right] \{\delta_{gm}\} - \{\bar{\epsilon}^{(g)}\} \qquad (30)$$

The potential energy functional of Equation (21), Section III is discretized using Equation (27) to obtain:

$$\Phi_m = 1/2 \lfloor \delta_{gm} \rfloor [K^{(g)}] \{\delta_{gm}\} - \lfloor \delta_{gm} \rfloor \{F_\epsilon^{(g)}\} \qquad (31)$$

wherein the stiffness $[K^{(g)}]$ and prestrain load $\{F_\epsilon^{(g)}\}$

matrices for the quadrilateral membrane finite element are:

$$[K^9] = \int_0^1 \int_0^1 [D_m]^T [I_{mk}] [D_m] \, d_\eta d_\mu \qquad (32)$$

$$\{F_e^9\} = \int_0^1 \int_0^1 [D_m]^T \{I_{me}\} \, d_\eta d_\mu \qquad (33)$$

126

Two principal steps remain in the development of the finite element representation. Consideration must be given to the particularization of Equation (30) to specific points within the finite element and the integrations indicated in Equations (32) and (33) must be carried out.

V.   Calculation of the Element Matrices

It is convenient to invoke numerical quadrature to obtain numerical values for the finite element matrices. All quantities, in the integrals to be evaluated to obtain the element matrices, are functions of the assumed mode shapes {H} and the gridpoint values $\{\hat{x}_g\}$ and $\{\hat{y}_g\}$. Thus, to obtain the values of the integrands, as is required in the numerical quadrature calculation, it is necessary to evaluate the mode shapes {H} at the sample points. Then, with these, numerical values can be calculated for all terms in the integrands.

Gaussian quadrature is employed. For the interval of interest ($0 \leq \S \leq 1$) the set of sample points {p} and weights {w} for one dimensional quadrature are:

2-point
$$\{p\}^T = \lfloor 0.21132487, \; 0.78867483 \rfloor \qquad (34)$$
$$\{\omega\}^T = \lfloor 0.5 \qquad , \; 0.5 \qquad \rfloor \qquad (35)$$

3-point
$$\{p\}^T = \lfloor 0.11270165, \; 0.5 \qquad , \; 0.88729811 \rfloor \qquad (36)$$
$$\{w\}^T = \lfloor 0.27777777, \; 0.44444444, \; 0.27777777 \rfloor \qquad (37)$$

These one-dimensional sets of sample points and weights permit the construction of two-dimensional sets. Let I (η,μ), for example, denote an integrand defined on the two-dimensional domain $0 \leq \eta,\mu \leq 1$. Furthermore, let the sample points p_r and weights ω_r along the η - coordinate line be R in number. Similarly, let there be S sample points p_s and weights w_s along the μ- coordinate. The Gaussian product

127

formula for this two-dimensional integration follows as:

$$\int_0^1 \int_0^1 I(\eta,\mu) \, d\eta \, d\mu = \sum_{r=1}^R \sum_{s=1}^S w_r w_s I(\eta,\mu)\Big|_{(p_r,p_s)} \qquad (38)$$

The quadrature problems posed by Equations (32) and (33) Section IV involve integrands expressed in terms of $\{H\}$, $\{H,\eta\}$ and $\{H,\mu\}$. Therefore, in preparation for quadrature these vectors are evaluated at the quadrature points. The collective results are given symbolic definitions as:

$$\{H\}^T = \lfloor \lfloor H\rfloor_{11}, \lfloor H\rfloor_{12}, \ldots, \lfloor H\rfloor_{15},$$
$$\lfloor H\rfloor_{21}, \lfloor H\rfloor_{22}, \ldots, \lfloor H\rfloor_{25}, \qquad (39)$$
$$\vdots$$
$$\lfloor H\rfloor_{R1}, \lfloor H\rfloor_{R2}, \ldots, \lfloor H\rfloor_{R5} \rfloor$$

$$\{H,\eta\}^T = \lfloor \lfloor H,\eta\rfloor_{11}, \lfloor H,\eta\rfloor_{12}, \ldots, \lfloor H,\eta\rfloor_{15},$$
$$\lfloor H,\eta\rfloor_{21}, \lfloor H,\eta\rfloor_{22}, \ldots, \lfloor H,\eta\rfloor_{25}, \qquad (40)$$
$$\vdots$$
$$\lfloor H,\eta\rfloor_{R1}, \lfloor H,\eta\rfloor_{R2}, \ldots, \lfloor H,\eta\rfloor_{R5} \rfloor$$

$$\{H,\mu\}^T = \lfloor \lfloor H,\mu\rfloor_{11}, \lfloor H,\mu\rfloor_{12}, \ldots, \lfloor H,\mu\rfloor_{15},$$
$$\lfloor H,\mu\rfloor_{21}, \lfloor H,\mu\rfloor_{22}, \ldots, \lfloor H,\mu\rfloor_{25}, \qquad (41)$$
$$\lfloor H,\mu\rfloor_{R1}, \lfloor H,\mu\rfloor_{R2}, \ldots, \lfloor H,\mu\rfloor_{R5} \rfloor$$

wherein:

$$\{H\}_{rs} = \{H(\eta,\mu)\}\Big|_{(p_r,\, p_s)} \qquad (42)$$

$$\{H,\eta\}_{rs} = \frac{\partial}{\partial \eta}\{H(\eta,\mu)\}\Big|_{(p_r,\, p_s)} \qquad (43)$$

$$\{H,\mu\}_{rs} = \frac{\partial}{\partial \mu}\{H(\eta,\mu)\}\Big|_{(p_r,\, p_s)} \qquad (44)$$

128

The foregoing relations specify the quadrature operation completely. Using the evaluated mode shapes, the element stiffness $[K^{(g)}]$ and prestrain load $\{F_\epsilon^{(g)}\}$ matrices follow from Equations (32) and (33), Section IV by direct calculation, i.e.,

$$[K_m^{(g)}] = \sum_{r=1}^{R} \sum_{s=1}^{S} \omega_r \, \omega_s \, [D_m]^T \, \{I_{mK}\} \, [D_m] \Big|_{\{H,\eta\}_{rs},\{H,\mu\}_{rs}}$$

(45)

$$\{F_\epsilon^{(g)}\} = \sum_{r=1}^{R} \sum_{s=1}^{S} \omega_r \, \omega_s \, [D_m]^T \, \{I_{me}\} \Big|$$

(46)

$$\{H,\eta\}_{rs}, \ \{H,\mu\}_{rs}$$

The stress-displacement relation of Equation (30), Section IV provides the means to recover values for the stresses at any point within the finite element. This relation is particularized to a set of five display points similar to that employed in the original, number 21, membrane finite element, e.g.,

$$\{N^{(g)}\}_1 = [S_N]_1 \, \{\delta_{mg}\} - \{s_N\}_1$$

(47)

wherein:

$$[S_N^{(g)}]_1 = [E^{(g)}] \, [T_u(1,0)] \, [D_m(1,0)]$$

(48)

$$\{s_N\}_1 = \{\bar{e}^{(g)}(1,0)\}$$

(49)

The stress vectors at the other points $(\eta,\mu) = (1,1), (0,1), (0,0)$ and $(\frac{1}{2},\frac{1}{2})$ follow similarly. The $[S_N^{(g)}]$ and $\{s_N^{(g)}\}$ matrices are the matrices of Equation (5), Section II which complete the specification of the modifications made to the original thin shell element (number 21) to obtain the modified thin shell element (number 38).

129

A careful calculation of the gridpoint loads that are equivalent to a specified distribution of boundary loading should be based upon work equivalence rather than static equivalence. Such a calculation is not presently provided within the MAGIC II System for the membrane situation and must be made manually. An illustrative calculation is included to encourage the use of work equivalent gridpoint loads.

Consider an element side of Length L. For a coordinate o s L along the element side, the assumed displacement functions employed in finite element numbers 21 and 38 are quadratic, i.e.,

$$u(s) = \frac{2}{L^2} (s-L) (s- \frac{L}{2}) u_o$$

$$- \frac{4}{L^2} s (s-L) u_{L/2} \qquad (50)$$

$$+ \frac{2}{L^2} s (s- \frac{L}{2}) u_L$$

Let the traction component associated with this component of displacement have a specified distribution, say quadratic, e.g.,

$$p(s) = \frac{2}{L^2} (s-L) (s- \frac{L}{2}) p_o$$

$$- \frac{4}{L^2} s (s-L) p_{L/2} \qquad (51)$$

$$+ \frac{2}{L^2} s (s- \frac{L}{2}) p_L$$

The external work of associated components of boundary traction and displacement is given by:

$$W = \int_o^L u(s) \; p(s) \; ds \qquad (52)$$

130

This energy functional is specialized to the illustrative example by substitution from Equations (50) and (51), i.e.,

$$W = \int_0^L \lfloor u_o, u_{\frac{L}{2}}, u_L \rfloor \begin{bmatrix} \frac{2}{L^2}(s-L)(s-\frac{L}{2}) \\ -\frac{4}{L^2}s(s-L) \\ +\frac{2}{L^2}s(s-\frac{L}{2}) \end{bmatrix} \lfloor \frac{2}{L^2}(s-L)(s-\frac{L}{2}), -\frac{4}{L^2}(s-L)s, \frac{2}{L^2}s(s-\frac{L}{2}) \rfloor \begin{bmatrix} p_o \\ p_{L/2} \\ p_L \end{bmatrix} ds \quad (53)$$

The result of this integration is,

$$W = \lfloor u_o, u_{L/2}, u_L \rfloor \begin{bmatrix} P_o \\ P_{L/2} \\ P_L \end{bmatrix} = \frac{L}{60} \lfloor u_o, u_{L/2}, u_L \rfloor \begin{bmatrix} 8, & 4, & -2 \\ 4, & 32, & 4 \\ -2, & 4, & 8 \end{bmatrix} \begin{bmatrix} p_o \\ p_{L/2} \\ p_L \end{bmatrix} \quad (54)$$

from which the vector of gridpoint loads is obtained, as:

$$\begin{bmatrix} P_o \\ P_{L/2} \\ P_L \end{bmatrix} = \frac{L}{60} \begin{bmatrix} 8, & 4, & -2 \\ 4, & 32, & 4 \\ -2, & 4, & 8 \end{bmatrix} \begin{bmatrix} p_o \\ p_{L/2} \\ p_L \end{bmatrix} \cdot \quad (55)$$

This result permits convenient manual calculation of the gridpoint loads that correspond to a quadratic distribution of boundary traction specified by its intensity at the element gridpoints.

131

VI. Convergence

The example chosen to illustrate the convergence characteristics of finite element number 38 is the parabolically loaded membrane shown in Figure II-12. This same problem was considered previously in evaluation of the original finite element, number 21.

The membrane is constructed of isotropic material and the distributed loading is replaced by work equivalent grid-point loads obtained in the manner outlined in Section V. Only one quadrant of the membrane is considered explicitly in the analysis. This quadrant is idealized using square finite elements. The idealization for the case of four finite elements is shown in Figure II-13.

This example prolem was analyzed using idealizations of 1, 4 and 16 finite elements. Finite element types 21 and 38 were considered as well as a bi-cubic element referred to throughout as the COMEC finite element. Additionally, a solution obtained by an alternative method of analysis is included in the comparison. The displacement at the point of maximum load, u_q, and the total potential energy Φ are taken to characterize the predicted behavior.

The numerical results are presented in Table II-1. These numerical results are given graphical interpretation in Figure II-14. It is clear from Figure II-14 that the maximum displacement is predicted accurately by all three types of finite elements. Moreover, the potential energy converges monotonically for each type of finite element. Specific displacements need not converge monotonically and indeed they do not for the case illustrated in Figure II-14.

$$\overline{N}_x = 100 \left[1-\left(\frac{y}{16}\right)^2\right]$$

t = 0.1 in.

E = 30 x 10⁶ lb/in.²   ν = 0.3
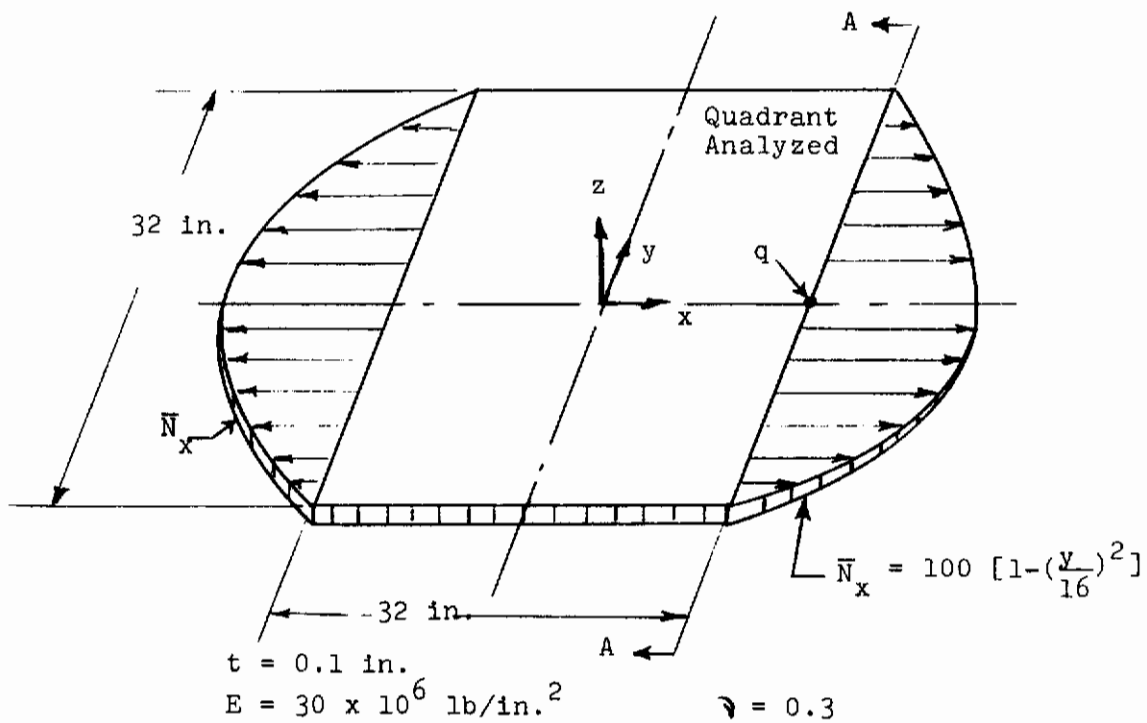
FIGURE II-12   PARABOLICALLY LOADED MEMBRANE DESCRIPTION

O ≡ Gridpoint Numbers
Δ ≡ Profile Numbers
▢ ≡ Element Numbers
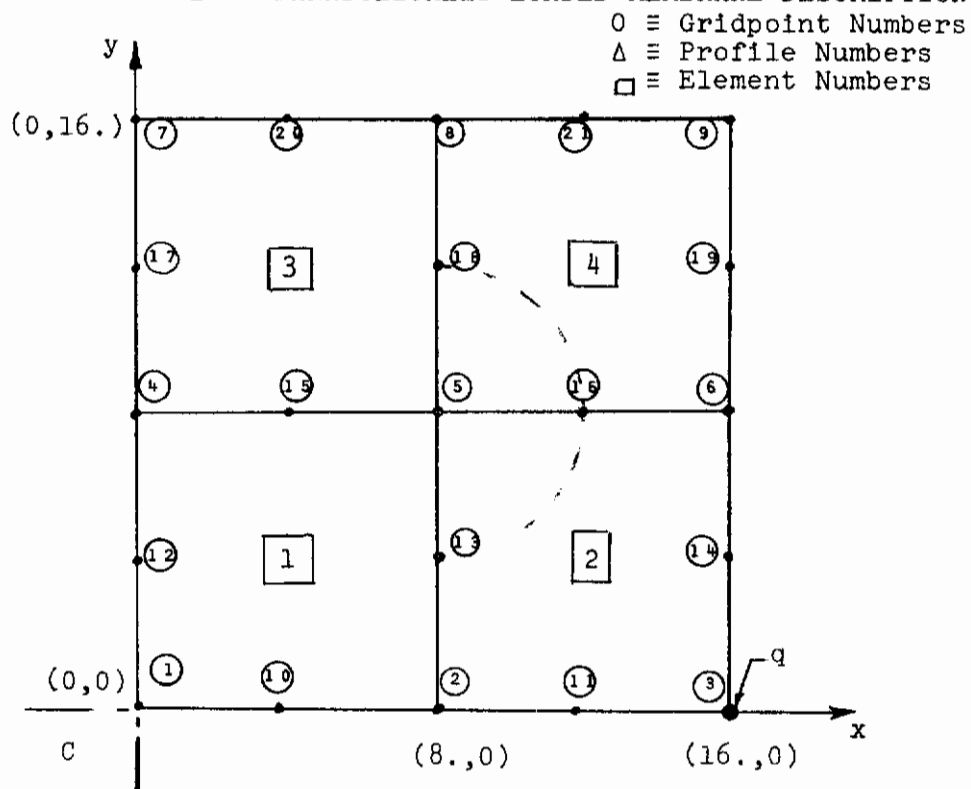
FIGURE II-13   PARABOLICALLY LOADED MEMBRANE IDEALIZATION

TABLE II-1

PARABOLICALLY LOADED MEMBRANE CONVERGENCE RESULTS

Number of Elements	Element Type	No. D.O.F.	Pot. Energy Φ	Displacement u_q	$E_u\%$
	EXACT	-	-	0.000492	-
1	Magic Plug #21	10	-0.2138	0.000492	0.0
	Magic Plug #38	10	-0.2147	0.000496	0.8
	COMEC	16	-0.2162	0.000489	0.6
4	Magic Plug #21	32	-0.2155	0.000492	0.0
	Magic Plug #38	32	-0.2167	0.000492	0.0
	COMEC	50	-0.2169	0.000493	0.2
16	Magic Plug #21	107	-0.2167	0.000492	0.0
	Magic Plug #38	112	-0.2169	0.000492	0.0
	COMEC	162	-0.2169	0.000492	0.0

D.O.F. = Degrees of Freedom

134

FIGURE II-14   PARABOLICALLY LOADED MEMBRANE CONVERGENCE

135

VII.   Shape Sensitivity

The parabolically loaded membrane problem of Figure II-12 is employed to obtain an indication of the sensitivity of finite element number 38 to distortion of its shape at ordinary aspect ratios. The baseline idealization is comprised of four square finite elements as shown in Figure II-13. Idealizations of elements of distorted shape are obtained by moving the central gridpoint (No. 5) to selected positions on the dashed circle shown in Figure II-13.
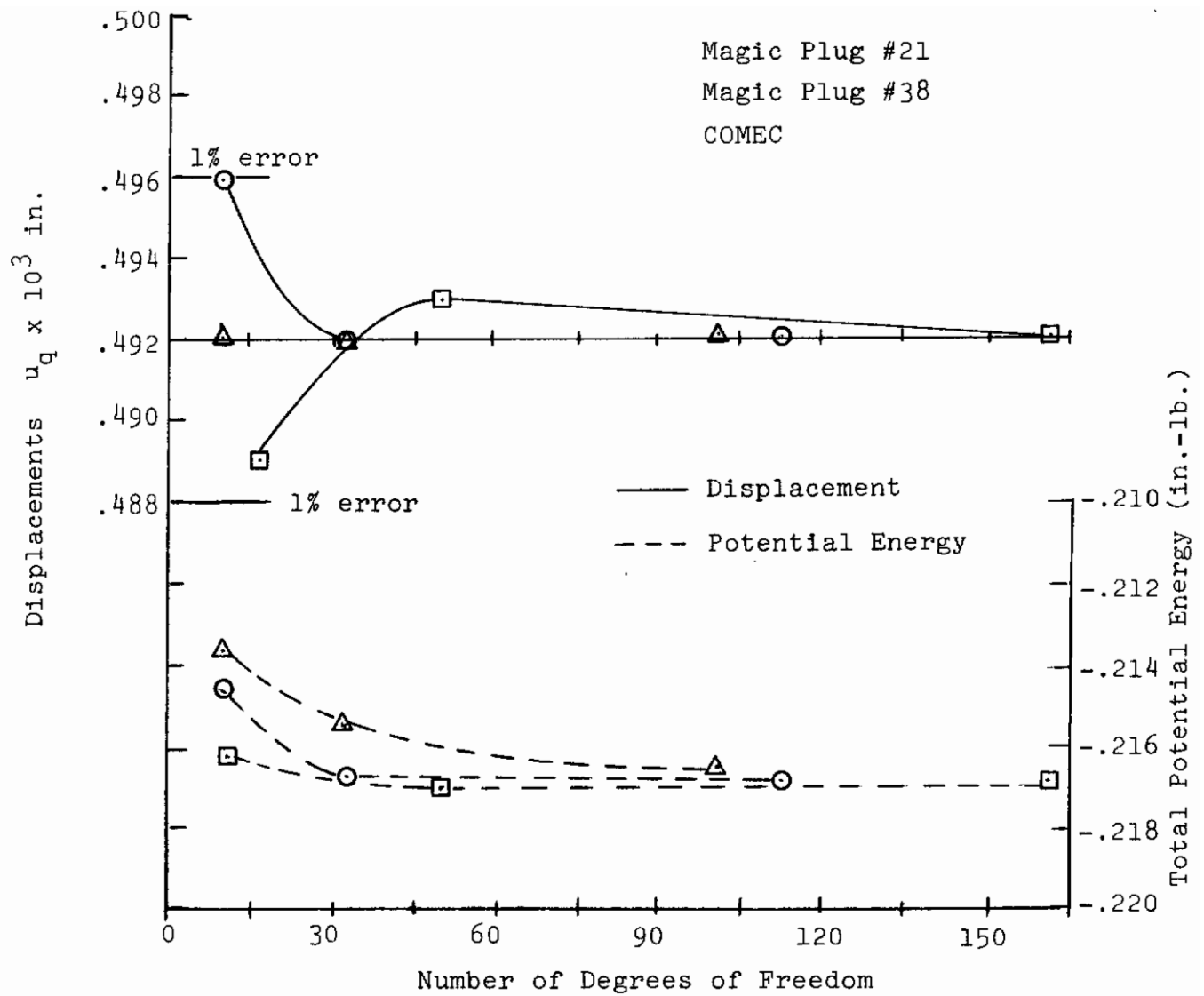
The displacement u_q and the potential energy are taken to characterize the predicted behavior. The results obtained using finite element number 21 are shown in Table II-2, together with results obtained using finite element number 38 and the COMEC finite element. This comparison is portrayed graphically in Figure II-15.

Observation of the results of Table II-2 and Figure II-15 indicates that the considerable distortion imposed does not greatly affect the accuracy of the behavior predicted by finite element number 38. It is concluded at this point that the new finite element number 38 may be used in conjunction with the original finite element number 21 without significant adverse effects upon the predicted behavior. Indeed, the performance of the new simpler finite element is nearly equivalent to that of finite element number 21.

VIII.   Bending At High Aspect Ratio

It is useful to separate the evaluation of the performance of finite element number 38 at high aspect ratios into two parts. First, bending is considered. Subsequently, the type of deformation which predominates in structural joints will be examined.

Consideration of bending at high aspect ratios is included principally to emphasize the need for caution in applications where shear deformations are relied upon to represent flexural behavior. The example problem chosen to illustrate the difficulty of coping with behavior of this type is shown in Figure II-16.

TABLE II-2   PARABOLICALLY LOADED MEMBRANE SHAPE STUDY RESULTS

CASE	ELEMENT TYPE	POT. ENERGY $\mathfrak{D}$	DISPLACEMENT U_q	E_u %
	EXACT	--	0.000492	--
1	Magic Plug #21 Magic Plug #38 Comec	-0.2155 -0.2167 -0.2169	0.000492 0.000492 0.000493	0.0 0.0 0.2
2	Magic Plug #21 Magic Plug #38 Comec	-0.2164 -0.2168	0.000492 0.000494 0.000492	0.0 0.4 0.0
3	Magic Plug #21 Magic Plug #38 Comec	-0.2165 -0.2166	0.000491 0.000492 0.000489	0.2 0.0 0.6
4	Magic Plug #21 Magic Plug #38 Comec	-0.2166 -0.2168	0.000491 0.000490 0.000492	0.2 0.4 0.0
5	Magic Plug #21 Magic Plug #38 Comec	-0.2166 -0.2162	0.000491 0.000490 0.000490	0.2 0.4 0.4
6	Magic Plug #21 Magic Plug #38 Comec	-0.2166 -0.2168	0.000492 0.000491 0.000492	0.0 0.2 0.0

* 4 FINITE ELEMENTS
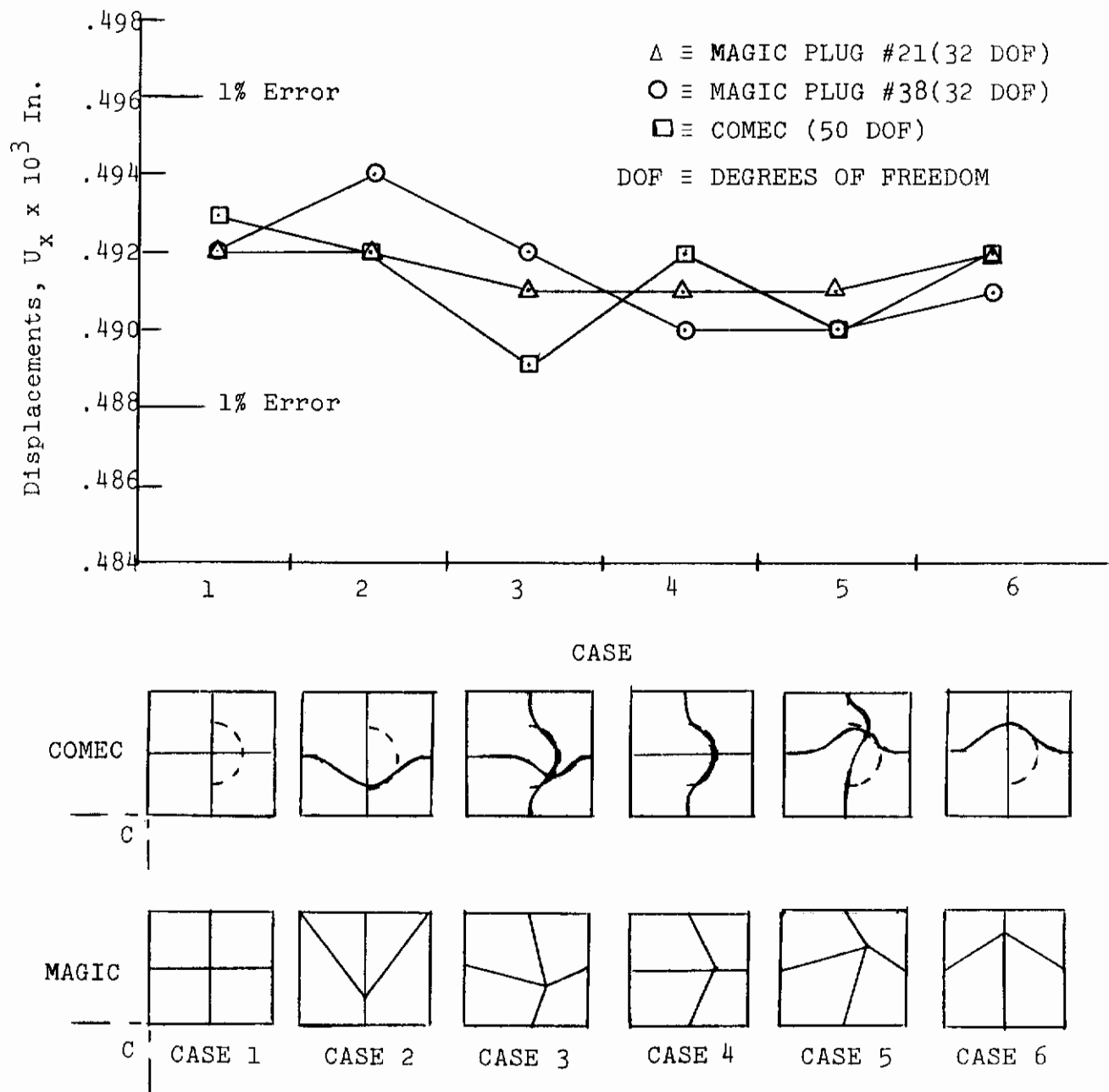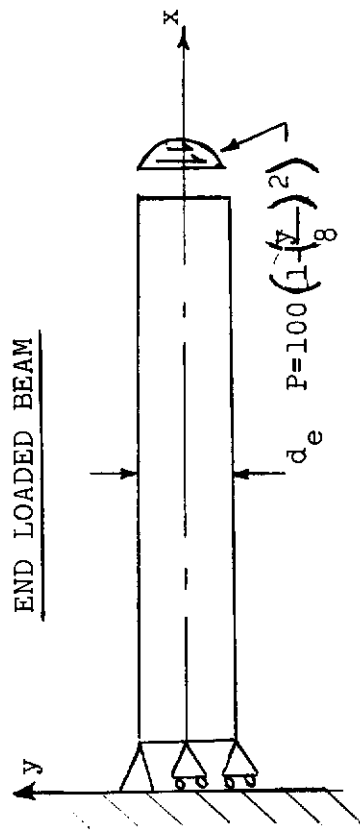
FIGURE II-15   PARABOLICALLY LOADED MEMBRANE SHAPE SENSITIVITY

MATERIAL PROPERTIES

$E = 30. \times 10^6$ #/in.^{2}

$\nu = 0.3$

$t = 0.1$ in.

$d_e = 16.0$ in.

END LOADED BEAM

$P = 100 \left(1 - \left(\frac{y}{8}\right)^2\right)$

MAGIC IDEALIZATION
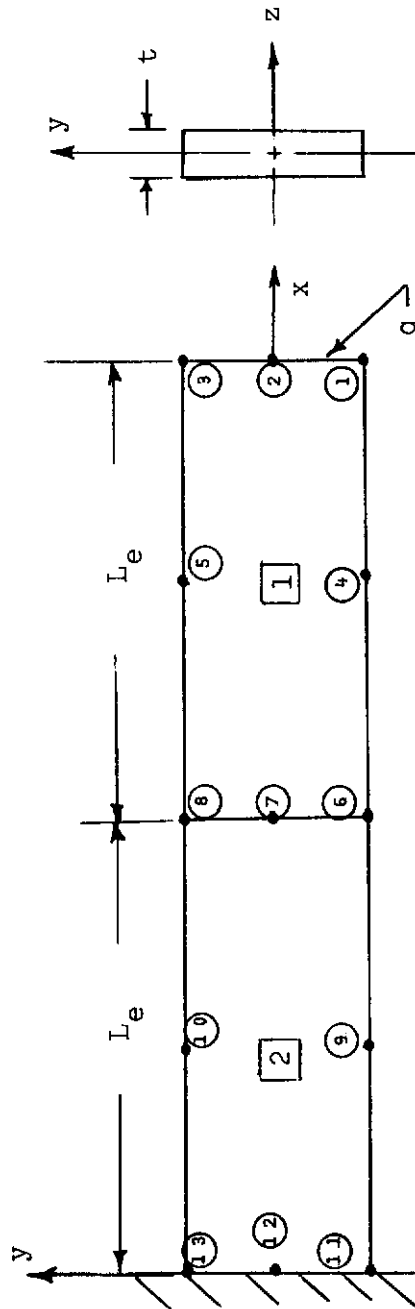
$0 \equiv$ GRIDPOINT NUMBERS

$\square \equiv$ ELEMENT NUMBERS

FIGURE II-16   CANTILEVER BEAM DESCRIPTION

The cantilever beam of Figure II-16 is loaded with a parabolically distributed shear load. Two elements, each extending over the entire depth are employed to idealize the structure. A sequence of cases involving increasing aspect ratios of the finite elements is obtained by holding the depth and number of finite elements constant while increasing the length of the beam.

The displacements, potential energy and reactions are taken to characterize the predicted behavior of the cantilever beam. These results are presented in Table II-3 for finite element number 38. Corresponding results obtained from finite element number 21, the COMEC finite element and beam theory are also shown in Table II-3. Dimensional, nondimensional and error values are included.

Interpretation of these results is accomplished more conveniently using the graphical representation of Figure II-17. At a finite element aspect ratio of unity, the structure is not a slender beam but the finite element results are in agreement with each other within a fraction of a percent.

At aspect ratios of two and four, the finite element results achieve reasonable approximations of beam results and, more importantly are in satisfactory agreement with each other except for the anomalous 7.4% error in the reaction predicted using finite element number 38. The difficulty of representing bending behavior with membrane elements is more apparent for the increased aspect ratio of 8.0. While this is not considered to be especially high, the system stiffness matrix did not admit accurate solution using single precision arithmetic on the IBM 360/65 computer. The The reactions obtained using finite element numbers 21 and 38 are grossly in error. Although not shown, for slightly higher aspect ratios, the reaction obtained using the COMEC finite element was also grossly in error.

140

TABLE II-3 CANTILEVERED BEAM, RESULTS *

Element Aspect Ratio	Element Type	Displacement U_q	Pot. Energy π	Reaction	δ $(\delta/L) \times 10^6$	ϵ_δ %	M $(T/L) \times 10^6$	ϵ_M %	P-R	ϵ_R %
All	Beam	-	-	1066.7	0.3472	-	-185.2	-	0.0	-
1	Magic Plug #21	0.0130	-6.928	1066.5	0.3968	-14.3	-211.48	-14.2	0.2	.018
	Magic Plug #38	0.0133	-7.085	1066.2	0.4060	-16.9	-216.28	-16.8	0.5	.047
	COMEC	0.0132	-7.07	1066.1	0.4060	-16.9	-216.0	-16.6	0.0	0.0
2	Magic Plug #21	0.0913	-48.679	1070.0	0.3483	- 0.3	-185.72	- 0.3	-3.3	-.309
	Magic Plug #38	0.0928	-49.507	1066.4	0.3541	- 2.0	-188.89	- 2.0	0.3	.028
	COMEC	0.092	-49.115	1064.4	0.3500	- 0.8	-187.50	- 1.2	2.3	.215
4	Magic Plug #21	0.6986	-372.54	1069.3	0.3331	4.1	-177.65	4.1	-2.6	.24
	Magic Plug #38	0.7368	-392.93	1145.7	0.3514	-1.2	-187.38	-1.2	-79.0	7.4
	COMEC	0.7080	-378.66	1055.3	0.3380	2.6	-180.5	2.5	11.4	1.07
8	Magic Plug #21	11.411	-6086.2	3102.2	0.6812	-96.2	-363.36	-96.2	-2035.5	190.8
	Magic Plug #38	2.498	1332.0	407.6	0.1491	+57.0	79.52	57.1	659.1	61.8
	COMEC	5.6	-2995.0	1038.0	0.3340	3.8	-178.8	3.5	28.7	2.7

* 2 FINITE ELEMENTS

FIGURE II-17   CANTILEVERED BEAM BEHAVIOR

142

MATERIAL PROPERTIES

Isotropic	Orthotropic
$E = 30 \times 10^6$	$E_x = 16.622 \times 10^6$
	$E_y = E_z = 1.1405 \times 10^6$
$Y = 0.3$	$Y_{xy} = 0.292$
	$Y_{yz} = Y_{zx} = 0.020$
	$G_{xy} = 0.533 \times 10^6$
	$G_{yz} = G_{zx} = 0.582 \times 10^6$
	$t = 1.0$ in.
	$L_e = 10$ in.

LAP JOINT

$3 L_e$

$P = 200\#$ TOTAL

MAGIC IDEALIZATION

○ GRIDPOINT NUMBERS
□ ELEMENT NUMBERS

Line of Symmetry

LINE OF SYMMETRY
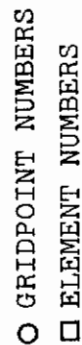
FIGURE II-18   STRUCTURAL JOINT, MATERIAL PROPERTIES AND IDEALIZATION

143

The point of special interest here is that the source
of the difficulty does not reside in the finite element deriva-
tions themselves. The difficulty is in the conditioning of the
system stiffness matrix. Thus, the above example emphasizes
the inappropriateness of this class of finite elements for bending
applications but does not constitute a meaningful evaluation
of the relative performance of members of this class at high aspect
ratios.

IX.   Tension-Shear At High Aspect Ratio

The results presented in prior sections have examined
considerations that are subordinate to the evaluation of the
finite element number 38 in the present context. In this section
of the report the performance of the modified finite element is
compared to that of finite element number 21 for an idealized
structural joint. Errors that arise in generating the stiffness
matrix for high aspect ratio shapes of finite element number 21
have severely restricted attempts to analyze structural joints
using the IBM 360/65 computer. The success of the modification
of the quadrilateral thin shell element hinges upon the analysis
of a structural joint using finite element shapes of substantially
higher aspect ratio than is possible with the original finite
element.

The highly idealized structural joint employed in this
evaluation is shown in Figure II-18. Symmetry permits explicit
consideration of one quadrant. A total of four identical finite
elements arranged as shown in Figure II-18 is used in each case
considered in this parametric study. The total load, uniformly
distributed over the end, and the length of the joint are held
constant. The parametric variation of the aspect ratio of the
finite elements is accomplished by varying the thickness of the
joint.

The displacement u_q on the centerline at the load, the
potential energy and the reaction at the line of symmetry
opposing the load are taken to characterize the behavior of the
joint. Of these, the reaction is the most sensitive measure.
The results obtained using finite element number 38 are compared
with those obtained using the original finite element and the
COMEC finite element. Reference values are calculated consider-
ing the joint as a tensile bar.

Two distinct series are presented corresponding to the
use of isotropic and orthotropic material properties. The
complete set of numerical results for the isotropic series is
presented in Table II-4. The principal results are portrayed
graphically in Figure II-19. It is clear from Figure II-19 that
the various predictions are in agreement at the outset. When
the aspect ratio is increased beyond 8 the original finite
element representation leads to an unsatisfactory error. On the
other hand, the modified element representation performs satis-
factorily up to a value of 64.0. Thus the modified finite
element exhibits an improvement of a factor of 8 over finite
element number 21. The relative accuracy of the COMEC finite
element which involves polynomials of higher order was unexpected.

The same calculations were repeated for the case of an
orthotropic material. Table II-5 contains the numerical results
and Figure II-20 presents the corresponding graphical interpre-
tation. The original finite element performs satisfactorily to
an aspect ratio of 16.0 while the modified finite element is
apparently satisfactory even beyond an aspect ratio of 128.0.
These results reinforce the factor of 8 improvement inferred
from the results obtained for the isotropic series.

TABLE II-4   ISOTROPIC LAP JOINT* - RESULTS

ELEMENT ASPECT RATIO	ELEMENT TYPE	DISPLACE-MENT U_g $\times 10^{-4}$	POT. ENERGY π	REACTION R	$U_g d_e$ $\times 10^{-4}$	$\epsilon_{u_{gde}}$ (%)	ϕ $(\pi\, d_e)$	ϵ_ϕ(%)	P-R	ϵ_R(%)
ALL	BAR	--	--	100.	0.8333	--	.00417	--		--
1 $(d_e=10.)$	MAGIC PLUG #21	0.182	.00091	99.993	1.82	118.	.0091	118.2	0.007	0.007
	MAGIC PLUG #38	0.188	.00094	99.975	1.88	126.	.0094	125.4	0.025	0.025
	COMEC	0.180	.00091	100.007	1.80	116.	.0091	118.2	-.007	-0.007
2 $(d_e=5.)$	MAGIC PLUG #21	0.209	.00105	100.006	1.045	25.4	.00525	25.9	-.006	-0.006
	MAGIC PLUG #38	0.212	.00106	99.982	1.060	27.2	.00530	27.1	-.018	-0.018
	COMEC	0.209	.00105	100.005	1.045	25.4	.00525	25.9	-.005	-0.005
4 $(d_e=2.5)$	MAGIC PLUG #21	0.354	.00177	99.885	.8850	.20	.0044	5.52	0.115	0.115
	MAGIC PLUG #38	0.358	.00179	99.943	.8950	7.4	.00448	7.43	0.057	0.057
	COMEC	0.351	.00179	99.992	.8925	7.1	.00448	7.43	0.008	0.008
8 $(d_e=1.25)$	MAGIC PLUG #21	0.702	0.0035	106.21	.8775	5.3	.00439	5.27	-6.210	-6.210
	MAGIC PLUG #38	0.685	0.0034	99.986	.8563	2.8	.00429	2.88	0.014	0.014
	COMEC	0.682	0.0034	99.996	.8530	2.4	.00426	2.16	0.004	0.004
16 $(d_e=0.625)$	MAGIC PLUG #21	1.89	.00945	178.47	1.1813	41.8	.0059	41.5	-78.48	-78.48
	MAGIC PLUG #38	1.35	.00675	101.09	.8438	1.3	.0042	.72	- 1.09	-1.09
	COMEC	1.33	.00666	99.995	.8313	-.24	.0042	.72	0.005	.005
32 $(d_e=0.3125)$	MAGIC PLUG #21									
	MAGIC PLUG #38	2.66	.0133	99.68	.8312	-.25	.0042	.72	0.32	0.32
	COMEC	2.64	.0132	99.959	.825	-1.0	.0041	-1.7	0.041	0.41
64 $(d_e=0.15625)$	MAGIC PLUG #21									
	MAGIC PLUG #38	4.85	.0243	84.573	.7578	-9.1	.0038	-8.9	5.427	5.427
	COMEC	5.21	.0260	98.389	.8141	-2.3	.0042	+.72	1.611	1.611
128 $(d_e=0.078125)$	MAGIC PLUG #21									
	MAGIC PLUG #38	4.44	.0222	15.874	.3473	-58.3	.0017	-59.2	84.126	84.126
	COMEC	10.3	.0519	97.125	.8047	-3.4	.0039	-6.5	2.875	2.875

*   4 FINITE ELEMENTS

146
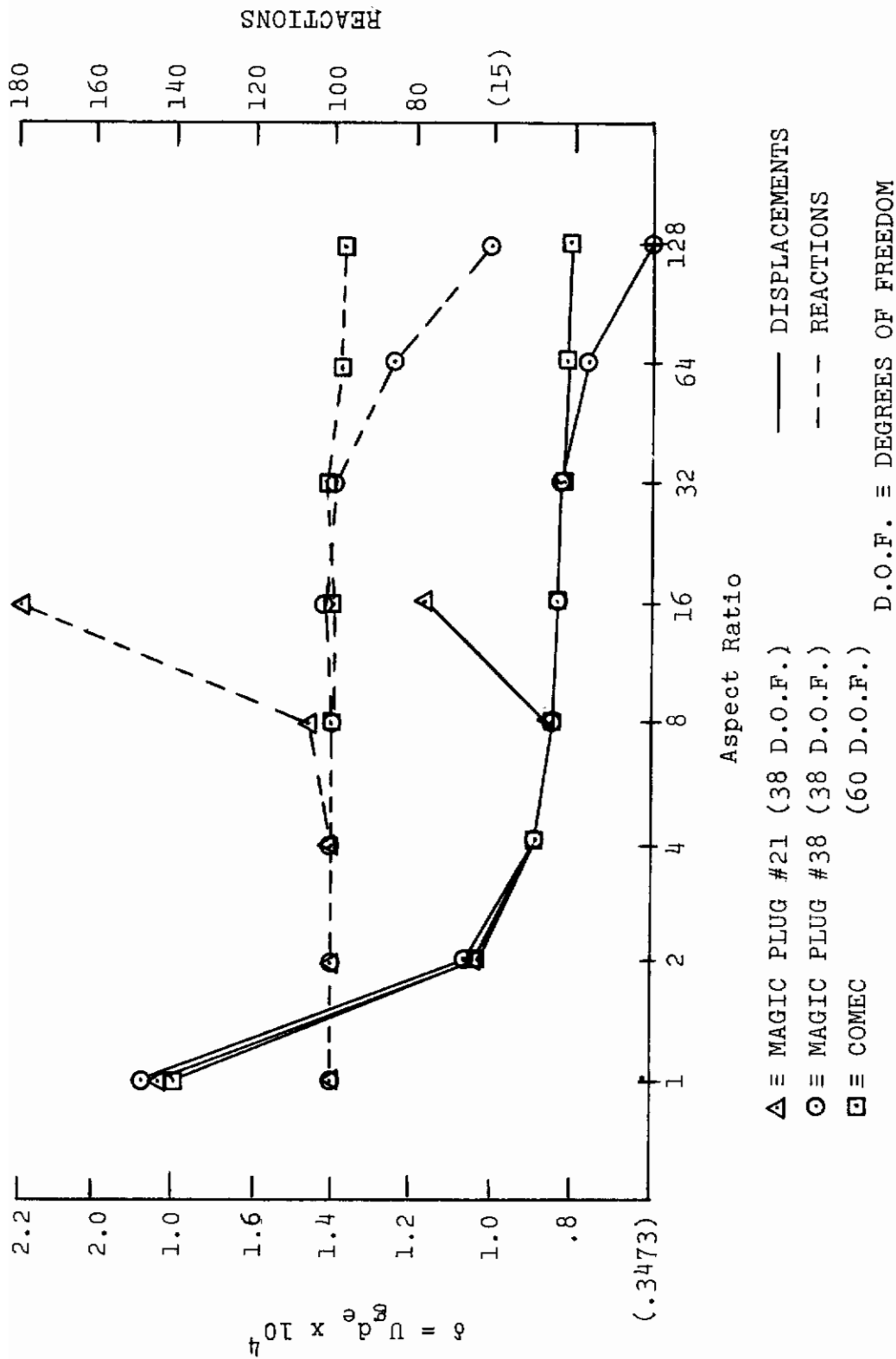
FIGURE II-19 ISOTROPIC LAP-JOINT, BEHAVIOR

△ ≡ MAGIC PLUG #21 (38 D.O.F.)
⊙ ≡ MAGIC PLUG #38 (38 D.O.F.)
▢ ≡ COMEC   (60 D.O.F.)

——— DISPLACEMENTS
– – – REACTIONS

D.O.F. ≡ DEGREES OF FREEDOM

TABLE II-5   ORTHOTROPIC LAP JOINT RESULTS

Element Aspect Ratio	Element Type	Displace-ment U_q x 10^{-4}	Pot. Energy π x 10^{-3}	Reac-tion R.	U_q de x 10^{-3}	ϵ_{uqde} %	$\bar{u}$ (πde) x 10^{-3}	ϵ_ϕ %	P-R	ϵ_R %
ALL	Bar	-	-	100.0	.1504	-	7.52	-	0.	-
1 (de = 10.0)	Magic Plug #21	1.0256	5.0128	100.0115	1.0256	87.52	50.128	567.0	-.0115	-.0115
	Magic Plug #38	1.071	5.036	99.9874	1.0710	92.06	50.36	570.0	.0126	.0126
2 (de = 5.)	Magic Plug #21	.87148	4.3574	99.9987	.43575	28.54	21.787	190.0	.0013	.0013
	Magic Plug #38	.8930	4.465	99.983	.4465	29.61	22.325	197.0	.0170	.0170
4 (de = 2.5)	Magic Plug #21	.9164	4.582	99.9661	.2291	7.87	11.455	52.3	.0339	.0339
	Magic Plug #38	.9276	4.638	99.9805	.2320	8.16	11.595	54.2	.0195	.0195
8 (de = 1.25)	Magic Plug #21	1.384	6.92	97.1454	.1730	2.26	8.65	15.0	2.855	2.855
	Magic Plug #38	1.395	6.97	99.9871	.1744	2.40	8.71	15.8	.0129	.0129
16 (de = .625)	Magic Plug #21	2.488	12.44	97.794	.1555	.51	7.775	3.4	2.206	2.206
	Magic Plug #38	2.55	12.439	100.006	.1594	.9	7.774	3.4	-.0058	-.0058
32 (de = .3125)	Magic Plug #21	14.938	74.68	431.538	.467	31.64	23.34	210.0	-331.54	-331.54
	Magic Plug #38	4.932	24.66	99.264	.1541	.37	7.70	10.9	0.7364	.7364
64 (de = .15625)	Magic Plug #21	2.5517	1.2764	12.2311	.0399	-11.05	.199	97.4	87.77	87.77
	Magic Plug #38	9.673	48.37	99.634	.1511	.07	7.56	.53	.3660	.3660
128 (de = .078125)	Magic Plug #21 " Plug #38	19.179	95.89	98.85	.1498	-.06	7.49	.40	1.1488	1.1488
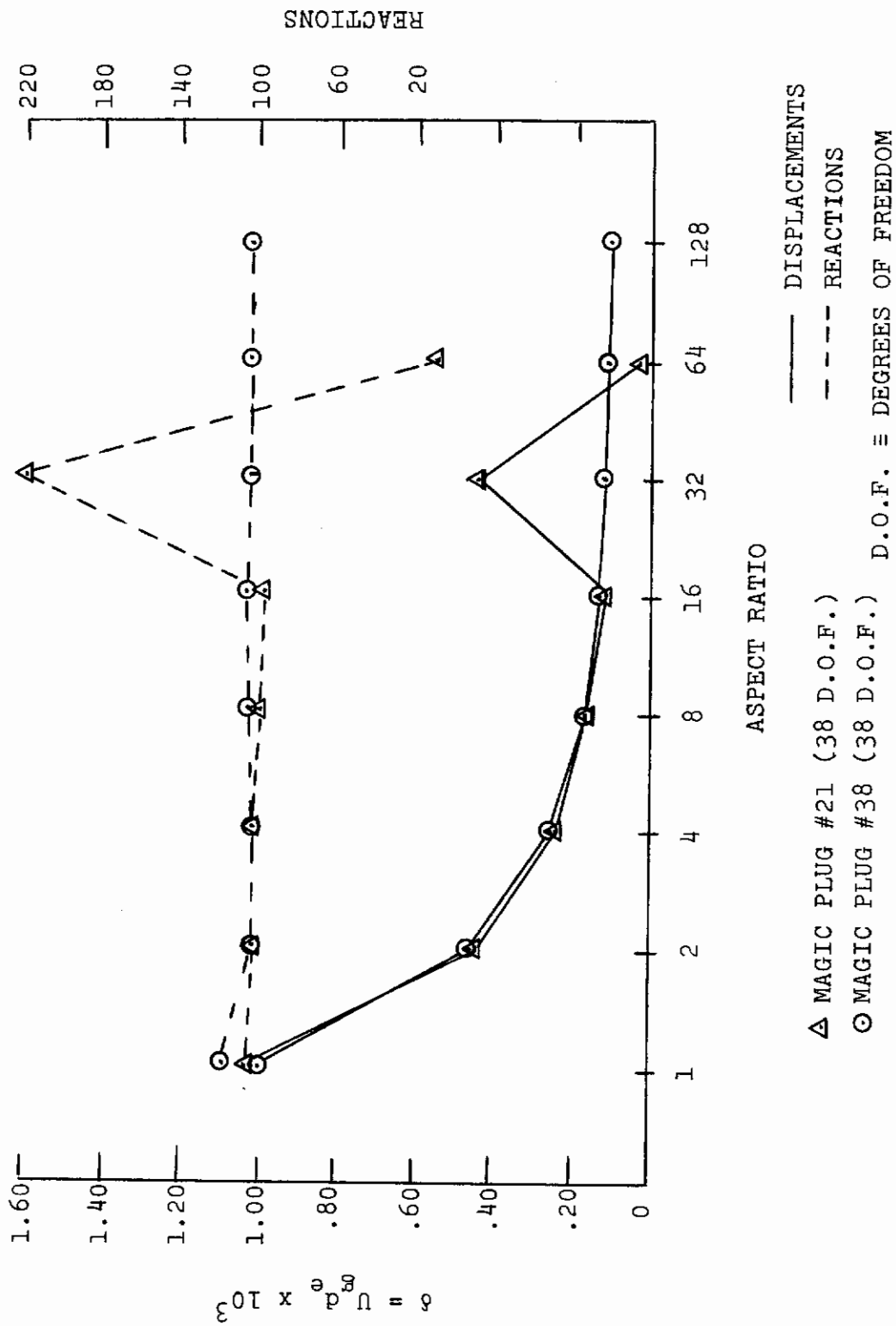
FIGURE II-20 ORTHOTROPIC LAP JOINT, BEHAVIOR

△ MAGIC PLUG #21 (38 D.O.F.)

⊙ MAGIC PLUG #38 (38 D.O.F.) D.O.F. ≡ DEGREES OF FREEDOM

―――― DISPLACEMENTS

――――― REACTIONS

149

X.   Summary and Conclusions

The modification of quadrilateral thin shell element
number 21 was undertaken to relax the aspect ratio constraint
on the in-plane portion of the representation. Attempts to
analyze structural joints had proved unsuccessful in that large
residuals (for instance, loss of load throughout the structure)
were obtained that were attributed to the unavoidable high
aspect ratios of the finite elements.

The development of finite element number 21 was examined
and the use of triangular subdivisions was judged to be the
limiting factor. Even at modest aspect ratios of the quadri-
lateral, the ratios of the sides of the triangular subdivisions
are extreme in comparison. Accordingly, the principal modifica-
tion in constructing finite element number 38 was the elimination
of the use of triangular subdivisions within the finite element.

The modification to obtain finite element number 38 is
presented in subsections I through V. A simple, low order dis-
placement approximation was chosen because experience has shown
that the simpler approximations are generally better conditioned.
Additionally, the gridpoints and gridpoint degrees of freedom of
the final form of the finite element representation were stipulated
at the outset to be the same as those of finite element number 21.
The resulting membrane representation of finite element 38 is
equivalent to the quadratic "serendipity" isoparametric finite
element representation.

The modified finite element representation is available in
the MAGIC III system as finite element 38. This new finite
element representation maintains all features present in finite
element 21. The program-analyst interface is unchanged. The
input data is the same. The displays of results have exactly the
same interpretation for the two finite elements.

The results presented for the membrane at different levels of grid refinement establish that the new membrane representation is satisfactory although somewhat less accurate than finite element number 21. Similarly, the results presented for idealizations of the membrane using distorted finite element shapes show that the new element performs satisfactorily at ordinary aspect ratios.

The cantilever beam problem emphasizes that this type of behavior is not predictable using full depth membranes (or shear panels) regardless of how accurately the element matrices are generated. The problem class of interest is represented by the idealized structural joint in which tension-shear behavior is dominant.

The idealized isotropic lap joint suggests an improvement of a factor of eight in the aspect ratio that can be employed using the new finite element number 38 in place of the original finite element number 21. This factor is substantiated by the analysis of the same joint configuration constructed of orthotropic materials.

The permissible aspect ratio limit of finite element number 38 relative to finite element number 21 is considered to be reasonably well established by the examples presented. However, the permissible absolute limit on aspect ratio depends upon computer characteristics, the size of the problem and the amount of bending present. All results presented herein were obtained using an IBM 360/65 computer. The problem sizes were chosen to be small for economic reasons. Clearly, the detrimental effects of bending were negligible in the illustrative lap joint examples.

The new quadrilateral thin shell element number 38 is recommended for use for elongated element shapes on the basis of the numerical evaluation presented herein. Its relative advantage is clear. Guidance for just how large finite element aspect ratios can be in specific applications must evolve from usage in practical design.

151

SECTION III

INCORPORATION OF NEW COMPUTATIONAL PROCEDURES

A.   INTRODUCTION

Several new computational modules have been incorporated into the MAGIC III System to support the structural analysis capability.

The first module is designated as ANALIC (Analysis in Core). This module can be used to perform a complete linear elastic stress analysis, selected portions of a linearily elastic analysis or as a general purpose equation solver. Four distinct equation solvers are available in this module and are described in the following subsection. The abstraction instructions required for this module and detailed instructions for its use are delineated in Volume II of this document (Reference 7).

In addition to the ANALIC module, an additional out-of-core equation solver has been added to MAGIC III. A variable bandwidth solver utilizing the square-root Cholesky technique is available for the decomposition of symmetric positive-definite matrices.

The theoretical details of the method are presented in a subsequent subsection while detailed instructions for its use in the MAGIC III System are given in The User's Manual[7], Volume II of this report.

152

B.   <u>ANALIC (ANALYSIS IN CORE)</u>

   I.   <u>Introduction</u>

        ANALIC is a MAGIC III module which can be used to perform a complete linear elastic stress analysis using in-core routines. This module may also be used to perform selected portions of a linear elastic analysis or as a general purpose equation solver. The ANALIC module is capable of solving problems of approximately 175 reduced degrees of freedom with 18,000 words of working storage. This module features "dynamic" storage which allows the maximum-size problem to fit in core.

   II.   <u>Equation Solvers In ANALIC</u>

      2.1   <u>Method of Bordering</u>

        The procedure described herein determines the inverse of a symmetric matrix by the bordering method. The given matrix A is regarded as the result of bordering a matrix of order (M-1), the inverse of which is assumed known. Thus let

$$
A_n = \begin{bmatrix} a_{11} & & & & \vdots & \\ a_{21} & a_{22} & & & \vdots & \\ a_{31} & a_{32} & & & \vdots & \\ a_{n-1,1} & & a_{n-1,\,n-1} & \vdots & \\ a_{n,1} & a_{n,2} & a_{n,n-1} & \vdots & a_{nn} \end{bmatrix} = \begin{bmatrix} A_{n-1} & \vdots & \\ \cdots & \vdots & \cdots \\ v_n & \vdots & a_{nn} \end{bmatrix} \qquad (1)
$$

Then, by seeking A^{-1} in the same form, we finally arrive at

$$
A_n^{-1} = \begin{bmatrix} A_{n-1}^{-1} + \dfrac{A_{n-1}^{-1}\, v_n^T v_n A_{n-1}^{-1}}{n} & \vdots & \\ \cdots & \vdots & \cdots \\ \dfrac{-v_n A_{n-1}^{-1}}{\alpha_n} & \vdots & \dfrac{1}{\alpha_n} \end{bmatrix} \qquad (2)
$$

where $\quad \alpha_n = a_{nn} - v_n A_{n-1}^{-1} v_n^T$

The algorithm used is a method of inverting a matrix by successive borderings. The system loops on the order of the desired matrix inverse and computes the inverse of a (1 x 1), (2 x 2), (3 x 3), ..., (n x n) in turn by using the preceding computed inverse. Each step of the process is accomplished on the basis of Equation (2).

The following operations are to be carried out in order to find A_n^{-1}:

(a) The computation of the row $-v_n A_{n-1}^{-1}$ with elements

$$\gamma_{n1}, \quad \gamma_{n2}, \quad \cdots, \quad \gamma_{n,n-1}$$

(b) The computation of the number

$$\alpha_n = a_{nn} + \sum_{i=1}^{n-1} a_{in} \gamma_{ni}$$

(c) The determination of the elements a_{ik} of the inverse matrix by the relationships

$$a_{ik} = a'_{ik} + \frac{\gamma^2_{ni}}{\alpha_n} \qquad (i \leq n-1, \ k \leq i)$$

$$a_{nk} = \frac{\gamma_{nk}}{\alpha_n} \qquad (k \leq n-1)$$

$$a_{nn} = \frac{1}{\alpha_n}.$$

Storage for the subroutine used, consists of n $\left(\frac{n+1}{2}\right)$ locations for matrix A (symmetric stored in the lower half by rows) and one column of length n. The solution for displacements is computed by multiplying the total load column by the computed inverse.

154

2.2 Gauss Elimination

The subroutine presented in this section solves a system of simultaneous linear equations with symmetric coefficient matrix by Gauss elimination. Consider the system of simultaneous linear equations

$$A * X = R \qquad (1)$$

with symmetric m by m coefficient matrix, the upper triangular part of which is stored by column in m* (m+1)/2 successive storage locations, and an m by n right-hand side matrix R stored by column in m * n successive storage locations. Solution is done by Gauss Elimination with pivoting in the main diagonal of matrix A. If matrix R is the identity matrix, solution X is the inverse of matrix A. Solution matrix X is placed in positions of the right-hand side matrix R and is stored by column also. Thus, the computation of the solution requires no extra m by n array of storage. Only an auxiliary storage array named AUX with (m-1) storage locations is necessary.

Explicitly, the given system (1) is of the form:[+]

$$
\begin{bmatrix}
a_{11} & a_{12} & a_{13} & \cdots & a_{1m} \\
a_{21} & a_{22} & a_{23} & \cdots & a_{2m} \\
a_{31} & a_{32} & a_{33} & \cdots & a_{3m} \\
a_{m1} & a_{m2} & a_{m3} & \cdots & a_{mm}
\end{bmatrix}
*
\begin{bmatrix}
x_{11} & x_{12} & \cdots & x_{1n} \\
x_{21} & x_{22} & \cdots & x_{2n} \\
x_{31} & x_{32} & \cdots & x_{3n} \\
x_{m1} & x_{m2} & \cdots & x_{mn}
\end{bmatrix}
$$

$$
=
\begin{bmatrix}
r_{11} & r_{12} & \cdots & r_{1n} \\
r_{21} & r_{22} & \cdots & r_{2n} \\
r_{31} & r_{32} & \cdots & r_{3n} \\
r_{m1} & r_{m2} & \cdots & r_{mn}
\end{bmatrix}
\qquad (2)
$$

+ Note that subroutine GELS requires only the upper triangular part of matrix A; that is, the elements a_{11}; a_{12}; a_{22}; a_{23}; a_{33}; ...; a_{1m}, a_{2m}, ..., a_{mm}. These elements are underlined in Equation (2).

155

The first step is to search the main diagonal of matrix A for the element of greatest absolute value, say a_{jj}, and to select it as first pivot ($p = a_{jj}$). The reason for pivoting only in the main diagonal of A is that rest-matrices of $A^{(k)}$ ($k = 1,2,\ldots,m-1$) must remain symmetrical during the whole algorithm. With a_{jj}, generate the internal absolute tolerance for testing usefulness of the symmetric algorithm in the following way:

$$tol = \left| a_{jj} \right| \cdot \varepsilon \tag{3}$$

with a given relative tolerance ε.

Suppose that pivot element a_{jj} is equal to a_{11}. If it is not, interchange the first rows of matrices A and R with the jth and the first column of matrix A with the jth, and save column interchange information by storing the difference $(j-1)$ of pivot column index j and step counter $k = 1$ [interchanging column 1 with column j means interchanging variables x_{11} with x_{1j} ($1 = 1,2,\ldots,n$)].

Now transform the elements of pivot rows in matrices A and R by division with p, and the other elements by adding $-a_{\nu 1}$ times the new first rows of these two matrices to the other ν rows, obtaining:[++]

$$a_{1l}^{(1)} = \frac{a_{1l}}{p} \quad (l = 1,2,\ldots,m) \tag{4}$$

$$r_{1l}^{(1)} = \frac{r_{1l}}{p} \quad (l = 1,2,\ldots,n) \tag{5}$$

$$a_{\nu l}^{(1)} = a_{\nu 1} - a_{\nu 1} \cdot a_{1l}^{(1)} \quad \begin{pmatrix} l = 2,3,\ldots,n; \\ \nu = 2,3,\ldots,m \end{pmatrix} \tag{6}$$

$$r_{\nu l}^{(1)} = r_{\nu 1} - a_{\nu 1} \cdot r_{1l}^{(1)} \quad \begin{pmatrix} l = 1,2,\ldots,n; \\ \nu = 2,3,\ldots,m \end{pmatrix} \tag{7}$$

[++] Note that transformation of pivot row in matrix A destroys pivot column, which is, due to symmetry, stored in the same location. As pivot column is used unchanged for transformation of rest of A and R, it has to be saved in auxiliary array AUX before transforming pivot row.

As column interchange information is saved in the first position
of the main diagonal, the result of the first step is the two
matrices:

$$A^{(1)} = \begin{bmatrix} \underline{(j-1)} & a_{\underline{12}}^{(1)} & a_{\underline{13}}^{(1)} & \cdots & a_{\underline{1m}}^{(1)} \\ 0 & a_{\underline{22}}^{(1)} & a_{\underline{23}}^{(1)} & \cdots & a_{\underline{2m}}^{(1)} \\ 0 & a_{\underline{32}}^{(1)} & a_{\underline{33}}^{(1)} & \cdots & a_{\underline{3m}}^{(1)} \\ \cdots\cdots\cdots\cdots\cdots\cdots\cdots\cdots\cdots\cdots \\ 0 & a_{m2}^{(1)} & a_{m3}^{(1)} & \cdots & a_{\underline{mm}}^{(1)} \end{bmatrix}$$ and

$$R^{(1)} = \begin{bmatrix} r_{11}^{(1)} & r_{12}^{(1)} & \cdots & r_{1n}^{(1)} \\ r_{21}^{(1)} & r_{22}^{(1)} & \cdots & r_{2n}^{(1)} \\ r_{31}^{(1)} & r_{32}^{(1)} & \cdots & r_{3n}^{(1)} \\ \cdots\cdots\cdots\cdots\cdots\cdots\cdots\cdots\cdots \\ r_{m1}^{(1)} & r_{m2}^{(1)} & \cdots & r_{mn}^{(1)} \end{bmatrix}$$

It is easily seen from equations (4) - (7) that the rest of the
matrix $A^{(1)}$ -- that is, matrix $A^{(1)}$ without the first row and first
column -- is symmetric and that actually only the underlined
elements must be calculated and stored. Therefore, the range of
index 1 in formula (6) reduces to $1 = \nu$, $\nu + 1$, ..., m.

   This procedure is now repeated m-2 times, starting
at each step with the matrix $A^{(k)}$ of the step before without the
first k rows and first k columns, and the matrix $R^{(k)}$ without the first
k rows. The total result after m-1 steps is the matrices:

$$A^{(m-1)} = \begin{bmatrix} (j_1-1) & a_{12}^{(1)} & a_{13}^{(1)} & \dots & a_{1m}^{(1)} \\[6pt] 0 & (j_2-2) & a_{23}^{(2)} & \dots & a_{2m}^{(2)} \\[6pt] 0 & 0 & (j_3-3) & \dots & a_{3m}^{(3)} \\[6pt] \multicolumn{5}{c}{\dotfill} \\[6pt] 0 & 0 & 0 & \dots & (j_m-m) \end{bmatrix} \quad \text{and}$$

$$R^{(m-1)} = \begin{bmatrix} r_{11}^{(1)} & r_{12}^{(1)} & \dots & r_{1n}^{(1)} \\[6pt] r_{21}^{(2)} & r_{22}^{(2)} & \dots & r_{2n}^{(2)} \\[6pt] r_{31}^{(3)} & r_{32}^{(3)} & \dots & r_{3n}^{(3)} \\[6pt] \multicolumn{4}{c}{\dotfill} \\[6pt] r_{m1}^{(m)} & r_{m2}^{(m)} & \dots & r_{mn}^{(m)} \end{bmatrix}$$

Now work backward and set:

$$\left. \begin{aligned} r_{m-1,1}^{(m)} &= r_{m-m,1}^{(m-1)} - a_{m-1,m}^{(m-1)} \cdot r_{m1}^{(m)} \quad (1=1,2,\dots,n) \\[10pt] r_{m-2,1}^{(m)} &= r_{m-2,1}^{(m-2)} - a_{m-2,m-1}^{(m-2)} \cdot r_{m-1,1}^{(m)} \\[6pt] &\quad\ \dots\dots\dots\dots \\[6pt] r_{11}^{(m)} &= r_{11}^{(1)} - a_{12}^{(1)} \cdot r_{21}^{(m)} - a_{13}^{(1)} - r_{31}^{(m)} \\[8pt] &\quad - a_{m-2,m}^{(m-2)} \cdot r_{m1}^{(m)} \quad (1=1,2,\dots,n) \\[8pt] &\quad - \dots\ - a_{1m}^{(1)} \cdot r_{m1}^{(m)} \quad (1=1,2,\dots,n) \end{aligned} \right\} \qquad (8)$$

After each step of back substitution, rows of solution matrix
$X = R^{(m)}$ have to be back-interchanged according to interchange
information in the corresponding main diagonal element of matrix
$A^{(m-1)}$, in order to get the correct sequence of right-hand side
column elements corresponding to the sequence of left-hand side
row elements.

The only case in which the procedure described above can
fail to give a solution occurs when at any step all elements in
the main diagonal of the rest-matrix of $A^{(k)}$ become zero, and no
pivot element can be found. In this case, the procedure is by-
passed and the error message ier = -1 is given. This may --but
not necessarily--mean, that matrix A is singular. Possibly
subroutines GELG or DGELG (which are working with complete pivoting)
will be able to find a solution in cases where subroutines GELS
or DGELS fail. Actually, because of rounding errors, a further
check of the absolute values of pivot elements is performed by
the procedure. If at elimination step k this absolute value
becomes less than tol (see Equation 3), it is likely that there
was loss of significance in the computation of the diagonal
elements. But as this may not necessarily be the case, and as
this test depends highly on the choice of the relative tolerance
ε [+], the procedure gives only the warning ier = k-1, which indicates
that there is a possible loss of significance in the results
computed by the algorithm.[++] But here it is also possible that
subroutines GELG or DGELG will give better results. If there
is only one equation to solve (m=1), the test on loss of significance
is suppressed.

[+] For subroutine GELS, a relative tolerance between 10^{-6} and
10^{-7} is suggested; and for subroutine DGELS, between 10^{-14} and 10^{-16}.

[++] For example, $\varepsilon = 10^{-5}$ and warning ier = 3 mean that there is a
possible loss of about five or more significant digits in the
initial values of elimination step 4.

2.3   Cholesky Triangularization

Given an n by n symmetric positive definite matrix A, compute an upper triangular matrix R such that

$$A = R^T R$$

The elements r_{ik} of R are computed using the following recursive relationships:

$$r_{1k} = a_{1k}/r_{11} \qquad\qquad k=1,2,3,\ldots,n$$

$$r_{jk} = (1/r_{jj}) \, (a_{jk} - \sum_{i=1}^{j-1} r_{ij}r_{ik}) \qquad \begin{array}{l} j=2,3,\ldots,n \\ k=j,j+1,\ldots,n \end{array}$$

The determinant of A is $det(A) = \left(\prod_{i=1}^{n} r_{ii} \right)^2$.

The given matrix A is assumed stored columnwise in compressed form, that is upper triangular part only. MFSD stores the solution R in the same locations as A.

If any calculated radicand r_{kk}^2 (k = 1,2,...,n) is not positive, further calculation is bypassed, and the error parameter IER is set to -1. This means that A is not positive definite, possibly due to roundoff errors. IER is also set to -1 if the input parameter n is less than 1.

Let all radicands be positive and let r_{kk}^2 be the first radicand which is no longer greater than the internal tolerance TOL = $\left| EPS \, a_{kk} \right|$. The subroutine then gives the warning IER = k-1; however, calculation is continued. The warning indicates that there may be loss of significance at factorization step k due to loss of significant digits in the calculation of r_{kk}^2.

Given a general matrix A and a nonsingular upper
triangular matrix T, the subroutine MTDS will perform one of the
following six operations, depending on the value of an input
parameter IOP:

IOP=1:   A is replaced by $T^{-1}A$.

IOP=-1:   A is replaced by AT^{-1}.

IOP=2:   A is replaced by $(T^{-1})^T A$.

IOP=-2:   A is replaced by $A(T^{-1})^T$.

IOP=3:   A is replaced by $(T^T T)^{-1}A$.

IOP=-3:   A is replaced by $A(T^T T)^{-1}$.

With the above information available:

(i)   Calculation of $X=T^{-1}A$ is done using backward
substitution to obtain X from TX=A.

(ii)   Calculation of $Y=(T^{-1})^T A$ is done using forward
substitution to obtain Y from $T^T Y=A$.

(iii)   Calculation of $Z=(T^T T)^{-1}A$ is done by first
solving $T^T Y=A$ and then solving TZ=Y.

The remaining three operations are reducible to the
above three.

This particular module may also be used to compute
the solution of a system of equations BX=A with symmetric positive
definite coefficient matrix B. The first step towards the solution
is the triangular factorization of B. The second step, which may
be repeated for different sets of righthand sides A, is the
calculation of $(T^T T)^{-1}A$. Another useful application is the
computation of the product $A^T B^{-1}A$ with symmetric positive definite
B and arbitrary A in only three steps and without additional
storage requirements:

161

(i)   Replace B to T where $B=T^T T$.

(ii)   Replace A by $C=(T^T)^{-1}A$.

(iii)   Replace B by $C^T C$.

2.4   Gauss Wavefront

This method uses a modified Gauss solution algorithm. A wavefront approach is used to manipulate the data and solve the symmetrix matrix of linear equations. The routine is a modified version of the method described in Reference 20.   .

Given:

$$\begin{bmatrix} K_{11} & K_{12} \\ K_{12}^T & K_{22} \end{bmatrix} \begin{bmatrix} U_1 \\ - \\ U_2 \end{bmatrix} = \begin{bmatrix} \bar{P}_1 \\ P_2 \end{bmatrix} \tag{1}$$

where $\bar{U}_2$ are prescribed displacements and $\bar{P}_1$ are given forces. From (1) we can write:

$$K_{11}U_1 + K_{12}\bar{U}_2 = \bar{P}_1 \tag{2}$$

We can decompose K_{11} as

$$K_{11} = L_{11}DL_{11}^T \tag{3}$$

where L_{11} is lower triangular

D   is diagonal with $d_{ii} = l_{ii}$

L_{11}^T is L_{11} transpose

and the elements of L_{11} are given by

$$l_{ij} = k_{ij} - \sum_{n=1}^{i-1} \frac{l_{nj} l_{ni}}{l_{n,n}} \qquad (i \le j) \tag{4}$$

162

Substituting into (2) we can write:

$$L_{11}DL_{11}^{T}U_1 = \bar{P}_1 - K_{12}\bar{U}_2 \qquad (5)$$

Now setting

$$y = DL_{11}^{T}U_1 \qquad (6)$$

we write

$$L_{11}y = \bar{P}_1 - K_{12}\bar{U}_2 \qquad (7)$$

and solve for y by forward substitution. Finally we obtain the unknown displacements U_1 by using backward substitution in Equation (7).

The stiffness matrix is stored in wavefront format which contains columns consisting of the first non-zero row to the diagonal element. The subroutines in ANALIC operate on the data in this format. Subroutines are called in turn to convert the symmetric matrix to wavefront format, decompose the matrix, perform forward substitution, and finally back substitution.

IV CONCLUSIONS

It is concluded that the MAGIC III System is a logical and consistent extension of the MAGIC I and II Systems, and that the additional capabilities realized with MAGIC III have met or exceeded the requirements of Contract No. F33615-71-C-1390. The satisfactory achievement of the overall objectives is given substantiation by a number of subsidiary conclusions. Specifically, it is concluded that:

(1) The addition of the solid finite element representations to the MAGIC III System provides enhanced capability to predict general three dimensional states of stress in structures of arbitrary profile.

(2) The addition of the triangular cross-section ring finite element which accommodates asymmetric mechanical and thermal loading on axisymmetric structures provides capability for the analysis of thick-walled and solid axisymmetric structures of finite length.

(3) The addition of the modified quadrilateral thin shell element provides enhanced capability for the prediction of structural response of membranes and plane-strain sections that require elongated finite element shapes.

(4) The addition of the ANALIC (Analysis In Core) Module provides an in-core equation solution capability designed for "moderate-sized" applications. Four equation solution techniques are provided.

(5) The out-of-core variable bandwidth equation solver utilizing the square root Cholesky technique has been provided for the decomposition of "large order" positive definite symmetric matrices.

164

(6) The MAGIC III Agendum Library has been expanded and includes computational procedures for the following:

a. STATICSASYM   (Linear Elastic Displacement and Stress Analysis, Triangular Ring - Asymmetric Loading)

b. STATICS   (Linear Elastic Displacement and Stress Analysis)

c. STATICSC   (Linear Elastic Displacement and Stress Analysis with Condensation)

d. STATICS2   (Linear Elastic Displacement and Stress Analysis With Prescribed Displacements)

e. STABILITY   (Linear Elastic Instability Analysis Using Cholesky Triangularization)

f. STABILITYA   (Linear Elastic Instability Analysis Using Matrix Inversion)

g. DYNAMICS   (Vibration Frequencies, Mode Shapes, Generalized Mass and Stiffness for Supported Structures)

h. DYNAMICSF   (Free-Free Vibration Frequencies, Mode Shapes, Generalized Mass and Generalized Stiffness for Unsupported Structures)

i. DYNAMICSC   (Vibration Frequencies, Mode Shapes, Generalized Mass and Generalized Stiffness with Condensation for Supported Structures)

j. DYNAMICSCF   (Free-Free Vibration Frequencies, Mode Shapes, Generalized Mass and Generalized Stiffness with Condensation for Unsupported Structures)

These computational procedures listed above enable the conduct of linear displacement, stress, and stability analyses in the presence of general prestrain

165

and thermal loading as well as distributed and concentrated mechanical loading. Additionally, vibration analyses for free-free or supported structures can be employed with or without the use of condensation techniques.

(7) The versatile MAGIC III System finite element library, which is composed of sixteen finite elements, enables effective idealization of most linear structures.

(8) The stability analysis procedure provided in the MAGIC III System enables the prediction of critical load levels for general built-up shell structures.

(9) The preprinted input data forms facilitate the rapid and reliable specification of problem data as evidenced by their wide acceptance with the original MAGIC I and II Systems.

(10) The output provided by the MAGIC III System is oriented to the engineering user, is consistent with MAGIC II, and facilitates clear and concise interpretation of output parameters.

(11) The computer program organization of the MAGIC III System is logical in design and is well suited to generalization.

166

SECTION V

REFERENCES

1. Mallett, R. H. and Jordan, S. "MAGIC: An Automated General Purpose System for Structural Analysis: Volume I. Engineer's Manual", AFFDL-TR-68-56, Volume I, Air Force Flight Dynamics Laboratory, Wright-Patterson AFB, Ohio, January 1969.

2. Jordan, S; Mallett, R.H. and Maddux, G.E., "MAGIC: An Automated General Purpose System for Structural Analysis: Volume II. User's Manual", AFFDL-TR-68-56, Volume II, Air Force Flight Dynamics Laboratory, Wright-Patterson AFB, Ohio, July 1969.

3. DeSantis, D., "MAGIC: An Automated General Purpose System for Structural Analysis: Volume III. Programmer's Manual", AFFDL-TR-68-56, Volume III, Air Force Flight Dynamics Laboratory, Wright-Patterson AFB, Ohio, January, 1969.

4. Jordan, S., "MAGIC II: An Automated General Purpose System for Structural Analysis: Volume I Engineer's Manual (Addendum)", AFFDL-TR-71-1, Volume I, Air Force Flight Dynamics Laboratory, Wright-Patterson AFB, Ohio, May 1971.

5. Jordan, S. "MAGIC II: An Automated General Purpose System for Structural Analysis, Volume II. User's Manual", AFFDL-TR-71-1, Volume II, Air Force Flight Dynamics Laboratory, Wright-Patterson AFB, Ohio, January, 1971.

6. Gallo, A.M., "MAGIC II: An Automated General Purpose System for Structural Analysis, Volume III. Programmer's Manual", AFFDL-TR-71-1, Volume III, Air Force Flight Dynamics Laboratory, Wright-Patterson AFB, Ohio, January 1971.

7. Jordan, S. and Batt, J. R., "MAGIC III: An Automated General Purpose System for Structural Analysis, Volume II. User's Manual", AFFDL-TR-72-42 Volume II, Air Force Flight Dynamics Laboratory, Wright-Patterson AFB, Ohio, July, 1972.

8. Gallo, A. M., "MAGIC III; An automated General Purpose System for Structural Analysis, Volume III. Programmer's Manual", AFFDL-TR-72-42, Volume III, Air Force Flight Dynamics Laboratory, Wright-Patterson AFB, Ohio, July, 1972.

9. Melosh, R., "Structural Analysis of Solids", American Society of Civil Engineers, Journal of the Structural Division, August, 1963.

10. Gallagher, R. H., Padlog, J. and Bijlaard, P. O., "Stress Analysis of Heated Complex Shapes", American Rocket Society Journal, Volume 32, No. 5, May, 1962.

11. Mallett, R. H., "Formulation and Evaluation of a Tetrahedron and Triangular Prism Discrete Element", Bell Aerospace Company, Report No. 9500-941001, 1967.

12. Przemieniecki, J. S., "Inertia and Stiffness Properties of Tetrahedron Elements for the Matrix Analysis of Three-Dimensional Elastic Media", AIAA Journal.

13. Helle, E. "Formulation and Evaluation of a Triangular Cross-Section Ring Discrete Element", BAC Technical Report No. 9500-941-003, June 1966.

14. Mallett, R. H. and Jordan, S., "Formulation and Evaluation of a Trapezoidal Cross-Section Ring Discrete Element", BAC Technical Report No. 9500-941004, November 1966.

15. Jordan, S. and Helle, E., "Formulation and Evaluation of a Two-Dimensional Core Discrete Element", BAC Technical Report No. 9500-941006, February 1967.

16. Clough, R. W., and Rashid, Y., "Finite Element Analysis of Axisymmetric Solids", J. Eng. Mech. Dir. 91, 71-85, 1965.

17. Wilson, E. L., "Structural Analysis of Axisymmetric Solids", AIAA Journal 3, 12, 2267-2274, December 1965.

18. Apostal, M. C. and Braun, F. W., "C-141 Wheel Rim Analysis - Theoretical Development and Evaluation", BAC Report No. 2500-941034.

19. Mallett, R. H., "Mathematical Models for Structural Discrete Elements", BAC Technical Note, June 1966.

20. Melosh, R. J. and Bamford, R. M., "Efficient Solution of Load-Deflection Equations", J. ASCE (Structures Division) Paper No. 6510, 661-676 (1969).

DOCUMENT CONTROL DATA - R & D

(Security classification of title, body of abstract and indexing annotation must be entered when the overall report is classified)

1. ORIGINATING ACTIVITY (Corporate author)	2a. REPORT SECURITY CLASSIFICATION
Bell Aerospace Company A Division of Textron Buffalo, New York 14240	Unclassified
	2b. GROUP N/A

3. REPORT TITLE

MAGIC III - An Automated General Purpose System for Structural Analysis - Volume I - Engineer's Manual

4. DESCRIPTIVE NOTES (Type of report and inclusive dates)

Final Report

5. AUTHOR(S) (First name, middle initial, last name)

James R. Batt and Stephen Jordan

6. REPORT DATE	7a. TOTAL NO. OF PAGES	7b. NO. OF REFS
August, 1972		

8a. CONTRACT OR GRANT NO.	9a. ORIGINATOR'S REPORT NUMBER(S)
AF 33615-71-C-1390	AFFDL-TR-72-42 Volume I
b. PROJECT NO. 1467	
c. Task No. 146702	9b. OTHER REPORT NO(S) (Any other numbers that may be assigned this report)
d.	

10. DISTRIBUTION STATEMENT

This document has been approved for public release and sale; its distribution is unlimited.

11. SUPPLEMENTARY NOTES	12. SPONSORING MILITARY ACTIVITY
None	Air Force Flight Dynamics Laboratory Structures Division for Wright-Patterson AFB, Ohio 45433

13. ABSTRACT

An automated general purpose system for analysis is presented. This system, identified by the acronym, "MAGIC III" for Matrix Analysis via Generative and Interpretive Computations, is an extension of the structural analysis capability available in the initial MAGIC System. MAGIC III provides a powerful framework for implementation of the finite element analysis technology and provides diversified capability for displacement, stress, vibration, and stability analyses.

Additional elements have been added to the MAGIC element library in this phase of MAGIC development. These are the solid elements; rectangular prism, tetrahedron, triangular prism, symmetric triangular prism, and triangular ring (asymmetrical loading). Also included are the symmetric shear web element and a revised quadrilateral thin shell element. The finite elements listed include matrices for stiffness, mass, prestrain load, thermal load, distributed mechanical load, pressure and stress.

Documentation of the MAGIC III System is presented in three parts; namely, Volume I: Engineer's Manual, Volume II: User's Manual and Volume III: Programmer's Manual.

DD FORM 1 NOV 65 1473

14. KEY WORDS	LINK A		LINK B		LINK C	
	ROLE	WT	ROLE	WT	ROLE	WT
1. Structural Analysis						
2. Matrix Methods						
3. Matrix Abstraction						
4. Digital Computer Methods						
5. Finite Element Techniques						

Unclassified

Security Classification